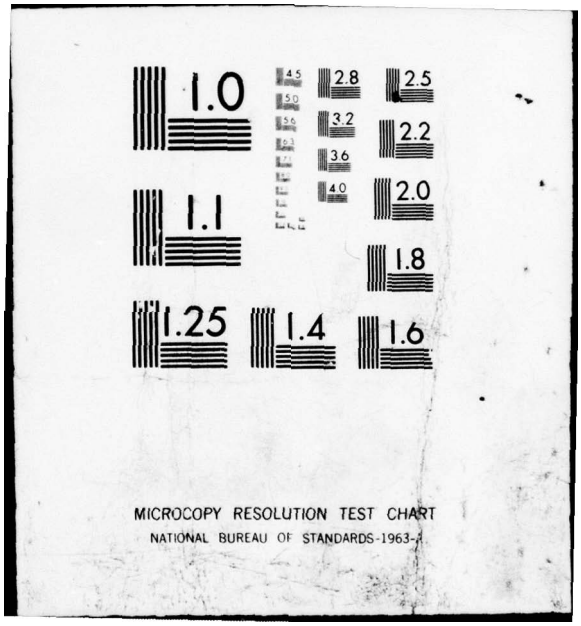
AD-A065 237 POLYTECHNIC INST OF NEW YORK BROOKLYN F/G 7/4
COMPOUNDS WITH DEFECT LATTICE STRUCTURES.(U)
NOV 78 E BANKS DAAG29-75-G-0096

UNCLASSIFIED ARO-12613.1-C NL

1 OF 2
AD A065237




1.0
1.1
1.25
1.4
1.6
1.8
2.0
2.2
2.5
2.8
3.2
3.6
4.0
4.5
5.0
5.6
MICROCOPY RESOLUTION TEST CHART
NATIONAL BUREAU OF STANDARDS-1963-A

ARO 12613.1-C
ARO 15558.1-C

(12) LEVEL III

740 204

AD A065237

DDC FILE COPY

POLYTECHNIC INSTITUTE OF NEW YORK
333 Jay Street, Brooklyn, New York
11201

See 1473 in back

FINAL REPORT

on

Grant No. DAAG29-75-G-0096
Project No. P-12513-C

and

Grant No. DAAG-29-78-G-0105
Project No. P-15558-C

COMPOUNDS WITH DEFECT LATTICE STRUCTURES

Covering the Period
1 March 1975 to 31 DECEMBER 1978

THIS DOCUMENT IS BEST QUALITY PRACTICABLE.
THE COPY FURNISHED TO DDC CONTAINED A
SIGNIFICANT NUMBER OF PAGES WHICH DO NOT
REPRODUCE LEGIBLY.

DDC
RECEIVED
MAR 5 1979
B

U.S. Army Research Office (Durham)
Durham, North Carolina

DISTRIBUTION STATEMENT A
Approved for public release;
Distribution Unlimited

79 02 26 001

DISCLAIMER NOTICE

THIS DOCUMENT IS BEST QUALITY PRACTICABLE. THE COPY FURNISHED TO DDC CONTAINED A SIGNIFICANT NUMBER OF PAGES WHICH DO NOT REPRODUCE LEGIBLY.

POLYTECHNIC INSTITUTE OF NEW YORK
333 Jay Street
Brooklyn, New York
11201

FINAL REPORT

on

Grant No. DAAG29-75-G-0096
Project No. P-12513-C

and

Grant No. DAAG-29-78-G-0105
Project No. P-15558-C

COMPOUNDS WITH DEFECT LATTICE STRUCTURES

Covering the Period
1 March 1975 to 31 DECEMBER 1978

Prepared by Prof. E. Banks

U.S. Army Research Office (Durham)
Durham, North Carolina

November 15, 1978

APPROVED FOR PUBLIC RELEASE;
DISTRIBUTION UNLIMITED

79 02 26 001

THE FINDINGS IN THIS REPORT ARE NOT TO BE CONSIDERED AS AN OFFICIAL DEPARTMENT OF THE ARMY POSITION, UNLESS SO DESIGNATED BY OTHER AUTHORIZED DOCUMENTS.

Table of Contents

		Page
	Introduction	1
I.	New Bivalent Rare-Earth Magnesium Fluorides	3
	A. Synthesis	3
	B. Structural Studies	5
	C. Luminescence	6
	D. Energy Transfer from Eu^{2+} to Sm^{2+}	9
	E. Magnetic Susceptibility Measurements	11
II.	Complex Transition Metal Fluorides	29
	A. Preparation of New Samples and Crystal Growth	30
	B. Phase Transitions	32
	C. Site Preferences of Bivalent Ions in $K_xM^{II}_xM^{III}_{1-x}F_3$	34
III.	Upconversion and NMR Studies of CdF_2:Rare Earth	36
IV.	Synthesis of Potential Solid Electrolytes	38
V.	Eu Mössbauer Study of Eu_xMoO_4	42
VI.	Phase Transition and ESR of Cr(V) in Fluorapatite	43
	A. X-ray Data	43
	B. Differential Thermal Analysis	46
	C. Reinvestigation of ESR of CrO_4^{3-} in Fluorapatite	46
VII.	Possible Linear Conductors Based on (VO) Phthalocyanine	49
	References	51
	Degrees Awarded During Contract Period	52
	Appendix	53

e Section
Section
UNANNOUNCED
JUSTIFICATION
BY
DISTRIBUTION/AVAILABILITY CODES
AIL. and/or SPECIAL
A 23

List of Figures

Page

Section I.

Figure No.

1.1 Emission Spectrum of $EuMgF_4$ at Room Temperature 14

1.2 Excitation Spectrum of $EuMgF_4$ at Room Temperature 15

1.3 Brightness vs. Composition, $Sr_{1-x}Eu_xMgF_4$ 16

1.4 Excitation Spectrum of $SmMgF_4$ at Room Temperature 17

1.5 Emission Spectrum of $SmMgF_4$ at Room Temperature 18

1.6 Brightness vs. Composition $Sr_{1-x}Sm_xMgF_4$ 19

1.7 Emission Spectrum of $SmMgF_4$ at 77 K. 20

1.8 Emission Spectrum of $Eu_{0.9}Sm_{0.1}MgF_4$ at Room Temperature - λ_{exc} = 350 nm 21

1.9 Emission Spectrum of $Eu_{0.99}Sm_{0.01}MgF_4$ at Room Temperature - λ_{exc} = 350 nm 22

1.10 Excitation Spectrum of 681 nm Sm^{2+} Line (Room Temp.) in $Eu_{0.99}Sm_{0.01}MgF_4$ 23

1.11 Eu^{2+} Fluorescent Lifetime vs. Sm^{2+} Concentration in $Eu_{1-x}Sm_xMgF_4$ (Room Temp.) 24

1.12 Reciprocal Susceptibility vs. Temperature, $EuMgF_4$ 25

1.13 Reciprocal Susceptibility vs. Temperature, $Eu_{0.5}Sm_{0.5}MgF_4$ 26

1.14 Reciprocal Susceptibility vs. Temperature, $SmMgF_4$ 27

1.15 Effective Magnetic Moment of Sm^{2+} in $SmMgF_4$ vs. Temperature; Comparison with $SmBr_2$ 28

List of Figures (Concluded)

Page

Section VI.

Figure No.

6.1 Differential Thermal Analysis of Fluorapatite - Comparison of DTA run after Cooling to run after holding sample at -160°C for four hours 48

Introduction

This report is the last in a long series of reports on research in solid-state chemistry and physics, under the general title, "Compounds with Defect Lattice Structures". Over the years, a wide variety of investigations had been undertaken, often going beyond the literal meaning of the title, although the behavior of solids containing varying concentrations of point imperfections and their complexes has been the major theme. The overriding goal has been the search for interesting magnetic, dielectric, conductive and luminescent behavior which may find application in solid-state electronic devices or assist in the explanation of the behavior of related materials which find application in such devices.

In the following pages, the research done in these areas at the Polytechnic Institute of New York since 1975 will be described. During this period, a number of studies following up work described in the final report on the previous grant[1] were undertaken, completed work was published, several new exploratory studies were undertaken, and as a result of the latter, two major new areas were opened up - one on a new approach to the synthesis of potential new solid electrolytes, which has become the basis for a new grant from

ARO[2], and a second - the discovery of new luminescent fluorides of divalent rare earths, which is the subject of one completed Ph.D. dissertation and of another ongoing investigation by a part-time graduate student. The work completed in this area, comprising Section I in this report, is discussed in detail there. Work reported in other sections will be referred to appendices for published papers and in the body of the text for material as yet unpublished.

I. New Bivalent Rare-Earth Magnesium Fluorides

In recent years, numerous reports of the piezoelectric and antiferromagnetic behavior of ternary fluorides formed between BaF_2 and fluorides of bivalent transition metals have appeared, and our interest in magnetic interactions in fluorides drew our attention to the report on the crystal structure of piezoelectric $BaMnF_4$[3] which became antiferromagnetic at low temperatures. We attempted to prepare $EuFeF_4$ by solid state reaction of EuF_2 and FeF_2. The purpose was to obtain a crystalline product which contained two strongly paramagnetic ions, Eu^{2+} ($4f^7$ - S = 7/2) and Fe^{2+} ($3d^6$ - S = 2). The result of heating EuF_2 with FeF_2 was the reduction of FeF_2 to metallic iron, indicating the very strong reducing power of Eu^{2+}.

A. Synthesis

Interest in phases of this type was revived by the appearance of a report by Bergmann and Crane[4] on the non-linear optical behavior of $BaMgF_4$. Reasoning that MgF_2 would be much more difficult to reduce than FeF_2, we attempted to prepare $EuMgF_4$ from EuF_2 and MgF_2 in sealed platinum tubes. These experiments yielded products showing new X-ray diffraction peaks, EuF_3 peaks, a few spots showing blue fluorescence under 365 nm ultraviolet excitation, and blackening of the walls of the Pt contaniers, evidently caused by

alloying of Mg metal with the platinum. This suggested that the reduction equilibrium between EuF_2 and MgF_2 was being displaced by removal of Mg from the reaction. To avoid this problem, we turned to the use of sealed graphite containers which yielded the first preparation of the new phase. X-ray diffraction showed the presence of a new orthorhombic phase whose unit cell parameters were similar to (and uniformly smaller than) those of $BaMgF_4$. A similar preparation using SrF_2 yielded a similar phase, $SrMgF_4$, with cell dimensions almost identical to those of $EuMgF_4$. For the europium compound, the most successful method to date is heating of the trifluoride EuF_3 with MgF_2 and excess Mg metal over that required to reduce the EuF_3 to EuF_2. The same method was used to prepare $SmMgF_4$, starting with SmF_3. The excess Mg metal (vapor at 800°C) appears to be needed to reduce any residual oxide present in the commercial starting materials. This oxide apparently inhibits the solid state reaction - a conclusion confirmed by the greater ease of conducting the solid state reaction when the commercial trifluorides are pretreated with ammonium fluoride.

In contrast to $BaMgF_4$, which melts congruently, the three new compounds decompose on melting (ca. 900°C) to the binary fluorides (e.g., $EuF_2 + MgF_2$). This creates a problem in single crystal growth, and we have not yet been able to

grow single crystals. The only relevant phase diagram information, on the system SrF_2-MgF_2, shows an apparent eutectic at 890° near the stoichiometric 1:1 composition[5].

B. Structural Studies

The orthorhombic unit cells of the three new fluorides are compared with that of $BaMgF_4$ below:

	a_o (A)	b_o (A)	c_o (A)
$BaMgF_4$	5.81	14.509	4.125
$SmMgF_4$	5.661	14.440	3.965
$EuMgF_4$	5.658	14.430	3.933
$SrMgF_4$	5.637	14.459	3.917

The cell parameters vary in a manner to be expected from the variation in ionic radii of the large cations, with a possible anomaly in the "b" axis of $SrMgF_4$.

Tests for second harmonic generation using a Nd glass laser were negative for all three compounds while a positive test was obtained with $BaMgF_4$ on the same apparatus. This indicates that they are probably centrosymmetric.

Structure factor calculations of the X-ray intensities, using the published parameters for $BaMnF_4$[3] did not yield good agreement for $EuMgF_4$, but the results suggest that the structures are related. The agreement is improved when the positional parameters are changed to parameters which are centrosymmetric. This suggests that the new phases may have structures corresponding to the hypothetical high-temperature

structure of $BaMgF_4$ (paraelectric phase). If this proves to be correct, we expect these phases will have transitions to a non-centric structure below room temperature. We are currently attempting to detect such transitions by low temperature X-ray diffraction and by ^{151}Eu Mössbauer spectroscopy.

C. Luminescence

The luminescence properties of these new compounds are quite unusual. At room temperature $EuMgF_4$ displays a bright blue fluorescence under excitation by a high pressure mercury vapor lamp (365 nm), the emission occurring in a broad band with a maximum at 437 nm. Excitation is in a broad band peaking at 354 nm. The room temperature emission and excitation spectra are shown in Figures 1.1 and 1.2. This compound shows complete solid solution with both $SrMgF_4$ and $SmMgF_4$. In solid solutions $Sr_{1-x}Eu_xMgF_4$, the maximum peak brightness was found at $x = 0.75$, as shown in Figure 1.3. Measurements of the quantum efficiencies of the sample with $x = 0.75$ and 1.00 were made in the laboratory of Dr. W. A. Thornton of the Westinghouse Electric Co., Bloomfield, N.J. The assistance of Dr. Thornton and Mr. E. Chen is gratefully acknowledged. The efficiency, under 365 nm excitation, of the $x = 0.75$ sample was 36% while that of pure $EuMgF_4$ was 34%, only about 5% less. This places $EuMgF_4$ in the class of "stoichiometric" phosphors, where the phenomenon of concentration quenching is negligible, such as NdP_5O_{14} [6-8] and

$LiNdP_4O_{12}$ [9,10]. The latter materials have been made into miniature solid state lasers, emitting in the infrared. If crystals of $EuMgF_4$ can be made, the intense blue band emission of Eu^{2+} suggests the possibility of tunable optically pumped lasers in the blue region, where the wavelength is selected by rotating a grating on one mirror of the optical cavity.

The quantum efficiency values cited above should be considered as lower limits because of the grey body color of the powders which is due, at least in part, to the presence of some graphite powder from the crucibles used in the preparation, and possibly a film of Mg metal deposited on the powders. If we are able to continue this research, we plan to use glassy carbon containers rather than machined graphite; this should eliminate graphite dust in the samples. In addition, measurement with 365 nm was off the true excitation peak of 356 nm. Correction for this would increase the measured values by about 8-10%.

Samarium magnesium fluoride, $SmMgF_4$, has a reddish body color and exhibits a weak red fluorescence under the Hg lamp. It is excited in a broad band peaking at 468 nm (Figure 1.4). The lines in the excitation spectrum are all identified as atomic emission lines of argon, superimposed on the band spectrum of the Ar discharge lamp used as excitation source in the Perkin-Elmer fluorescence spectrometer. They

do not represent transitions in the Sm^{2+} ion. Excitation is thus occurring to the $4f^5$ 5d manifold of Sm^{2+}, which is broadened by strong interactions with the crystal field. Under monochromatic excitation at 468 nm, the emission spectrum of $SmMgF_4$ consists, even at room temperature, of a series of rather sharp lines (Figure 1.5) in the red and near IR region. The strongest peak occurs at 681 nm.

In contrast to the behavior of $EuMgF_4$, the concentration dependence of the peak brightness of the Sm^{2+} emission (Figure 1.6) shows a maximum at about 10 mole % $SmMgF_4$ in $SrMgF_4$. Considerable concentration quenching is present in this case. On the assumption that the quenching mechanism is due to the crossover of the ground and excited states, spectra were recorded at 77 K. The emission spectrum at that temperature is shown in Figure 1.7. The brightness is considerably increased, although the magnitudes cannot be compared directly because of different sample geometry of the low temperature cell. This figure shows improved resolution and a proposed assignment of the transitions to states in the $4f^6$ manifold of Sm^{2+}. The assignment of the strong peak at 681 nm to the transition $^5D_o \longrightarrow {}^7F_o$ is made in analogy to results on Eu^{3+} fluorescence in crystals having low site symmetry. This transition is both Laporte and spin-forbidden, and can only be observed when the ion (Sm^{2+} or Eu^{3+}) is

located in a non-centrosymmetric site which introduces a linear term into the crystal potential. Although the present compounds are centrosymmetric, we believe that the local site symmetry must be non-centric, partly because of the above assignment.

D. Energy Transfer from Eu^{2+} to Sm^{2+}

The maximum in the excitation spectrum of $SmMgF_4$ occurs at 468 nm, which is very close to the emission peak of $EuMgF_4$ at 437 nm. This suggested that mixed samples might display energy transfer from Eu^{2+} to Sm^{2+}. Samples of composition $Eu_{1-x}Sm_xMgF_4$ were prepared with values of x ranging from 0.01 to 0.75. When these samples were excited at 350 nm (in the Eu^{2+} excitation band) no Eu^{2+} emission was observed for all samples having x greater than 0.1 - only the Sm emission is observed. Figure 1.8 shows the emission spectrum of $Eu_{0.9}Sm_{0.1}MgF_4$, excited in the Eu^{2+} excitation band. Only the line spectrum of Sm^{2+} is seen. In Figure 1.9, the spectrum of $Eu_{0.99}Sm_{0.01}MgF_4$ shows a very weak Eu^{2+} band in the blue region, and strong lines of the Sm^{2+} spectrum. The excitation spectra of these bands, monitored at the 681 nm Sm^{2+} line, show that both direct excitation in the Sm band and indirect excitation in the Eu band are occurring (Figure 1.10).

In an effort to determine whether this apparently total transfer of excitation energy was occurring by a radiative (photon transfer) process or a non-radiative (resonance transfer) process, two experiments were performed. Samples of $EuMgF_4$, $Eu_{0.995}Sm_{0.005}MgF_4$ and $Eu_{0.99}Sm_{0.01}MgF_4$ were measured for fluorescence lifetime, using an SLM series 400 lifetime meter. The instrument was set to detect the Eu blue fluorescence at 437 nm. The results, shown in Figure 1.11, indicate a significant decrease in Eu^{2+} fluorescence lifetime as the Sm concentration is increased. This behavior is characteristic for non-radiative energy transfer by resonance between excited Eu^{2+} ions and ground state Sm^{2+} ions. It was not possible to follow this lifetime shortening to higher Sm concentrations, owing to the complete quenching of the Eu^{2+} emission. This effect is considered to be additional evidence for a non-radiative energy transfer process, as some of the emitted Eu^{2+} radiation would be expected to escape from the samples if the photon transfer mechanism were the major mode of energy transfer.

To test for the possibility of radiative energy transfer, a mechanical equimolar mixture of $EuMgF_4$ and $SmMgF_4$ was prepared and the emission spectrum under 350 nm excitation was recorded. The spectrum showed the presence of both Eu^{2+} (blue band) and Sm^{2+} (red lines) emissions, although

excitation was solely within the Eu^{2+} band. This experiment shows that the radiative transfer mechanism is indeed feasible, but the absence of Eu^{2+} emission in solid solutions, as described above, indicates that resonant (non-radiative) energy transfer is the dominant mechanism, occurring at much higher rates than radiative transfer.

E. Magnetic Susceptibility Measurements

Samples of $EuMgF_4$, $SmMgF_4$ and solid solutions of the two at concentrations of 25 and 50 mole % were subjected to measurements of magnetic susceptibility using a Faraday balance at Brown University in the laboratory of Professor Aaron Wold, between room temperature and 80 K, and a vibrating sample magnetometer down to 4.2 K in the laboratory of Professor William O.J. Boo at the University of Mississippi. We acknowledge their assistance with gratitude. The results with both instruments were comparable in the temperature range where overlapping measurements were made.

The purpose of these measurements was to search for any possible ordering of the magnetic moments and to determine the strength of the nearest meighbor magnetic interactions from the magnitude of the Weiss constant θ in the Curie-Weiss Law: $X_m = C/T + \theta$. It was thought that the presence of strong exchange interactions might be correlated with the energy transfer processes described above.

Figures 1.12, 1.13 and 1.14 show the reciprocal of the molar susceptibility, $1/\chi_m$ plotted against absolute temperature for $EuMgF_4$, $Eu_{0.5}Sm_{0.5}MgF_4$ and $SmMgF_4$. The Weiss constant of -3 K for $EuMgF_4$ indicates that the magnetic exchange interactions are quite negligible. This result is not unexpected, as the Eu-Eu distances are expected to be large (about 4.4 A, if the structure resembles that of $BaMnF_4$ in any way). The magnetic moment calculated for Eu^{2+} from the slope of the linear high temperature region is 7.7 μ_B, compared to 7.8 μ_B expected for the $^8S_{7/2}$ configuration of Eu^{2+}. The curve for the 50 mole % mixture yields an average room temperature moment that would be expected for a random distribution of Sm^{2+} and Eu^{2+}, using the value of the room temperature moment of Sm^{2+} measured by Selwood[11] on $SmBr_2$. The magnetic moment of Sm^{2+} is expected to be temperature dependent, for the ground multiplet, ^7F_J consists of seven closely-spaced levels about 200 cm^{-1} apart, with the lowest state, ^7F_o, being non-magnetic. The susceptibility data on $SmMgF_4$ were substituted into the van Vleck formula for the susceptibility-temperature relation for the case where the multiplet splitting is comparable to kT, assuming zero for the Weiss constant. The magnetic moment of Sm^{2+} in Bohr magnetons is plotted against temperature in Figure 1.15, where Selwood's data on $SmBr_2$ are also shown. The two curves are

in reasonable agreement. There is a trend to higher values for $SmMgF_4$ at low temperatures and lower values at high temperatures. This may indicate some mixing of the J = 0 ground state with states of higher J values. If this is the case, it may be a factor which enhances the intensity of the nominally forbidden $^5D_o \longrightarrow {}^7F_o$ transition. Resolution of this question will require measurement of the Sm^{2+} emission spectrum at lower temperatures on an instrument of higher resolution than the Perkin-Elmer Spectrofluorimeter used in this research.

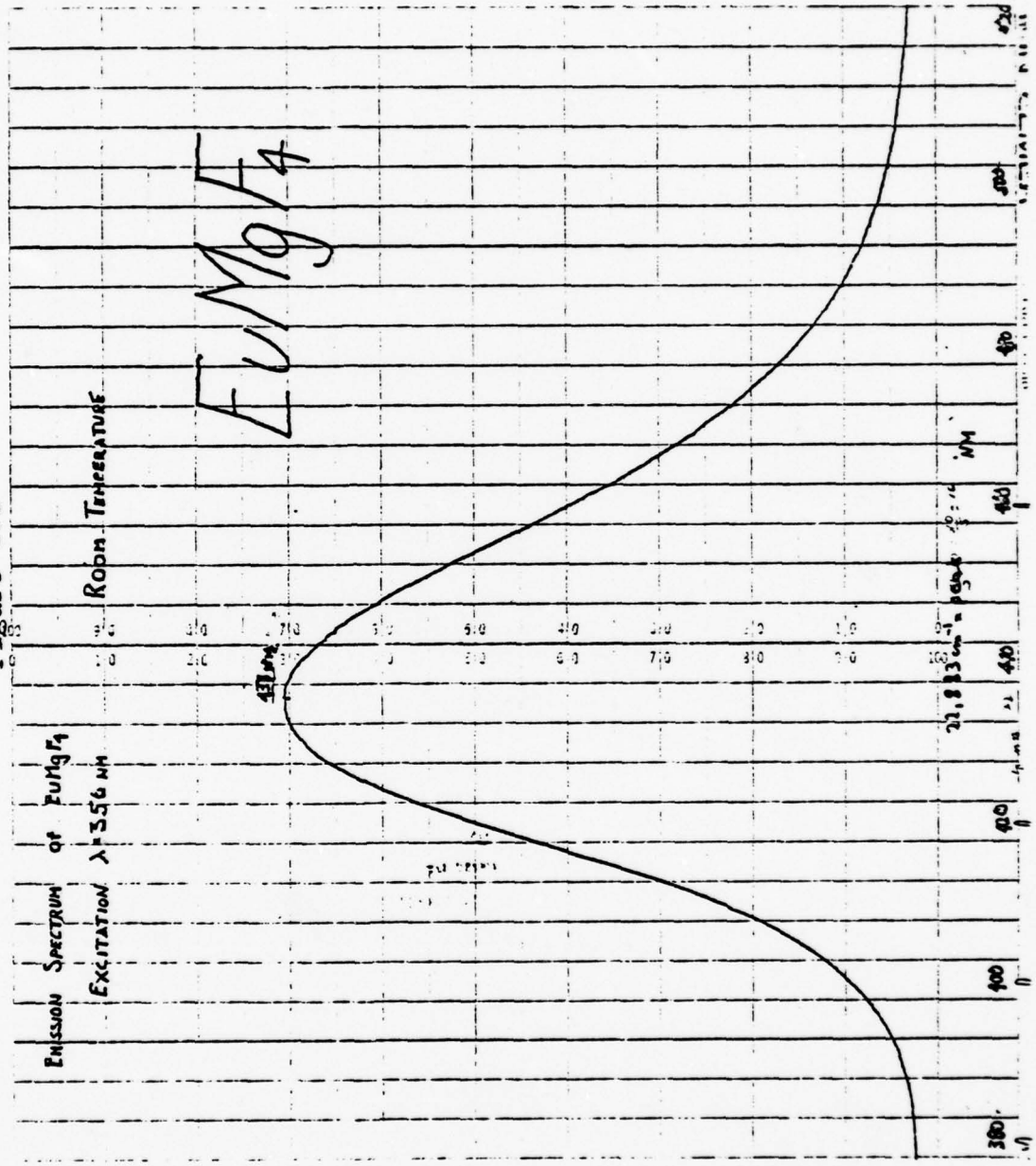

EuMgF4
Room Temperature
Emission Spectrum of EuMgF4
Excitation λ 356 nm

Figure 1.1

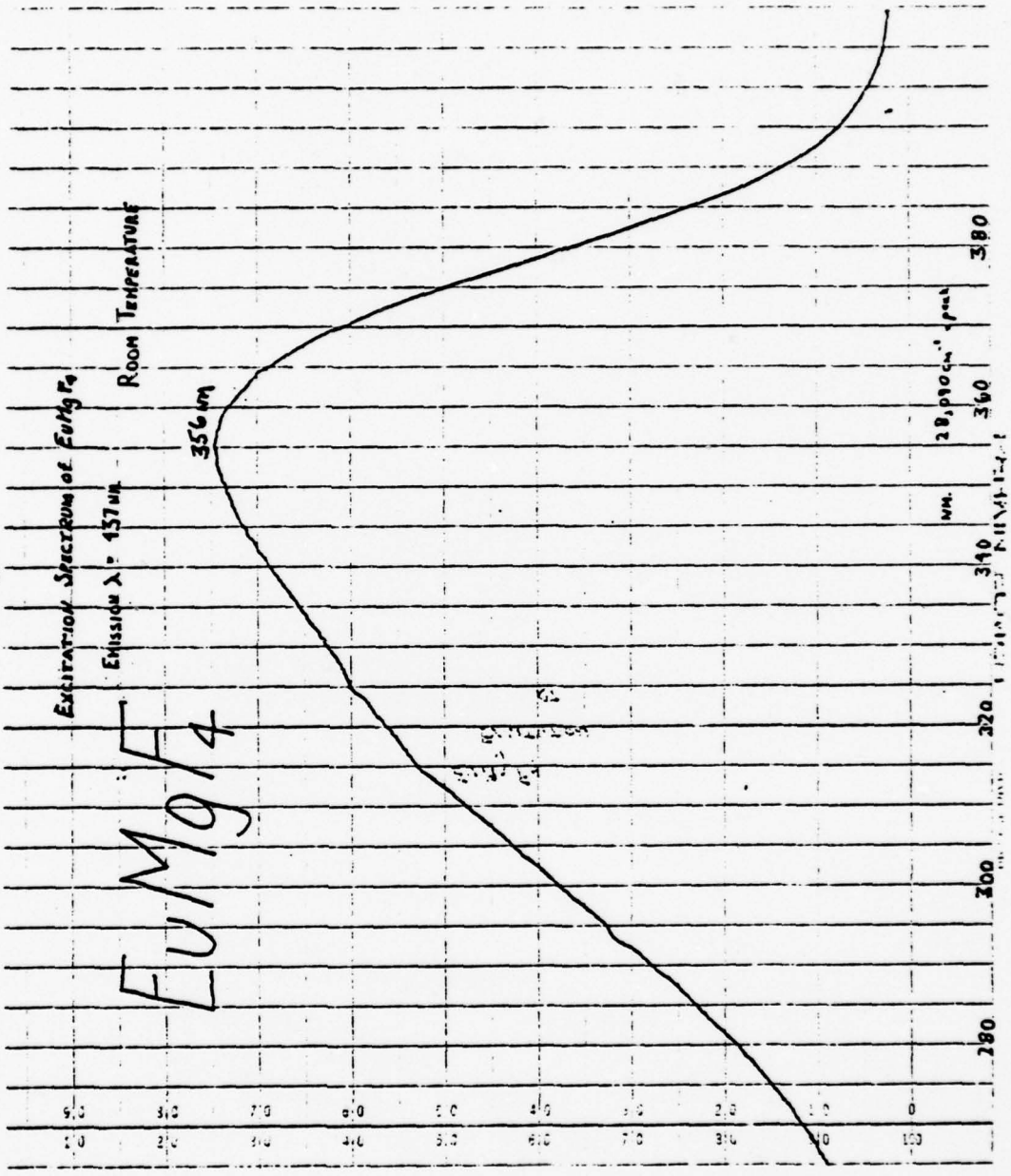

Excitation Spectrum of EuMgF4
Emission λ = 137 nm
Room Temperature
356 nm
EuMgF4
280
300
320
340
360
380
nm.

Figure 1.2

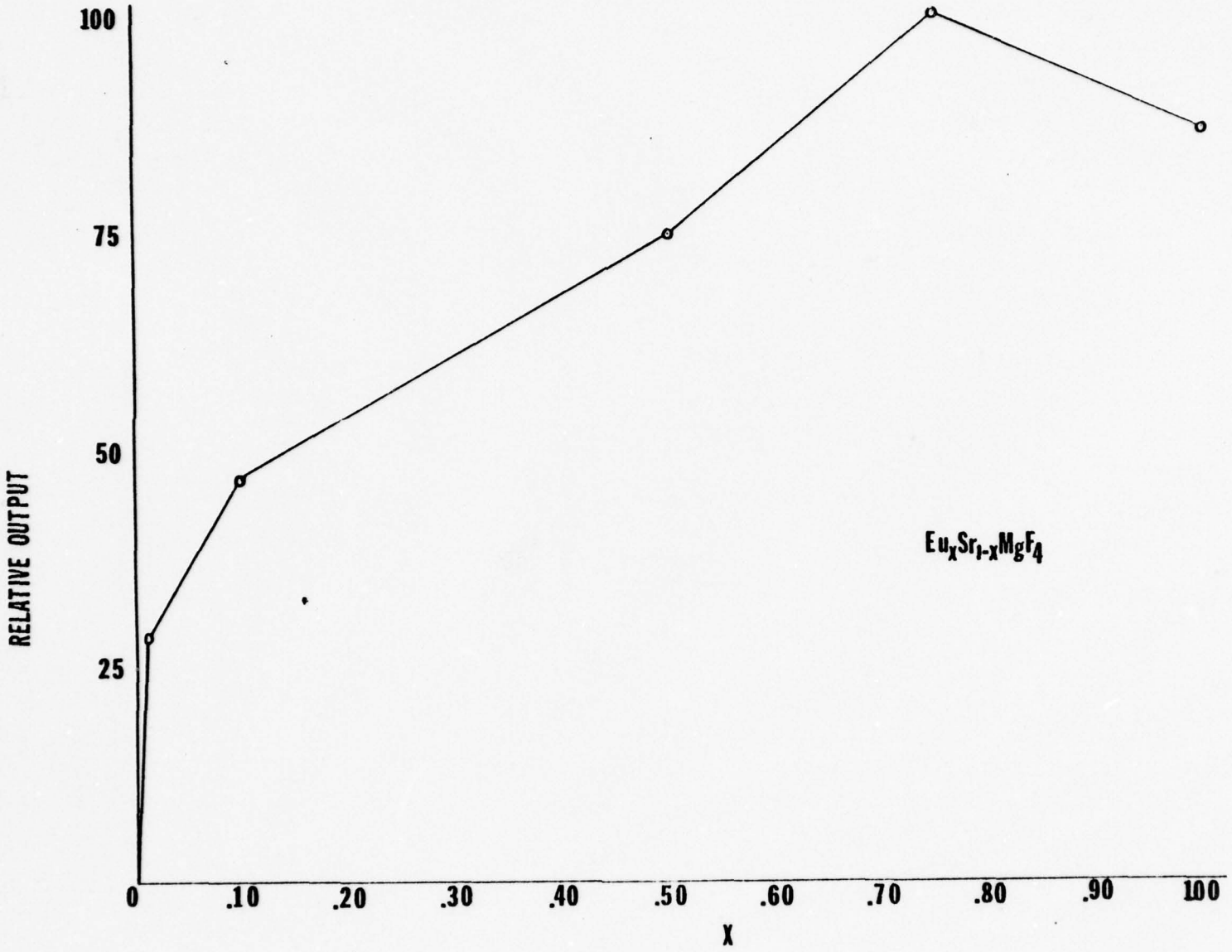


Figure 1.3

RELATIVE Eu^{2+} PEAK OUTPUT IN THE SERIES $Eu_xSr_{1-x}MgF_4$

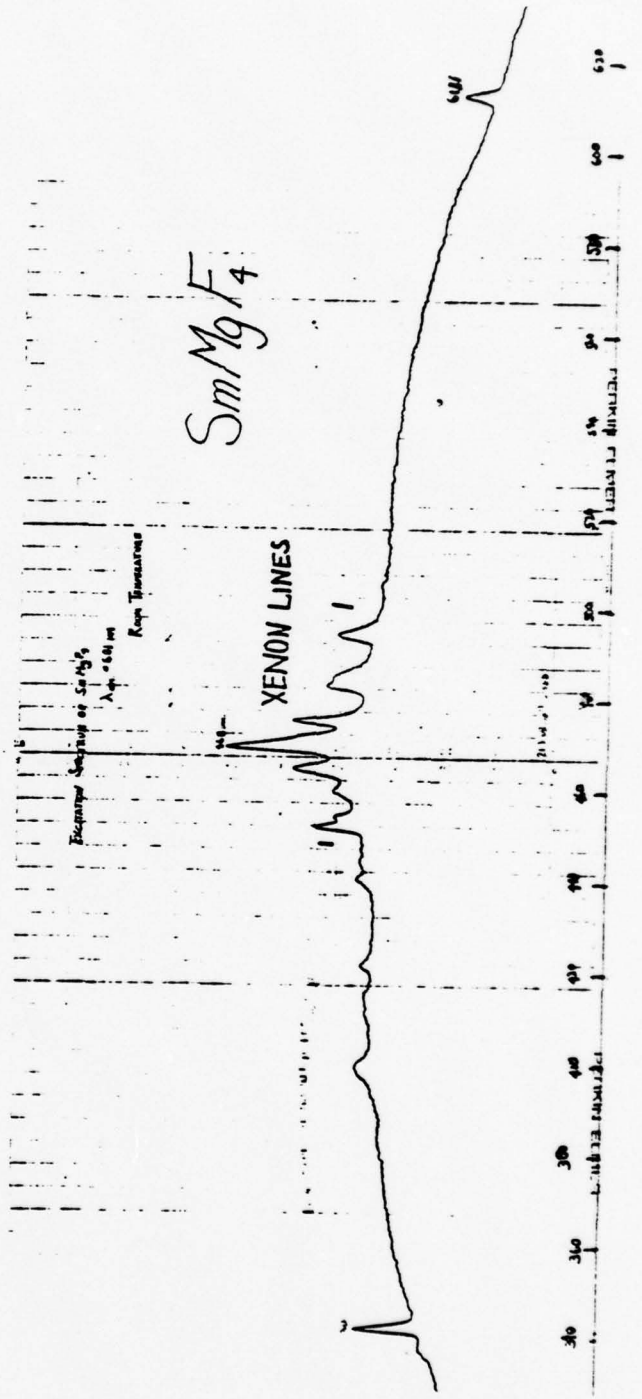


Figure 1.4

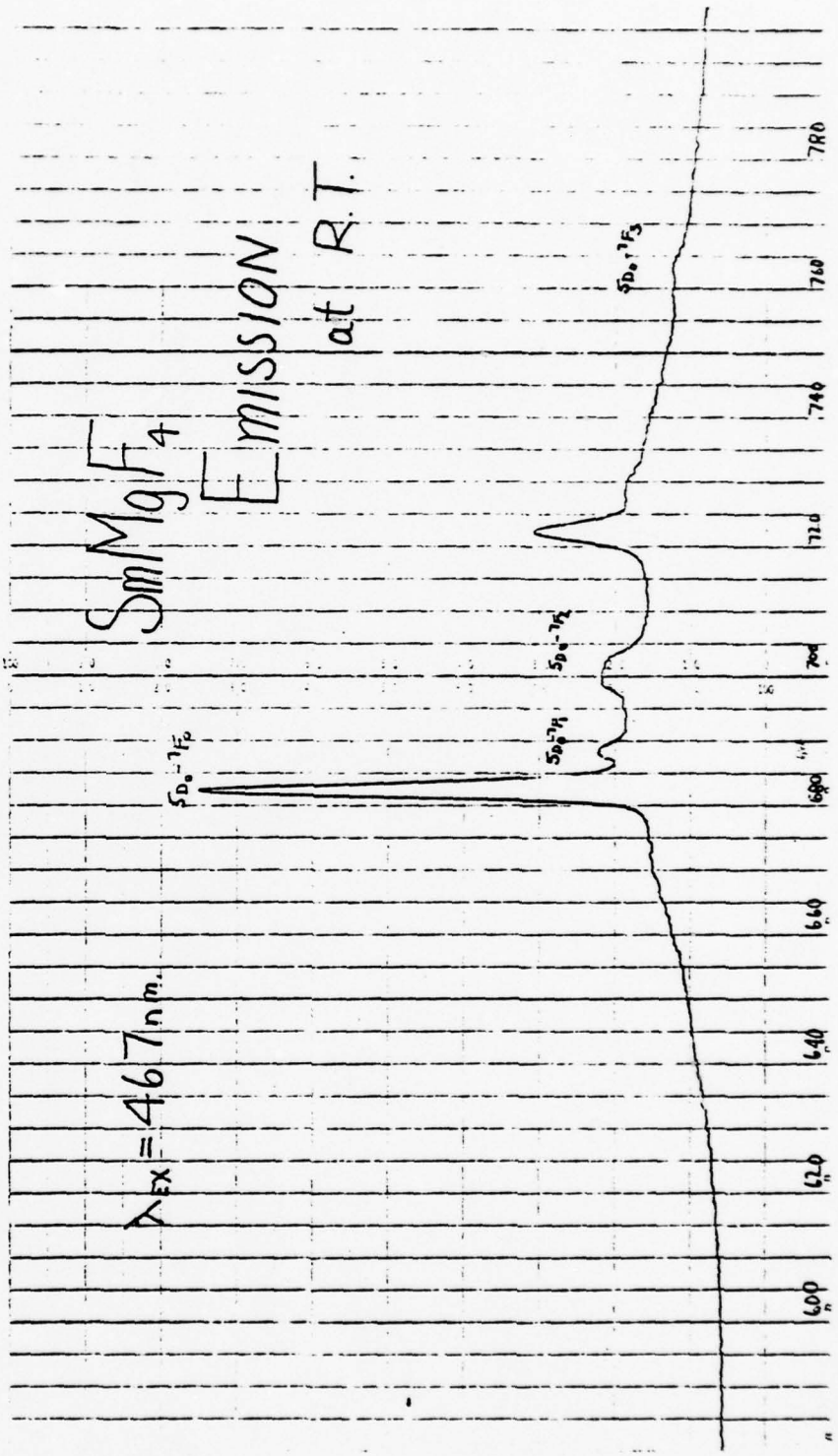

SmMgF4 Emission at R.T.
λEX = 467 nm.
5D0-7F0
5D0-7F1
5D0-7F2
5D0-7F3
600
620
640
660
680
700
720
740
760
780

Figure 1.5

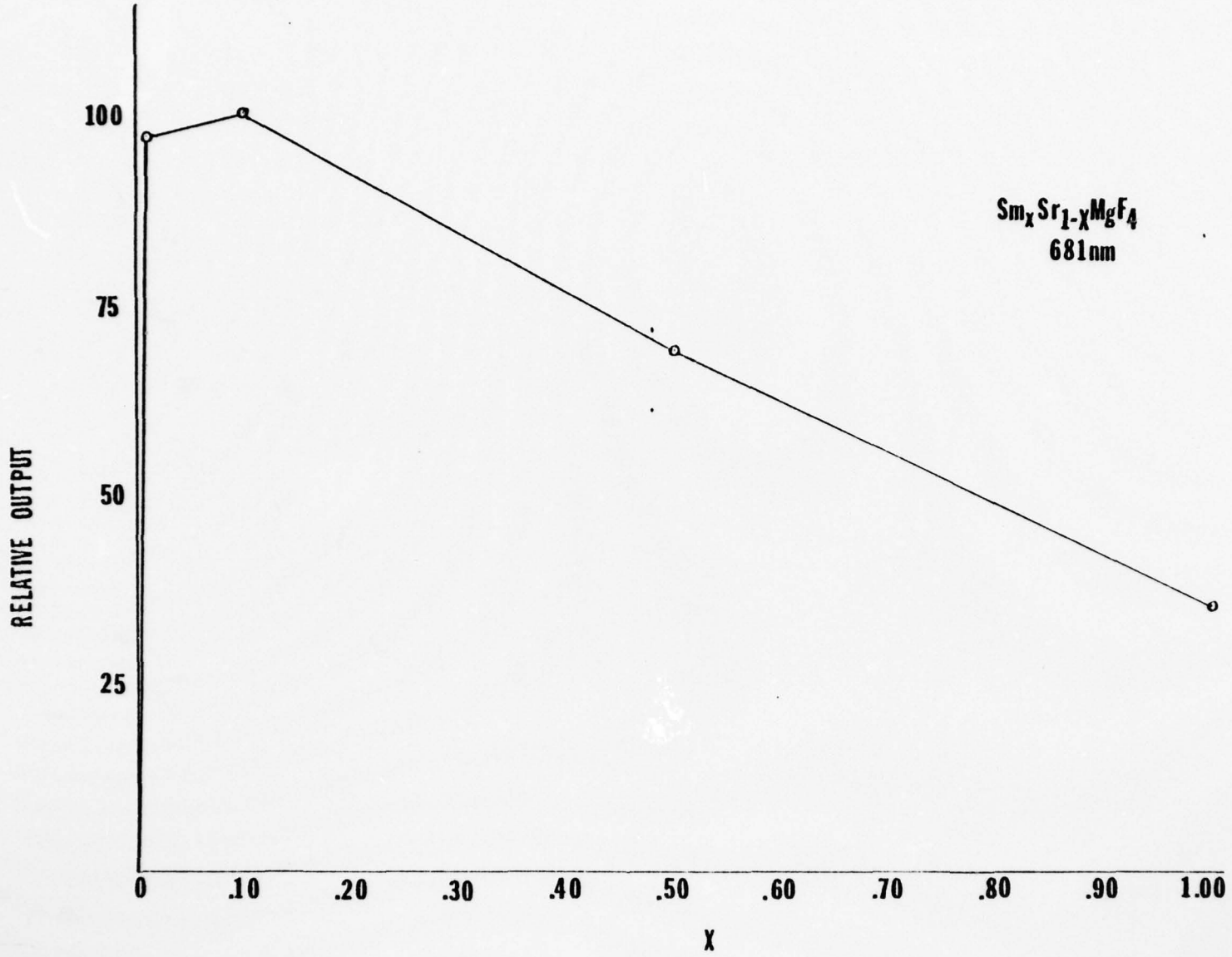


Figure 1.6

RELATIVE 681 nm PEAK OUTPUT IN THE SERIES $Sm_xSr_{1-x}MgF_4$

Figure 1.7

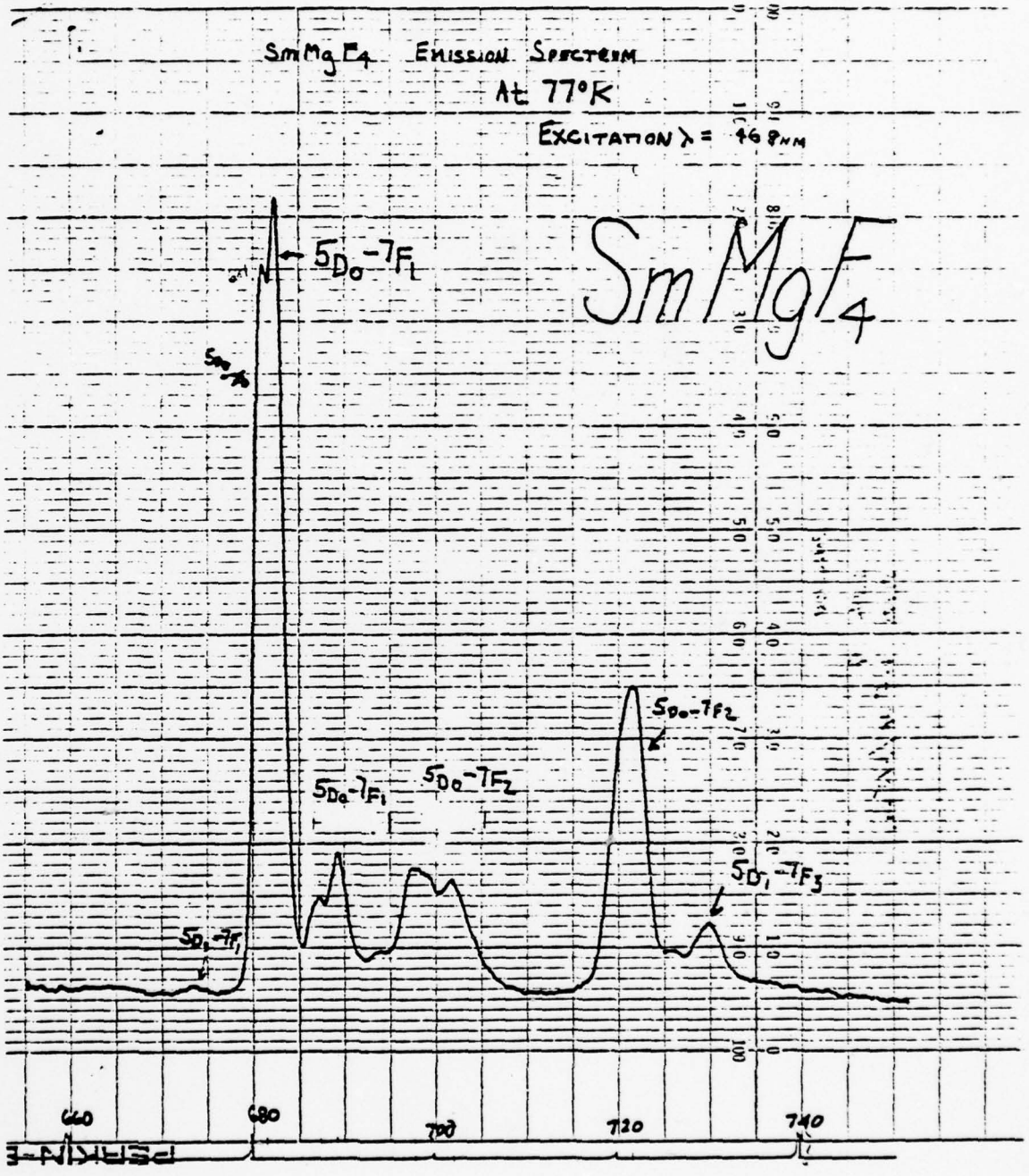

SmMgF4 Emission Spectrum
At 77°K
Excitation λ = 468 nm
SmMgF4
5D0-7F1
5D0-7F0
5D0-7F1
5D0-7F2
5D0-7F2
5D1-7F3
5D1-7F1
660
680
700
720
740

Figure 1.8

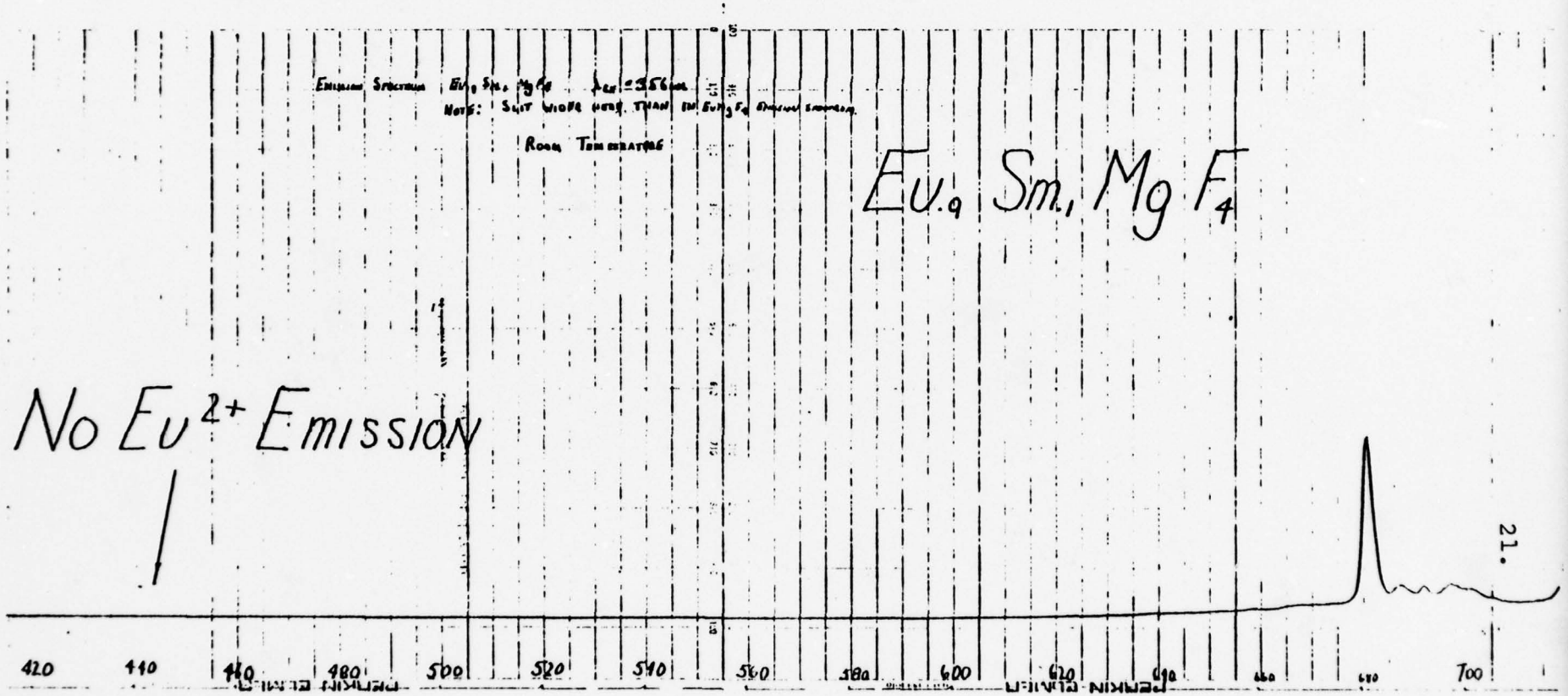

Eu.9 Sm.1 Mg F4
No Eu2+ Emission
420
440
460
480
500
520
540
560
580
600
620
640
660
680
700

Figure 1.9

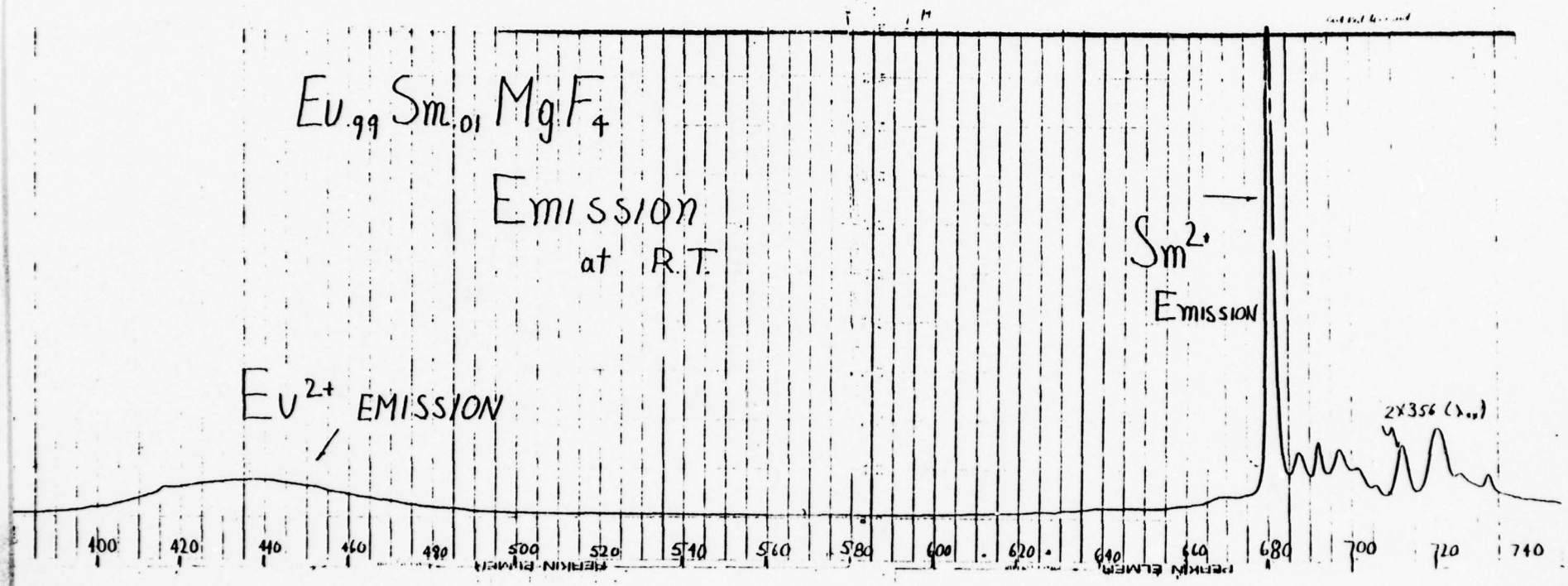

$Eu_{.99}Sm_{.01}MgF_4$
Emission
at R.T.
Sm^{2+}
Emission
Eu^{2+} EMISSION
2×356 (λ..)
400
420
440
460
480
500
520
540
560
580
600
620
640
660
680
700
720
740

Figure 1.10

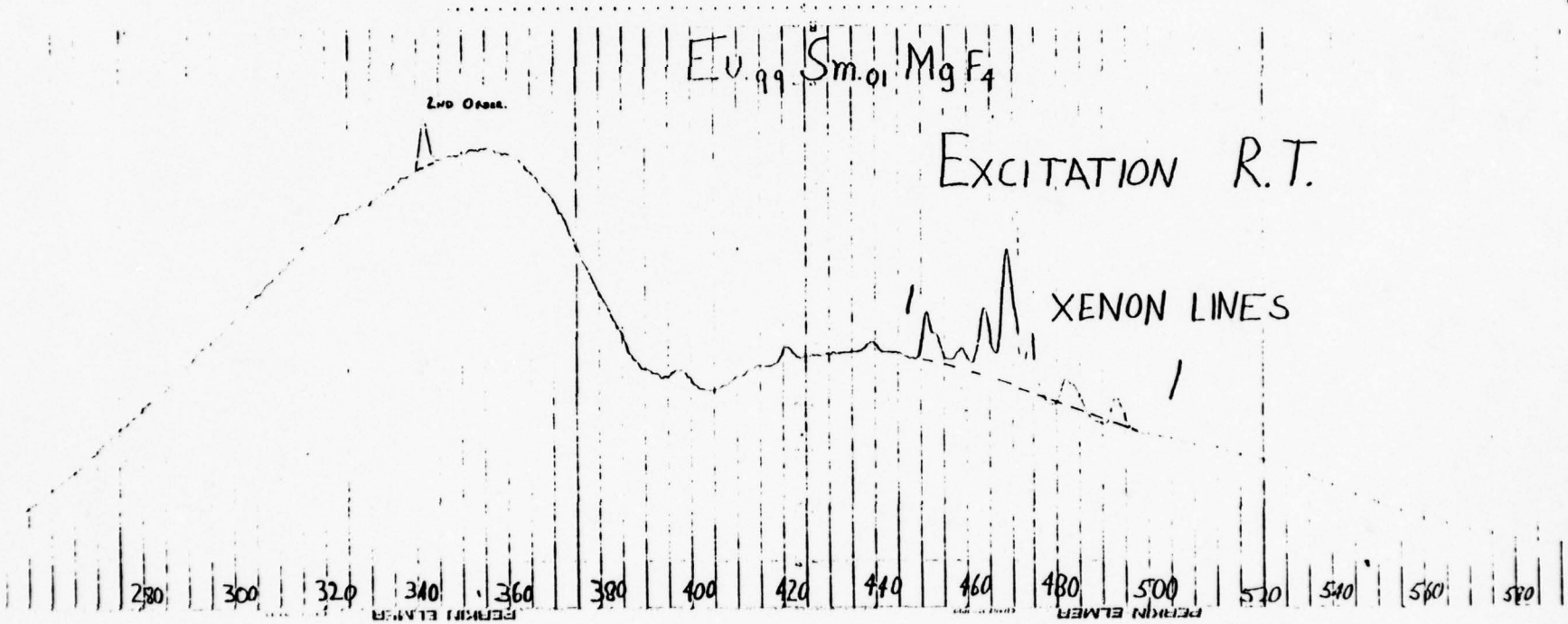
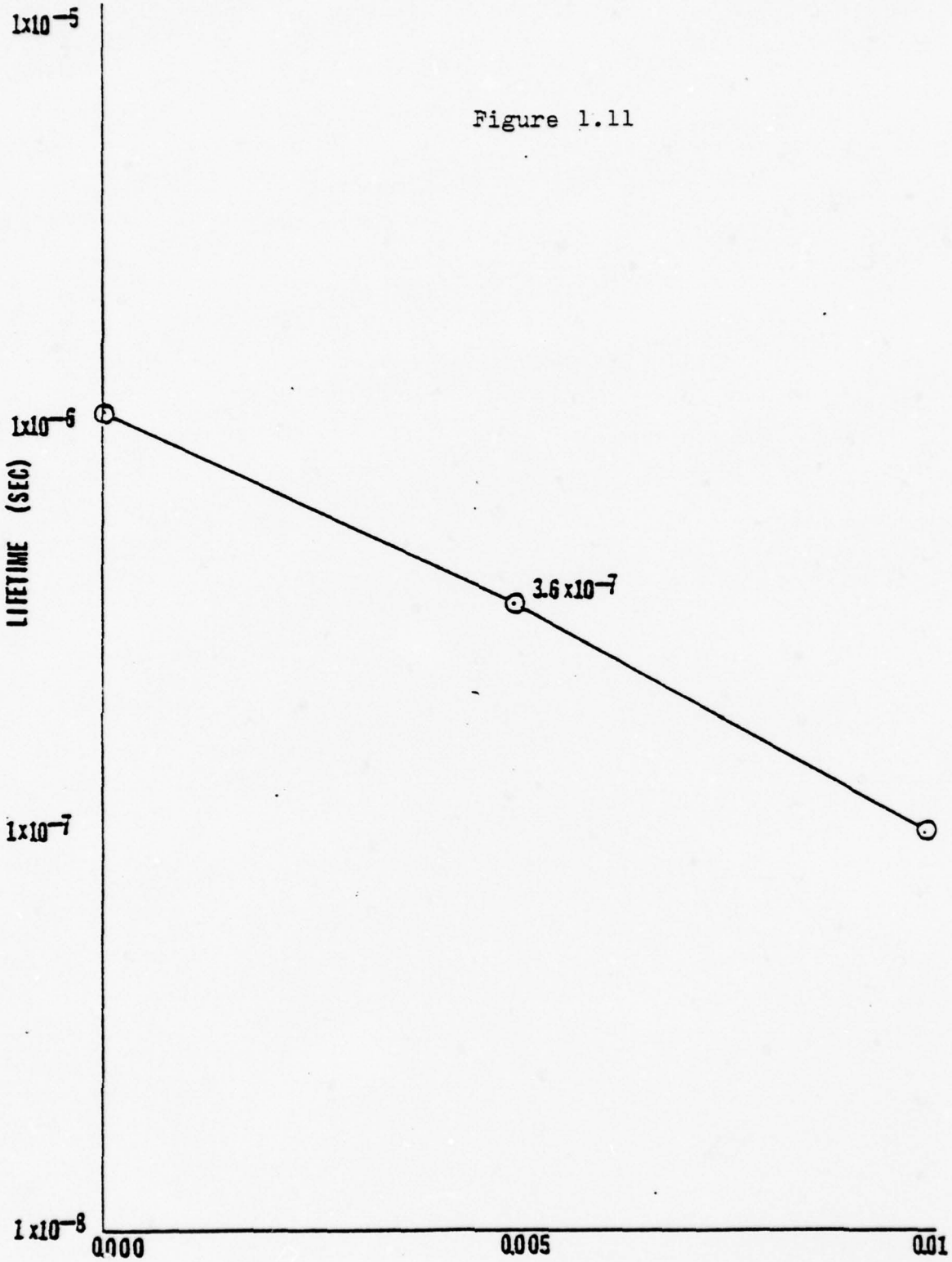

$Eu_{.99}Sm_{.01}MgF_4$
2ND ORDER.
EXCITATION R.T.
XENON LINES
280
300
320
340
360
380
400
420
440
460
480
500
520
540
560
580

Figure 1.11



LIFETIME OF 437 nm Eu^{2+} PEAK IN THE SERIES
$Sm_xEu_{1-x}MgF_4$

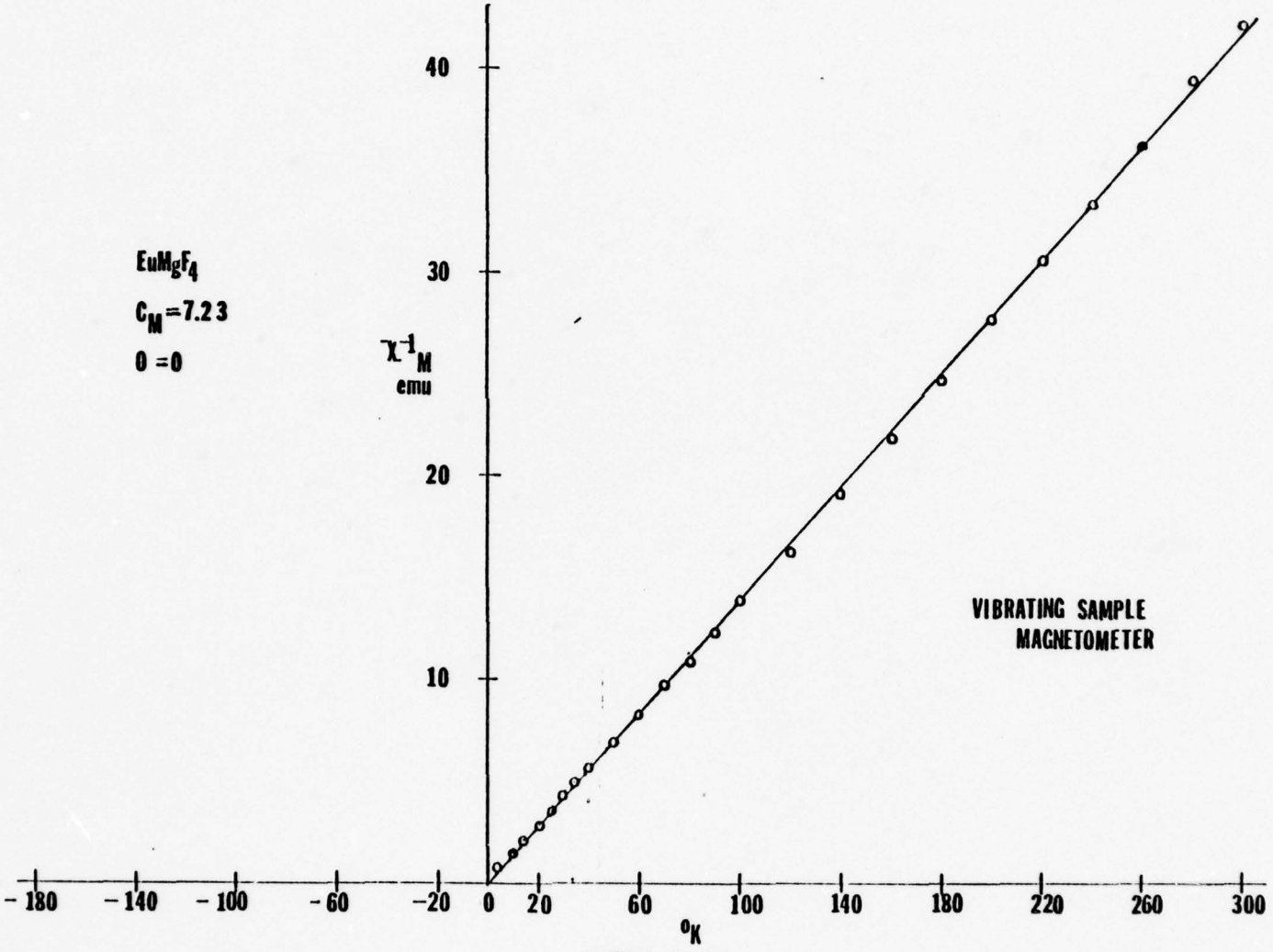


FIGURE 1.12

Plot of Reciprocal Susceptibility of $EuMgF_4$ (V.S.M.)

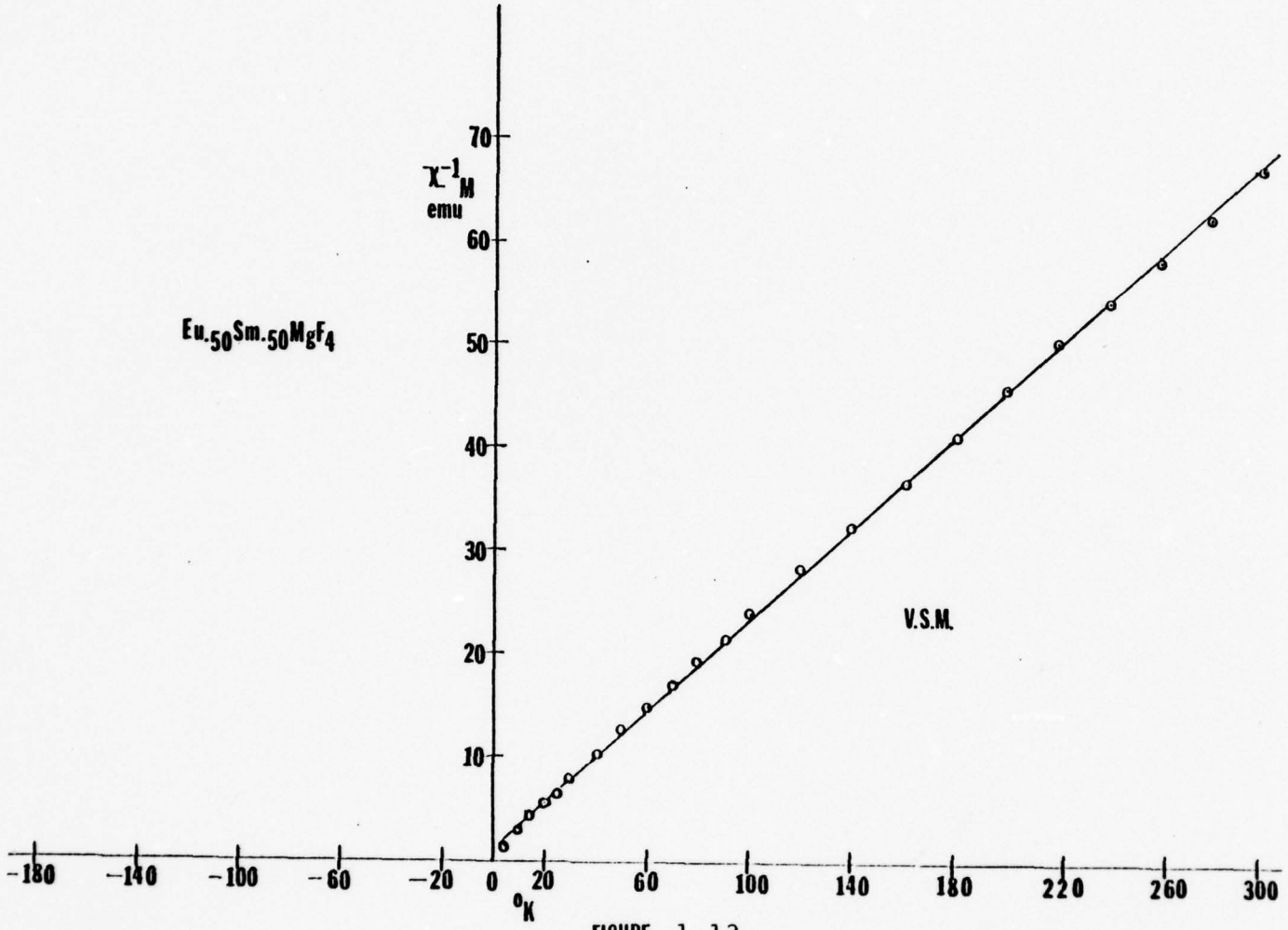


FIGURE 1.13

Plot of Reciprocal Susceptibility vs. Temperature for $Eu_{.50}Sm_{.50}MgF_4$ (V.S.M.)

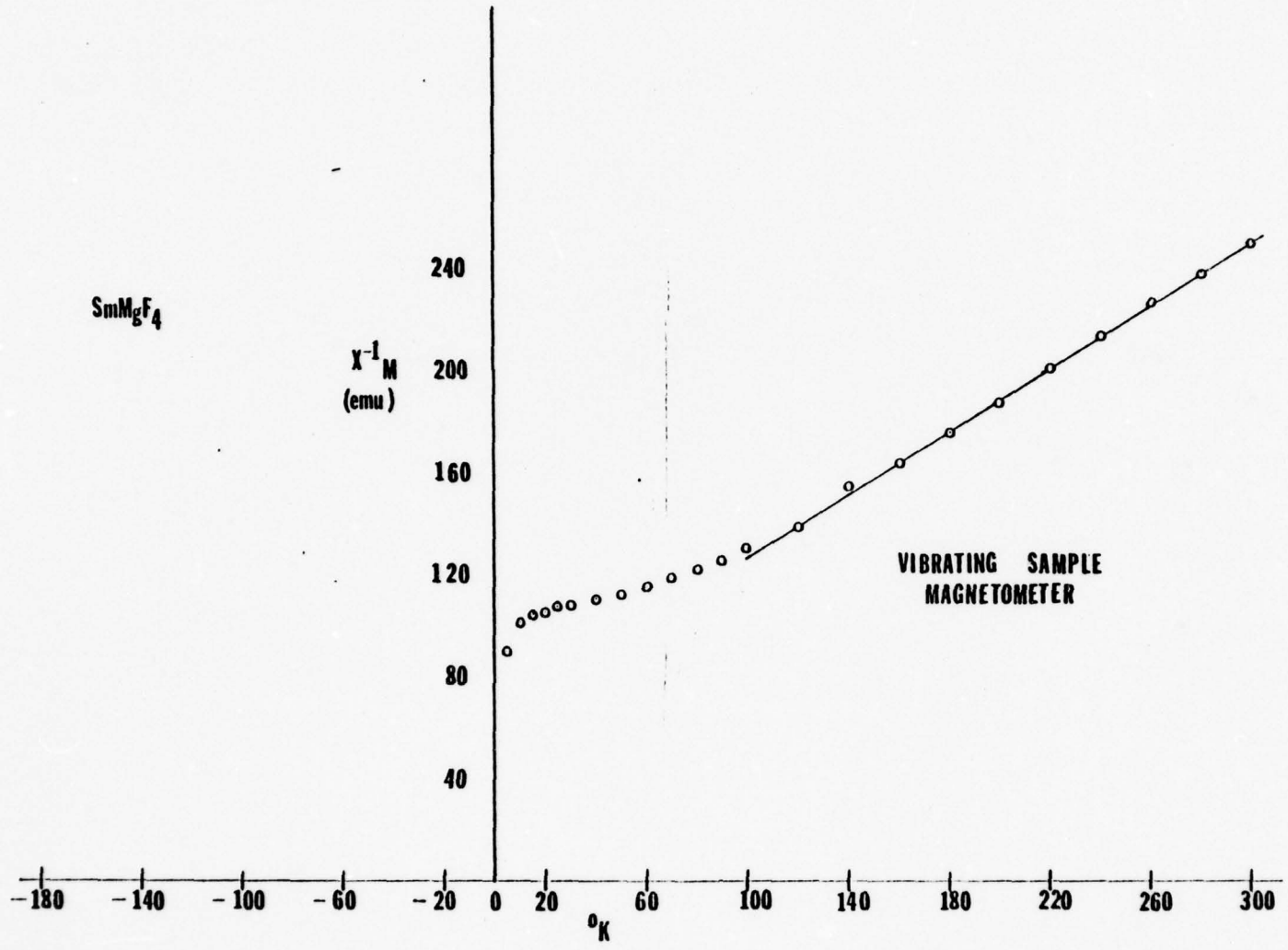
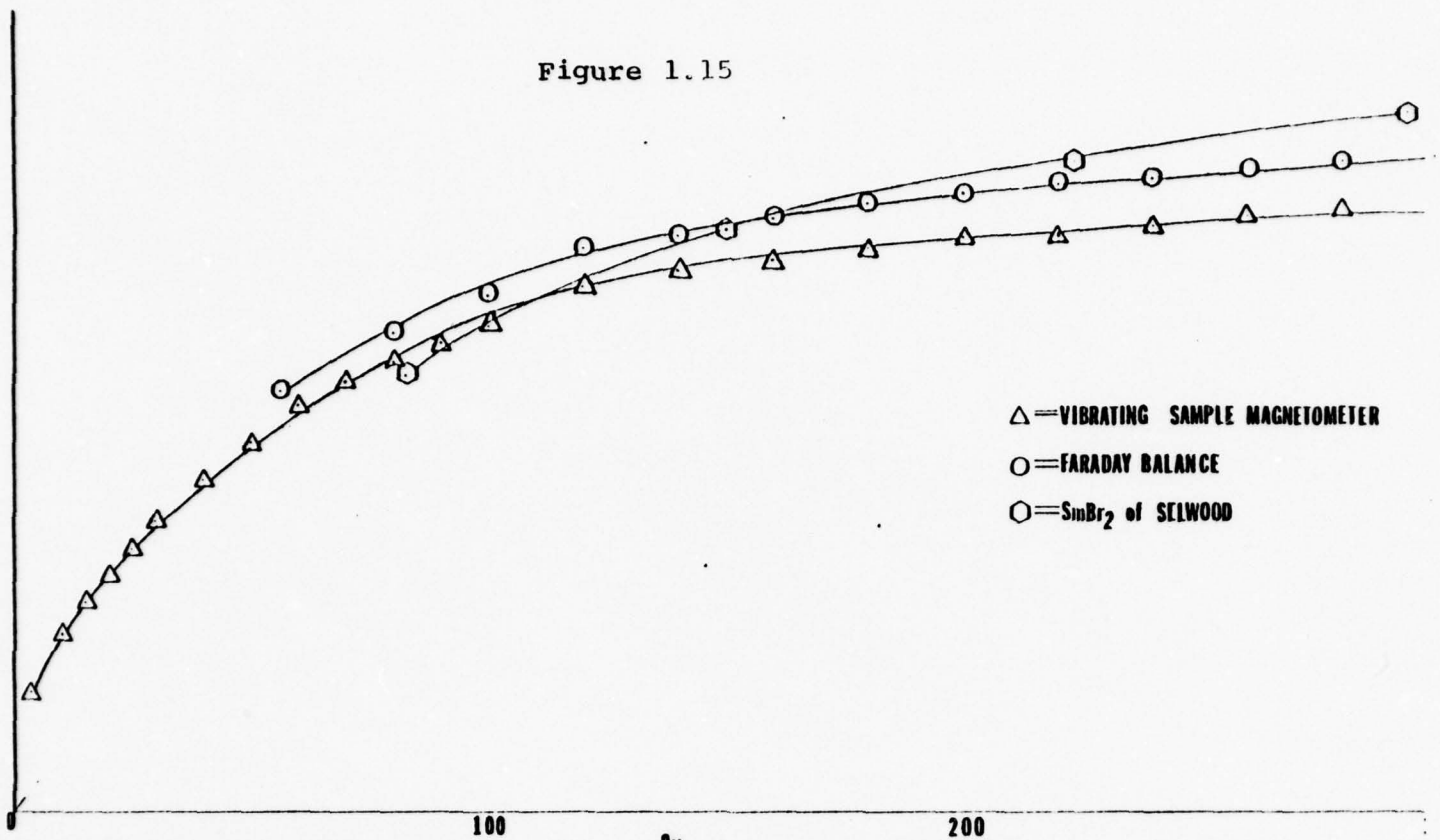


FIGURE 1.14
Plot of Reciprocal Susceptibility vs. Temperature for $SmMgF_4$ (V.S.M.)

Figure 1.15



EFFECTIVE BOHR MAGNETON NUMBER OF Sm^{2+} IN $SmMgF_4$ AND $SmBr_2$ VERSUS TEMPERATURE

II. Complex Transition Metal Fluorides

At the beginning of the present grant period, much emphasis was given to the study of the "tetragonal bronze" phase in the systems $K_xM^{II}_xM^{III}_{1-x}F_3$, where M^{II} and M^{III} are first-row transition metals. Previous studies had detected magnetic ordering in the temperature range of 135-140 K for KFe_2F_6 and $KMnFeF_6$, near the composition of x = 0.5 in the above formula. An X-ray study of a single crystal of KFe_2F_6 at room temperature had indicated that the structure was tetragonal, but anisotropic least-squares refinement yielded a discrepancy factor R = 0.07, which was too high for the precision of the experimental data. Neutron diffraction data on powder samples yielded a magnetic unit cell with a doubled "C" axis, but the magnetic structure could not be solved, using the tetragonal cell found at room temperature. The apparent existence of preferential site distributions over non-equivalent octahedral sites is one possible reason; this could also lead to ordering of Fe^{2+} and Fe^{3+} ions, with a consequent increase in unit cell parameters by some type of multiplication of the tetragonal "a" parameters. Another factor to be considered was the possibility that the crystals undergo a phase transformation below room temperature, requiring that the neutron diffraction data be analyzed in a space group of lower symmetry.

The research reported in this section (and the appendix) was largely devoted to resolving these questions. This involved the study of phase transitions below room temperature in samples in the K_xFeF_3 system, a study by Mössbauer spectroscopy of site preferences in a series of preparations near the x = 0.5 composition, single crystal X-ray studies on specimens in the K_xFeF_3 and $K_xMn_xFe_{1-x}F_3$ systems. New preparations were made in the Fe^{2+}-Cr^{3+} and Mn^{2+}-Cr^{3+} systems, for a systematic study of magnetic interactions. This project was abandoned for the time being because of the discovery of the new compounds described in Section I. The results are briefly summarized below; two papers which have been published and accepted for publication are reproduced in the Appendix.

A. Preparation of New Samples and Crystal Growth

Preparation of the series $K_xMn_xFe_{1-x}F_3$ were made, by solid state reaction in Ar-filled Pt crucibles; the tetragonal bronze phase appears to exist over the composition range $0.35 < x < 0.6$, with a continuous increase in the tetragonal lattice parameters with increasing x. In the series the a dimension increases from 12.53A at x = 0.4 to 12.70A at x = 0.6. the c dimension (undoubled) increases from 3.87A to 3.98A over the same interval. The c axis was found to be doubled in a piece of a single crystal obtained from a boule grown by

Bridgman pulling in a graphite crucible, in a melt of nominal value of x = 0.5. This led to the decision to study the crystal structure of such a crystal - see Appendix.

In the series $K_xFe_xCr_{1-x}F_3$, samples were prepared with x values from 0.25 to 0.60. The sample at x = 0.25 has the hexagonal bronze structure and the sample at x = 0.35 has an orthorhombic cell closely related to the hexagonal bronze structure. Higher values of x showed the expected tetragonal bronze structure.

Some preparations in the series $K_xLi_yFe^{II}_{x+y}Fe^{III}_{1-x}F_3$ were made, to determine if the small lithium ion could be inserted in the trigonal prism vacancies in the structure, as described by Banks and Goldstein[12] for the hexagonal potassium tungsten bronzes. Two preparations of the tetragonal phase had somewhat larger tetragonal lattice parameters than preparations with the same Fe^{2+}/Fe^{3+} ratio and potassium only. Attempts to prepare fully inserted phases were unsuccessful. A single crystal from a melt of composition $K_{0.6}Li_{0.2}FeF_3$ was found to have an orthorhombic supercell with $a' = \sqrt{2}\,a$, $b' = 2\sqrt{2}\,a$ and $c' = 2c$, where the unprimed axes pertain to the tetragonal subcell. This is the same supercell found on our single crystal of $K_{0.53}FeF_3$ (see below). Further work in this area was discontinued after the discovery of the new compounds described in Section I.

Some improvements in growth of crystals of these potassium transition metal fluorides were accomplished. Although no single-crystal boules were obtained, crystal sections of several mm dimensions were. The major improvements involved the addition of small amounts of KCl to the melt, which lowers the freezing point; the addition of NH_4F, which appears to eliminate the incorporation of oxide in the fluorides, and evacuation of the enclosure, which acts to eliminate voids in the boule due to entrapped gases.

B. Phase Transitions

The possibility mentioned above, that a structural phase transition may occur below room temperature and thus make the analysis of low temperature neutron diffraction data incorrect, was investigated by the use of a Heli-Tran low temperature X-ray diffractometer attachment. Samples of nominal composition $K_{0.5}FeF_3$, prepared at different times, were placed in the sample holder of the attachment and X-ray diffractograms were run at room temperature and at various lower temperatures down to 80 K. Silicon mixed with the powder sample was used as an internal standard. At low temperatures a new peak appeared near $2\theta = 24^{\circ}$. This peak was monitored between the lowest temperature and room temperature and the transition temperature was taken as the temperature above which the peak disappeared. The data for

these four samples are tabulated below. The room temperature lattice parameters, based on the tetragonal subecll, indicate an increase in the value of "x" in K_xFeF_3 with sample number although accurate values of x cannot be assigned. The presence of some FeF_2 lines in the patterns also indicates some variation in the x value of the nominally tetragonal phase.

Sample No.	Room Temp. Lattice Parameters		Apparent Transition Temp.
	a	c	
1	12.569 A	3.927 A	240 K
2	12.574	3.928	135 K
3	12.594	3.936	185 K
4	12.599	3.937	(above rm. temp.)

The peak near 24° was present at room temperature in sample 4, and was still present at 45°C. Since the published structure of $K_{0.6}FeF_3$ at room temperature is orthorhombic, it is tempting to suppose that this transition is to an orthorhombic and possibly non-centric structure. This would allow the transition metal ions to be displaced along the c axis in the low temperature structure and might assist in the interpretation of the magnetic neutron scattering. In the light of the structure results reported below, however, it would be wiser to determine the atomic arrangement from single crystal X-ray data at low temperature before proceeding.

C. Site Preferences of Bivalent Ions in $K_xM^{II}_xM^{III}_{1-x}F_3$

On the basis of earlier work on $K_{0.5}FeF_3$, we had suggested that the line broadening of the Fe^{2+} spectrum, relative to that of the Fe^{3+} spectrum, indicated that the Fe^{2+} ions have a preference for the (2c) sites in P4/mbm over the (8_j) sites, the broadening being due to the presence of Fe^{2+} ions in both sites. This was further investigated by a detailed Mössbauer study of the competition between Fe^{2+} and other bivalent ions in a variety of materials with substitution of Zn^{2+}, Mn^{2+}, Mg^{2+} for Fe^{2+}. This study has been published. (Banks, Torre, DeLuca, J. Solid State Chem., 22, 95-100(1977)). A copy of this paper will be found in the Appendix. The results show that the trivalent ions are located on the (8_j) sites exclusively and the divalent ions are distributed over the (2c) and (8_j) sites. The area ratios also suggest that Fe^{2+} ions show some preference for the (2c) sites when Mn^{2+} and Mg^{2+} are in competition. Much more work would be needed to correlate this with size and electronic factors.

D. Structural Studies

Precession photographs of two single crystals, nominally $K_{0.5}FeF_3$ and $KMn_{0.5}Fe_{0.5}FeF_3$, taken with long exposures, both showed superstructure spots. The iron compound had a unit cell with $a' = \sqrt{2}a$, $b' = 2\sqrt{2}a$ and $c' = 2c$. Previous refinement of the subcell in P4/mbm had yielded an

R factor of 0.07 with anisotropic thermal parameters, but the results were never published because the data were of such quality as to require an R value of the order of 0.02. The discovery of this orthorhombic supercell could improve the refinement, but this has not been done as yet. In the Mn-Fe crystal, the superstructure has c' = 2c, with the a parameters the same as the subcell. X-ray intensity data were collected at Brookhaven National Laboratory and the structure was refined in space group $P4_2bc$ (non-centrosymmetric). The results, given completely in the Appendix, indicate that three types of transition metal ion sites are present, one of which is mainly occupied by Mn^{2+}, another mainly by Fe^{3+}, and the third by a mixture of the two ions.

III. Upconversion and NMR Studies of CdF_2:Rare Earth

The work on upconverting $CdF_2:Yb^{3+},Er^{3+}$ crystals was completed. The maximum upconversion efficiency was found at a composition of about 86 CdF_2, 3 CaF_2, 10 YbF_3, 1 ErF_3. The quantum efficiency was about 0.7%, compared to about 0.1% for YF_3 and $BaYF_5$ doped with the same impurities. This work has been published (Greenblatt and Banks, J. Electrochem. Soc., 124, 409(1977) and a copy of that paper appears in the Appendix.

The Final Report on Grant DA-ARO-D-31-124-72-G7 described work on ^{19}F NMR which showed the existence of "dimers" of $(Re\text{-}F_i)_2$ in Er^{3+} and Yb^{3+} doped CdF_2, and a pre-print of a submitted paper was included in the Appendix. This report briefly discusses that result in the context of the infrared-visible conversion and the possibility that more complex structures may be involved instead of isolated dimers. The simplest interpretation of the observed (100) resonance is of "dimers" consisting of rare-earth-interstitial ion pairs in a square array in (100) planes of the fluorite structure. Other possibilities would be zigzag chains of rare earth-interstitial ions along (110) directions or helical arrays along (100) directions. These resonances show the dipolar shifts to be expected from the field due to a pair of rare earth ions at 90° to each interstitial fluoride, the shift

being proportional to the magnetic moment of the rare earth. The details are contained in the paper by Mustafa, et al. in J. Chem. Phys., 62, 2700(1975), which is included in the Appendix for reference.

Recent work on CdF_2 crystals doped with equal concentrations of Er^{3+} and Yb^{3+} has revealed a new resonance at fields intermediate between those due to the $(Er\text{-}F_i)_2$ and $(Yb\text{-}F_i)_2$ "dimers". The concentration of these mixed pairs $(Er\text{-}F_i)$ $(Yb\text{-}F_i)$ appears, from the intensity of the NMR signal, to be significantly higher than that to be expected on the basis of statistical distribution. This suggests that the postulated existence of such mixed pairs may explain the high upconversion efficiency of the crystals.

IV. Synthesis of Potential Solid Electrolytes

Solid electrolytes have become important in the development of rechargeable batteries of high energy density for applications to electric vehicles and utility load-leveling. The most advanced systems of this sort use a sodium-ion conductor based on $NaAl_{11}O_{17}$ (β-alumina) which has two-dimensional ion conduction pathways and is inherently a poorer electrolyte than a material which might have three-dimensional connections among the cation sites, which would be partially occupied to permit free movement of ions from one site to the other.

We have attempted to introduce alkali metal ions into the large interstices in cubic ZrP_2O_7 in the hope that these ions would be mobile. The large interstices can accommodate ions of radius up to about 1.2 A, and they are connected three-dimensionally. The first preparations were made using Y^{3+} as the charge-compensating species. This resulted in appreciable solid solution formation only in the case of lithium. Preparations of composition $Zr_{1-x}Y_xLi_xP_2O_7$ showed a cubic phase for values of x up to 0.1. Higher doping levels showed no further increase in lattice parameter and the appearance of a second phase pattern in X-ray diffractograms. No solid solution was observed for combinations of yttrium-sodium, gallium-sodium and gallium-lithium. A sample of

$Zr_{0.9}Y_{0.1}Li_{0.1}P_2O_7$ was submitted for ^7Li NMR to determine whether the lithium ions are mobile at temperatures up to 200°C. This experiment did not detect the ^7Li resonance, because of too little sample. Larger samples have not been prepared yet, because of our apparent success in obtaining a higher Li concentration using In^{3+} as the charge-compensating species (see below). The lattice parameters, measured for high angle diffraction peaks, for $Zr_{1-x}Li_xY_xP_2O_7$, are as follows:

x =	0.00	0.025	0.050	0.075	0.100
a_o(A) =	8.246	8.246	8.253	8.251	8.260

On the basis of ionic radius considerations, it was thought that these preparations might have lithium on normal Zr sites and yttrium in the large interstices. The X-ray intensities which are about the same for pure ZrP_2O_7 and the solid solution, discourage such an interpretation. With Y in the Zr sites, the 10% filling of the interstices by lithium would lead to a maximum of 2% change in intensity for the most sensitive reflections, whereas the distribution suggested above would give easily observable intensity changes.

Trivalent indium has a radius much closer to Zr^{4+} than does Y^{3+}. Similar preparations were made with this ion, and also with Eu^{3+}, as described below. The photoluminescence of Eu^{3+} can be used as a probe of the Eu environment, as shown by Hoefdrad, et al.[13].

Attempts were made to synthesize $Zr_{1-x}M^{I}_{x}M^{III}_{x}P_2O_7$, where M^{III} is In^{3+} or Eu^{3+} and M^{I} is Li^{+} or Na^{+}. Most of these were prepared by solid state reaction of mixtures of the constituent oxides, alkali carbonates and $NH_4H_2PO_4$, although some were made using precipitated $ZrO(H_2PO_4)_2 \cdot nH_2O$, which was the main technique used in the preparations described above for the Li-Y series. Single cubic phase products were obtained with the Li-In combination for x values up to 0.2, about twice the concentration found when Y^{3+} is the charge compensator. The lattice parameter decreases with increasing x, as would be expected from the smaller ionic radii of both Li^{+} and In^{3+} compared to that of Zr^{4+}. In the Li-Eu series, new X-ray peaks were observed at the lowest concentration attempted, but there appeared to be an expansion of the lattice. We have recently learned that GeP_2O_7 has a true unit cell, a = 22.854 A, triple the cell which we have been describing[14]. If this is also present in ZrP_2O_7, some of the extra lines in the Li-Eu solid solution may be extended. This is now being pursued. The samples containing Eu^{3+} display a bright orange fluorescence under long wavelength ultraviolet and fluorescence measurements will be made at the earliest opportunity. The position of the charge-transfer excitation band of the Eu^{3+} will provide a valuable clue as to the location of the trivalent ions in these solid solutions.

Because of the negative results of attempts to introduce sodium, an attempt was made to use $Na_4P_2O_7$ as a flux for single crystal growth. Single crystals of these materials would be valuable for future measurements. Heating an equimolar mixture of $Na_4P_2O_7$ and ZrP_2O_7 produced a single phase X-ray pattern corresponding to α-$Na_2Zr_2(PO_4)_3$, a material originally synthesized by H.Y-P. Hong as a possible solid electrolyte[15]. When excess $NH_4H_2PO_4$ (4 to 8 moles) was used, a cubic ZrP_2O_7 phase and an amorphous phase were formed. We have not yet determined whether any Na^+ is present in the ZrP_2O_7. If there is, it is possible that the sodium is present both on the Zr sites and in the interstitial positions.

V. Eu Mössbauer Study of Eu_xMoO_4

The previous final report included a report on rare-earth molybdate(V) compounds, with a description of the solid solution series Eu_xMoO_4 which postulated a cation vacancy model for the series ($0.67 \leq x \leq 1.00$) where the MoO_4 (VI) groups remain with molybdenum in the 6+ state and the introduction of Eu^{3+} is compensated by cation vacancies. A ^{151}Eu Mössbauer study, carried out at Professor N.N. Greenwood's laboratory on samples prepared here, has confirmed the vacancy model. The paper has been published in Inorganic Chemistry 15, 2317(1976) and a copy is reproduced in the Appendix.

VI. Phase Transition and ESR of Cr(V) in Fluorapatite

In our 1971 ESR study of CrO_4^{3-} in chlorapatite[16], we observed three crystallographically and magnetically inequivalent sites, in keeping with the monoclinic ($P2_1/b$) symmetry. In that paper we reported a similar splitting in fluorapatite, $Ca_5(PO_4)_3F$ which could not be analyzed at that time. However, we suggested that fluorapatite, which is hexagonal at room temperature, might undergo a phase transition on cooling. This cannot be directly observed by ESR of CrO_4^{3-}, because the Cr(V) resonance is not observable above liquid nitrogen temperature.

We report here some evidence of a phase transition in the neighborhood of 140 K, based on X-ray data and differential thermal analysis at low temperatures, and the results of a new ESR study of CrO_4^{3-} in fluorapatite which indicates that a lower symmetry structure exists at 4.2 K.

A. X-ray Data

A powdered sample of $Ca_5(PO_4)_3F$ was loaded into the low-temperature diffractometer and diffractograms were run at temperatures down to 20 K. The low temperature patterns showed extra lines, which could be indexed on the basis of a monoclinic unit cell with a' = a, b' = 2a, c' = c, the unprimed parameters being those of the original hexagonal cell; the non-standard labeling of the monoclinic axes is used to

emphasize the relation to the hexagonal cell. This cell is similar to the monoclinic cell of chlorapatite at room temperature. The extra reflections persisted up to well above liquid nitrogen temperature, recalling an earlier claim[17], based on dielectric constant measurements, that a phase transition occurs at about 140 K. DTA measurements with a liquid nitrogen cooled cell had indicated some thermal effect, but no sharp transition was observed.

A slice from a large cylindrical boule of fluorapatite, doped with 0.1% Mn, was cut perpendicular to the c axis and mounted on the sample holder of the low-temperature powder diffractometer. This permitted scanning of the (00ℓ) zone. The accepted space group of hexagonal fluorapatite is $P6_3/m$, which permits only even 00ℓ reflections. At room temperature these were the only ones observed. When the crystal was held overnight at liquid nitrogen temperature before recording the X-ray pattern, two new peaks appeared, which could be indexed as 001 and 003. The appearance of these peaks indicates that the screw axis is absent in the low temperature structure.

An attempt to observe the transition temperature by observing the disappearance of the odd order peaks during warming to room temperature failed because they persisted after the crystal returned to room temperature. However,

they disappeared after the crystal was held at room temperature overnight. This indicates that the transition is very sluggish indeed. Attempts to approach the transition from above indicated that no transition is found when the crystal is held at 133 K (-140°C) and that it is detected when it is held at 123 K (-150°C). This extreme thermal hysteresis is probably the reason that so many attempts to observe this transition have had negative results; most low temperature measurements are started as soon as the sample temperature has reached the desired value. The twenty-four hours required by our single crystal is an extreme case, the sample being about 1 mm thick and 1 cm in diameter. The DTA result below indicates that four hours is a sufficient time for a powder of the same composition.

A single crystal of fluorapatite doped with about 5% CrO_4^{3-} showed a monoclinic unit cell at room temperature. Time did not permit a structure analysis. This monoclinic structure may be an effect of the presence of high concentrations of the highly distorted CrO_4^{2-} ion, but it is not seen in crystals with lower concentrations and can certainly not account for the splitting described in the ESR study.

B. Differential Thermal Analysis

A sample of powdered fluorapatite containing about 0.1% CrO_4^{3-} was provided to Mr. John Elder, manager of the applications laboratory of the Mettler Corporation. DTA runs were made at a heating rate of 2°C/min. on the Mettler TA 2000 B Quantitative DTA System between -160°C and -100°C (113-153 K). The results (Figure 6-1),show that a transition is detected, when the sample was held at -160°C for four hours prior to running the heating curve, while it was not observed when the heating program was begun immediately after cooling. The extreme baseline drift is characteristic of the instrument operating at the extreme range of its sensitivity. This was confirmed with a sample of α-alumina which was the material used in the reference cell.

The small endotherm in the range -141 to -136°C appears to be the result of the transition expected in this range. The thermal effect is quite small, as would be expected for a second-order phase transition. Presumably there is some thermal hysteresis still present, so the true transition temperature would be somewhat lower, perhaps about 130 K.

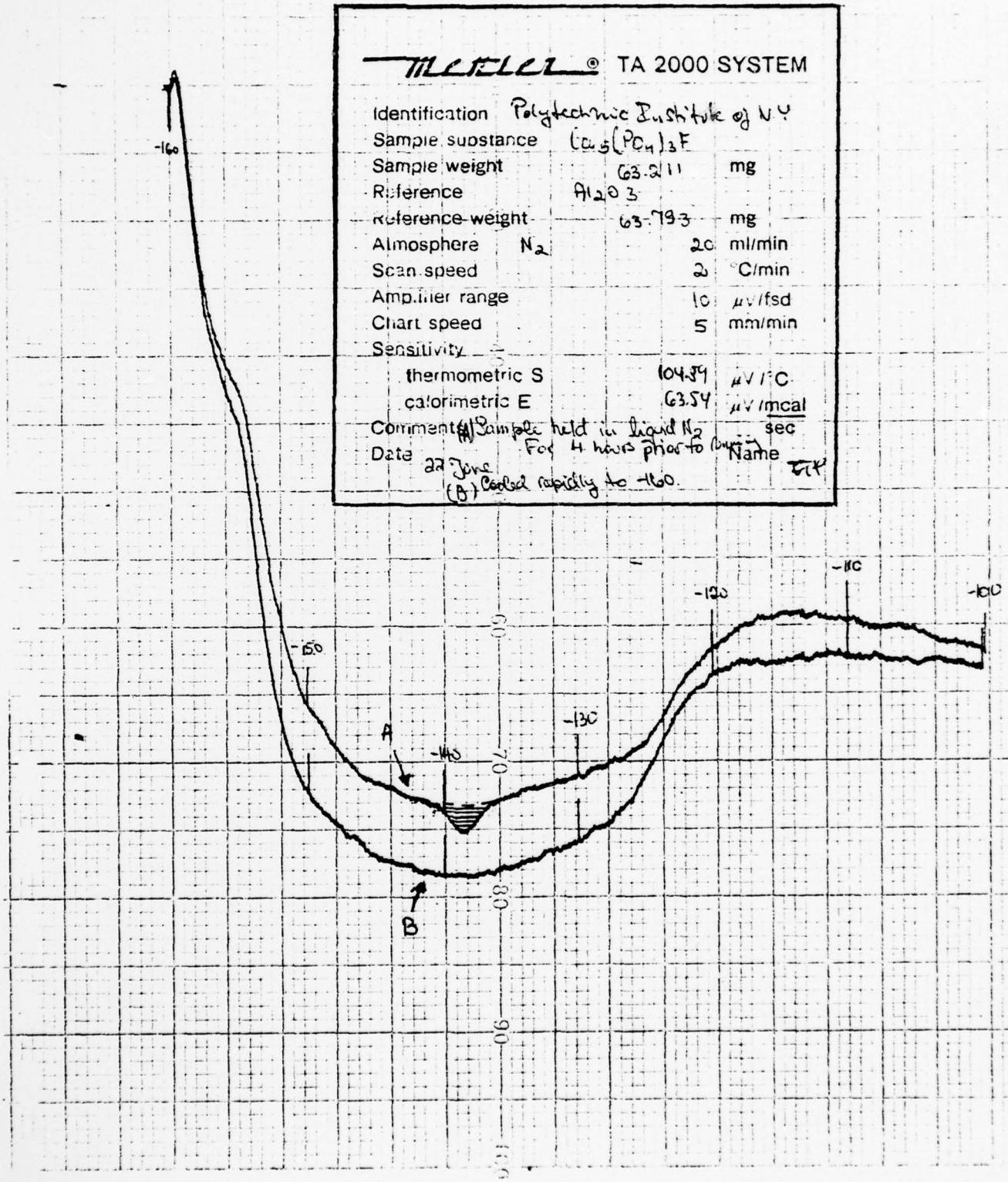
C. Reinvestigation of ESR of CrO_4^{3-} in Fluorapatite

If the X-ray evidence for the loss of the screw axis and for a monoclinic cell in the low temperature form of

fluorapatite are combined, the possible space groups are P2 and P2/b. The reinvestigation of the electron spin resonance of CrO_4^{3-} in fluorapatite indicates the presence of three crystallographically inequivalent PO_4^{3-} sites, consistent with monoclinic symmetry in a doubled unit cell of the type mentioned above. The data show a slight tendency for splitting of the three peaks, which would favor the choice of the non-centrosymmetric space group P2. However, such splitting could also be an effect of slight misorientation of the crystal. A test for second harmonic generation at low temperature showed a negative result, but the sample was not held at temperature for more than half an hour. This experiment should be repeated under the conditions described above.

A paper on the ESR study has been published (Greenblatt, Pifer and Banks, J. Chem. Phys., 66, 559(1977)) and a copy is reproduced in the Appendix.

Fig. 6-1


METTLER TA 2000 SYSTEM
Identification Polytechnic Institute of N.Y.
Sample substance $Ca_5(PO_4)_3F$
Sample weight 63.211 mg
Reference Al_2O_3
Reference weight 63.793 mg
Almosphere N_2 20 ml/min
Scan speed 2 C/min
Amplifier range 10 μV/fsd
Chart speed 5 mm/min
Sensitivity
thermometric S 104.54 μV/°C
calorimetric E 63.54 μV/mcal
Comments (A) Sample held in liquid N_2 sec
For 4 hours prior to Run
Date 22 June Name
(B) Cooled rapidly to -160.
-160
-150
-140
-130
-120
-110
-100
A
B

VII. Possible Linear Conductors Based on (VO) Phthalocyanine

There has been much recent interest in linear metallic conductors because of the possibility that they may provide a basis for superconductors with high Tc. Most of those involving transition metals are complexes of platinum in mixed valence states, and appear to owe their one-dimensional conductivity to the overlap of partially occupied d orbitals of the metal.

We have attempted to prepare similar materials by the partial oxidation of the vanadyl (VO^{2+}) ion in vanadyl phthalocyanine. If this could be done, the overlapping vanadium 3d orbitals would be connected through the 2p orbital of an intervening oxygen ion, and the behavior might be that expected of a one-dimensional analog of the tungsten and vanadium bronzes.

Two synthetic approaches were tried - the electrolysis of solutions of (VO) phthalocyanine in concentrated H_2SO_4 and the sealed tube oxidation of the phthalocyanine complex with I_2 and Br_2. Both yielded new phases as detected by powder X-ray diffraction. The optical properties of the products (transparency) suggested that they are insulators at room temperature.

Electrolysis of vanadyl phthalocyanine in concentrated sulfuric acid yielded small brown crystals, up to 0.1 mm in length. Vanadyl phthalocyanine when recrystallized from concentrated H_2SO_4, has a bright blue color. The X-ray pattern of the brown crystals showed a few strong sharp peaks with d-spacings of 3.27 and 2.01 A. This is quite different from the parent compound which has a very complex powder pattern. Most of the brown crystals were on the bottom of the vessel, but a few were found on the cathode, suggesting that they might be reduced to V^{3+}. Not enough product was obtained for magnetic susceptibility measurements or other means of determining the oxidation state.

Attempts to prepare partially oxidized materials by chemical vapor transport by I_2 led to the transport of some dark material whose X-ray pattern was somewhat different from that of the parent compound, and colorless crystals which were water-soluble, or reactive with water. X-ray data indicated a cubic lattice, either face-centered with A = 8.08 A or body-centered with a = 5.73 A. This product is probably the result of decomposition of the organic matter.

Work on this project was discontinued because of the approaching termination of the grant. It is evident that much more work would be required to understand these results and to study this problem in more detail.

References

(1) Final Report on Grant No. DA-ARO-D-31-124-72-G7, DA Project No. 20061102 B13B, dated March 26, 1975.

(2) Grant No. DAAG-29-78-G-0150.

(3) E.T. Keve, S.C. Abrahams and J.L. Bernstein, J. Chem. Phys., 51, 4928(1969).

(4) J.G. Bergman and G.R. Crane, J. Appl. Phys., 46, 4645(1975).

(5) Z.A. Mateiko and G.A. Bukhalova, Zhur. Neorg. Khim. 7, 165(1962); Russ. J. Inorg. Chem. (English Translation), 7, 84(1962).

(6) H.P. Weber, T.C. Damen, H.G. Danielmeyer and B.C. Tofield, Appl. Phys. Letts., 22, 534(1975).

(7) H.P. Weber, Optics and Quantum Electronics, 7, 431(1975).

(8) H.G. Danielmeyer, "Stoichiometric Laser Materials" in Festkörperprobleme XV Advances in Solid State Physics, Pergamon, N.Y. 1975, pp. 253-77.

(9) T. Yamada, K. Otsuka and J. Nakano, J. Appl. Phys., 45, 5096(1974).

(10) K. Otsuka, T. Yamada, M. Saruwatari and T. Kimura, IEEE J. Quantum Electronics QE-11, 330(1975).

(11) P.W. Selwood, J. Am. Chem. Soc., 55, 4689(1933); ibid. 56, 2392(1934).

(12) E. Banks and A. Goldstein, Inorg. Chem., 7, 466(1968).

(13) H.E. Hoefdrad, F.M.A. Stegers and G. Blasse, Chem. Phys., Letts., 32, 216(1975).

(14) H. Völlenkele, A. Wittmann and H. Nowotny, Monatsh. Chem., 94, 956(1963).

(15) H. Y-P. Hong, Mater. Res. Bull. 11, 173(1976).

(16) E. Banks, M. Greenblatt and B.R. McGarvey, J. Solid State Chem., 3, 308(1971).

References (Concluded)

(17) T. Arends, B.S.H. Royce, R. Smoluchowski and D.O. Welch, "Electrical and Transport Properties of Apatites", International Symposium on Structural Properties of Hydroxyapatite and Related Compounds, 12-14 September, 1968, Princeton University, Princeton, N.J.

Degrees Awarded During Contract Period

Professor E. Banks, Adviser

B.S. (Chemistry)

Synthesis of "Stuffed" Zirconium Pyrophosphates, Possible New Superionic Conductors, Charles H. Bush Polytechnic Institute of New York, June 1977, Thesis.

Ph.D. (Chemistry

New Divalent Rare Earth and Strontium Complex Fluorides, Michael Shone, Polytechnic Institute of New York, June 1979, Dissertation.

Appendix

Copies of Published Papers, Listed in Order of Reference in Text

Page

1. E. Banks, G. Torre and J.A. DeLuca, "Iron-57 Mössbauer Effect Study of the Distribution of Divalent and Trivalent Ions in Potassium Transition Metal Fluorides Having the Tetragonal Bronze Structure", J. Solid State Chem., 22, 95-100(1977). 55

2. E. Banks, S. Nakajima and G.J.B. Williams, "The Crystal Structure of $K_{0.54}(Mn,Fe)F_3$ at Room Temperature", Acta Cryst. B (in press) 61

3. M. Greenblatt and E. Banks, "CdF_2-YbF_3-ErF_3 - An Efficient Infrared to Visible Upconverting System", J. Electrochem. Soc., 124, 409-413 (1977) 92

4. M.R. Mustafa, W.E. Jones, B.R. McGarvey, M. Greenblatt and E. Banks, "Detection of Dimers by ^{19}F NMR in CdF_2 Doped with ErF_3 and YbF_3", J. Chem. Phys., 62, 2700-2706(1975). 97

5. N.N. Greenwood, F. Viegas, E. Banks and M. Nemiroff, "The Defect Model and Oxidation State of Europium and Molybdenum in Eu_xMoO_4", Inorganic Chem., 15, 2317-18(1976). 104

6. M. Greenblatt, J.H. Pifer and E. Banks, "Electron Spin Resonance of CrO_4^{3-} in Fluoroapatite, $Ca_5(PO_4)_3F$", J. Chem. Phys., 66, 559-62(1977). 106

The following two papers do not represent research done under this Grant. They are: a publication in which Professor Banks participated using materials prepared under previous ARO - supported research, and a review of recent developments in luminescence,

Page

including some material of relevance to the luminescence research reported in this report and its predecessors.

7. M. Campagna, G.K. Wertheim, H.R. Shanks, F. Zumsteg and E. Banks, "Local Character of Many-body Effects in X-ray Photoemission from Transition Metal Compounds: Na_xWO_3". Phys. Rev. Letters 34, 738-41(1975). 110

8. E. Banks, "Luminescence - The Past 25 Years", J. Electrochem. Soc., 125, 415C-418C(1978). 114

JOURNAL OF SOLID STATE CHEMISTRY 22, 95–100 (1977)

Iron-57 Mössbauer Effect Study of the Distribution of Divalent and Trivalent Ions in Potassium Transition Metal Fluorides Having the Tetragonal Bronze Structure

E. BANKS* AND G. TORRE†

Department of Chemistry, Polytechnic Institute of New York, Brooklyn, New York 11201

AND J. A. DELUCA

General Electric Corporate Research and Development, Schenectady, New York 12301

Received February 3, 1977; in revised form March 26, 1977

Mössbauer studies are reported for compounds of the type $KM^{II}M^{III}F_6$ (M = first-row transition metal ion, Zn, or Mg) which have the tetragonal bronze structure. The results of this investigation provide evidence that the trivalent ions are located on the 8(j) sites of the bronze structure and that the divalent ions are distributed over both the 8(j) and 2(c) sites.

Introduction

Since dePape's (*1*) report that $KFe^{II}Fe^{III}F_6$ ($K_{0.5}FeF_3$) has the tetragonal bronze structure (*2*), there have been prepared a number of similar tetragonal fluorides, such as the materials $KM^{II}Fe^{III}F_6$ (M = Mn, Co, Ni, Zn, Mg) and $KM^{II}Cr^{III}F_6$ (M = Mn, Fe, Co) reported by Hardy *et al.* (*3*).

In their Mössbauer effect study of $K_{0.5}FeF_3$ Buchanan *et al.* (*4*) infer from the linewidth data that the Fe^{3+} ions are on equivalent sites and that the Fe^{2+} ions are distributed over nonequivalent sites. Greenwood *et al.* (*5*) feel that the arguments based on linewidth data are not convincing because their 4.2°K Mössbauer spectra of $K_{0.4}FeF_3$ (also tetragonal) show an asymmetry in the outer lines of the Fe^{3+} magnetic hyperfine pattern which they interpret as evidence that the Fe^{3+} ions are not on equivalent sites, or at the very least, not equivalent over short distances. Both groups are restricted to interpretations based on linewidths and small asymmetries in an otherwise distinct magnetic hyperfine pattern because in neither their room- nor their low-temperature spectra is there direct evidence of absorption profiles arising from iron-ions of like charge occupying crystallographically nonequivalent sites. The room-temperature spectra of $K_{0.5}FeF_3$ and $K_{0.4}FeF_3$ can be described as an Fe^{3+} doublet with somewhat broadened linewidths and an Fe^{2+} doublet with very broad symmetrical absorption profiles one of which is totally unresolved as it is directly superimposed on the Fe^{3+} doublet. At

* Author to whom correspondence should be addressed.

† This paper is part of a dissertation to be submitted to the Polytechnic Institute of New York in partial fulfillment of the requirements for the degree of Doctor of Philosophy (Chemistry).

Copyright © 1977 by Academic Press, Inc.
All rights of reproduction in any form reserved.
Printed in Great Britain

ISSN 0022-4596

low temperatures one finds a single distinct Fe^{2+} magnetic hyperfine spectrum and a broad unresolved Fe^{2+} spectrum.

We began a Mössbauer effect study of selected compositions of "tetragonal bronze" fluorides in an effort to obtain direct evidence for the distribution of ions originally proposed by Buchanan *et al.* which we believed (*6*) was consistent with the limited data available. We reasoned that if the Fe^{2+} ions were on non-equivalent sites as proposed, then because of the sensitivity of the Mössbauer parameters of Fe^{2+} to changes in the local environment we might be able to prepare "tetragonal bronze" fluoride compositions in which the differences in the local environments of the 8(*j*) and 2(*e*) sites would be sufficient to result in a Mössbauer spectrum in which the contributions from the two kinds of Fe^{2+} ions are clearly resolved. By comparing the areas under the resolved spectra we could obtain a direct measure of the relative site occupancy.

Experimental

The tetragonal materials $KM^{II}M^{III}F_6$ were prepared by the method previously reported (*6*, *7*).

Mössbauer effect measurements were made on samples containing 10 mg Fe/cm^2, using a 10-mc Co^{57} in Pd source. An Elscint spectrometer (Model MD-3 transducer driven by a Model MFG-3A function generator) was used in the constant acceleration mode in conjunction with a Northern Scientific Model NS-900 multichannel analyzer. The spectrometer was calibrated with an α-iron foil, and a sodium nitroprusside standard was used as an isomer shift reference. A Ricor cryogenics attachment was used for measurements at 77°K. The spectra were computer fitted with the NBS program (*8*).

Results

A room-temperature Mössbauer spectrum typical of the samples containing Fe^{3+} and no Fe^{2+} is shown in Fig. 1a. All the Fe^{3+} spectra show a doublet with linewidths broader than the natural linewidth. The room-temperature spectrum of $K[Fe_{0.4}Mg_{0.6}]VF_6$ shown in Fig. 1b clearly shows spectra arising from two kinds of Fe^{2+} ions. The spectra for the other samples prepared to contain Fe^{2+} only are similar but differ in details such as the degree of overlap of the two Fe^{2+} spectra and the relative intensities of the peaks. The spectrum of $K[Fe_{0.4}Mn_{0.6}]FeF_6$ which contains both Fe^{2+} and Fe^{3+} is similar to the spectra reported for $K_{0.5}FeF_3$ and $K_{0.4}FeF_3$ with the exception that the higher velocity members of the Fe^{2+} profiles are resolved and do not combine to form a single very broad symmetrical absorption.

In analyzing the data we used the curve-fitting routine to fit only the absorption profiles that were clearly present to visual inspection. The probable errors listed along with the data in Table I are determined from those calculated for the various parameters of these curves as fit by the program. Inspection of the area fraction data for the Fe^{2+} spectra reveals an asymmetry between the lower velocity components and the higher velocity components. This asymmetry is due to the presence of an unresolved Fe^{3+} impurity spectrum which coincides with the lower velocity components of the Fe^{2+} spectra. At 77°K this impurity spectrum can be partly resolved, the effect being most pronounced in the sample $KFe^{II}_{1.4}Mn^{II}_{0.5}Cr^{III}F_6$ as shown in Fig. 2. In those instances where the overlap of Fe^{2+} and Fe^{3+} does not permit resolution of the component peaks, only approximate values of peak position-dependent parameters (isomer shift and quadrupole splitting) are listed in Table I. These are identifiable as the entries made without a corresponding error estimate. However, it can be seen that the isomer shift and quadrupole splitting values are typical of Fe^{3+}- and Fe^{2+}-containing fluorides. The higher velocity components of the Fe^{2+} spectra are not distorted by impurity contributions and the ratios listed in Table II can be used as a measure of the relative occupancy of the Fe^{2+}

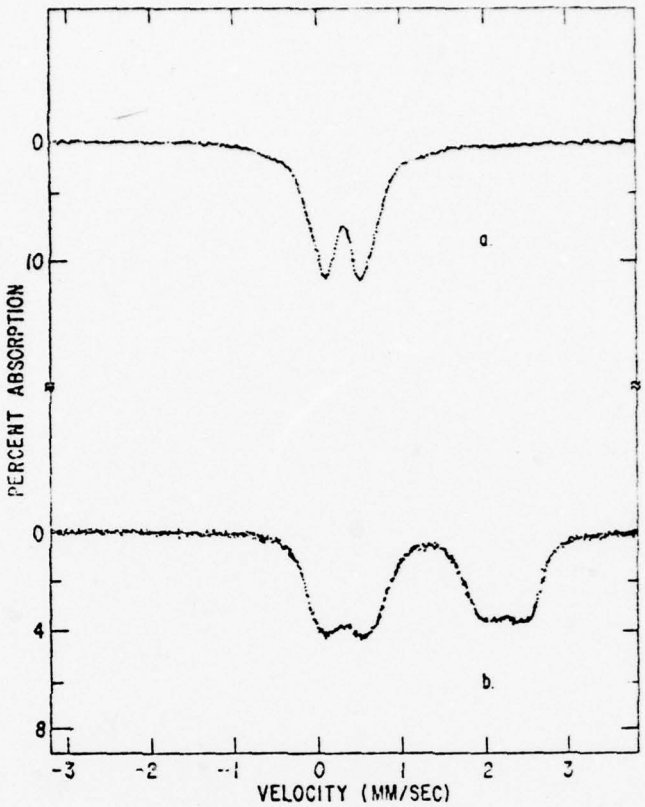


FIG. 1. Room-temperature Fe^{57} Mössbauer spectra of (a) $KCoFeF_6$ and (b) $K[Fe_{0.4}Mg_{0.6}]VF_6$.

ions on the nonequivalent sites of the tetragonal structures. The values given in Table II are computed by taking the ratio of the larger to the smaller of the undistorted higher velocity Fe^{2+} absorptions.

Discussion

There are five formula units, $KM^{II}M^{III}F_6$, per unit cell in the tetragonal bronze structure, and the ten multivalent ions (i.e., $5M^{II}$, $5M^{III}$) per unit cell fill the eight $8(j)$ and two $2(c)$ sites. If there is no site preference and both the divalent and trivalent ions distribute themselves randomly over the available sites, then the areas under the two Fe^{2+} spectra, resulting from Fe^{2+} on two different sites, should be in the ratio of 8:2. If the multivalent ions are distributed in the manner proposed by Buchanan *et al.*, then the M^{3+} ions must occupy five of the eight $8(j)$ sites (per unit cell) and the M^{2+} ions must then fill the remaining three $8(j)$ sites and two $2(c)$ sites. That is, if there exists the site preference proposed for the trivalent and divalent ions, then the areas under the Fe^{2+} absorptions for the two sites should be in the ratio of 3:2, such a ratio being obtainable only for the arrangement of ions proposed by Buchanan *et al.* (provided the Mössbauer fractions are equivalent).

We see in Table II that the area ratios measured for samples in which two Fe^{2+} spectra are resolved are ~3:2 for three of the samples and 5:4 for the remaining two samples. Thus, the data clearly indicate that there is a site preference for the divalent and trivalent ions and the area ratios measured

TABLE I
ROOM TEMPERATURE MÖSSBAUER PARAMETERS[a]

$KM^{II}M^{III}F_6$	Isomer shift[b]	Quadrupole splitting	Line half-widths[c]	Area fraction of total
$KZnFeF_6$	0.764 (±0.013)	0.504 (±0.022)	0.426 (±0.029)	0.50
			0.440 (±0.029)	0.50
$K_{0.9}[Mn_{0.4}Mg_{0.5}]Fe_{1.1}F_6$	0.719 (±0.005)	0.489 (±0.006)	0.376 (±0.008)	0.50
			0.368 (±0.008)	0.50
$KMnFeF_6$	0.721 (±0.005)	0.423 (±0.006)	0.341 (±0.007)	0.50
			0.333 (±0.007)	0.50
$KMgFeF_6$	0.716 (±0.005)	0.527 (±0.006)	0.447 (±0.007)	0.50
			0.452 (±0.007)	0.50
$KCoFeF_6$	0.723 (±0.005)	0.466 (±0.006)	0.386 (±0.008)	0.50
			0.379 (±0.008)	0.50
$KFeVF_6$	1.60	2.21	0.401 (±0.015)	0.18
			0.426 (±0.016)	0.19
	1.63	1.38	0.542 (±0.014)	0.36
			0.489 (±0.015)	0.28
$KFeCrF_6$	1.61	2.10	0.408 (±0.012)	0.27
			0.421 (±0.013)	0.25
	1.65	1.47	0.438 (±0.012)	0.30
			0.388 (±0.015)	0.18
$K[Fe_{0.4}Mg_{0.6}]VF_6$	1.73	2.48	0.451 (±0.013)	0.26
			0.413 (±0.014)	0.20
	1.63	1.35	0.488 (±0.013)	0.29
			0.482 (±0.015)	0.25
$K[Fe_{0.4}Mn_{0.6}]CrF_6$	1.61	2.19	0.359 (±0.012)	0.33
			0.337 (±0.017)	0.20
	1.67	1.49	0.406 (±0.013)	0.32
			0.428 (±0.023)	0.16
$K[Fe_{0.4}Mn_{0.6}]FeF_6$	0.72 (Fe^{3+})	0.42	0.358 (±0.006)	0.42
			0.337 (±0.006)	0.38
	—(Fe^{2+})		0.421 (±0.012)	0.08
			0.393 (±0.014)	0.12
	—(Fe^{2+})	—	Unresolved	—
			0.421 (±0.012)	0.08
	—(Fe^{2+})	—	Unresolved	—
			0.393 (±0.014)	0.12

[a] All values in mm-sec^{-1}.
[b] Relative to sodium nitroprusside.
[c] Lower velocity member listed first.

equal or are close to those predicted by the model of Buchanan *et al.*

The broader than normal linewidths observed for the Fe^{3+} and Fe^{2+} Mössbauer spectra are consistent with this interpretation. We have observed similar linewidths (*6*) in our studies of the modified pyrochlores $AM^{II}M^{III}F_6$ which have cubic structures in which the trivalent and divalent ions are distributed over the structurally equivalent 16(*c*) sites. Consideration of the tetragonal bronze structure (*2*) (the $Z = \frac{1}{4}$ plane is especially illustrative of this point) reveals that ions on the 8(*j*) sites have as nearest-neighbor multivalent cations ions on both 8(*j*) and 2(*c*) sites. The same is true for cations on the 2(*c*) sites. With both M^{3+} and M^{2+} ions distributed over the 8(*j*) sites and M^{2+} ions on the 2(*c*) sites one would not expect the local symmetry to be identical for all 8(*j*) sites (or for all 2(*c*) sites)

TABLE II
AREA RATIOS BETWEEN HIGHER VELOCITY COMPONENTS OF THE Fe^{2+} SPECTRA

$KM^{II}M^{III}F_6$	Area ratio
$KFeVF_6$	0.28/0.19 = 1.47
$KFeCrF_6$	0.25/0.18 = 1.40
$K[Fe_{0.4}Mg_{0.6}]VF_6$	0.25/0.20 = 1.25
$K[Fe_{0.4}Mn_{0.6}]CrF_6$	0.20/0.16 = 1.25
$K[Fe_{0.4}Mn_{0.6}]FeF_6$	0.12/0.08 = 1.50

even though we consider them structurally equivalent. We have a situation analogous to that occurring in the modified pyrochlores and this variation in local site symmetries is reflected in the broadened linewidths, and explains the slight asymmetry in the Fe^{3+} magnetic hyperfine pattern reported for $K_{0.4}FeF_3$ by Greenwood *et al.* without requiring that the Fe^{3+} ions be distributed on crystallographically nonequivalent sites.

In our study of fluorides having the "tetragonal bronze" structure we have prepared compositions for which the Mössbauer spectra clearly show the presence of two kinds of Fe^{2+}. The area ratios of these resolved absorptions provide a quantitative demonstration of the site distribution of Fe^{2+} in these materials which could only be inferred by Buchanan *et al.* from the very large linewidths observed for the Fe^{2+} absorption in $K_{0.5}FeF_3$. We have also shown that a careful analysis of the consequences of such a distribution of ions in the tetragonal structure explains not only the broadened linewidths observed but also removes the apparent discrepancy between the work of Buchanan *et al.* and Greenwood *et al.*

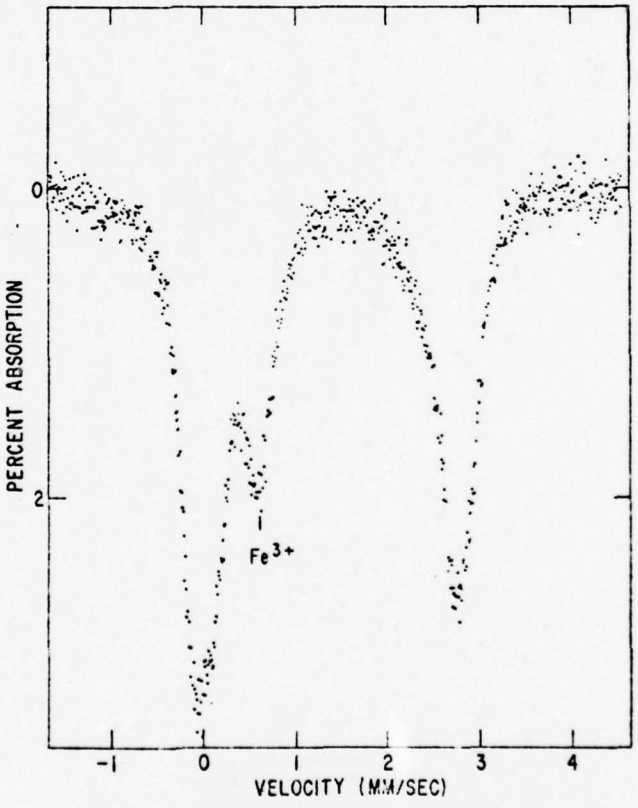


FIG. 2. The 77°K Fe^{57} Mössbauer spectrum of $K[Fe_{0.4}Mn_{0.6}]CrF_6$.

It should be noted that whereas a site preference does exist in the tetragonal bronze fluorides additional studies are required to determine if the mechanism of site preference is determined by the properties of the divalent *or trivalent ions.*

Acknowledgments

We wish to thank Dr. Lionel M. Levinson of General Electric Corporate Research and Development for the use of his Mössbauer facility and Robert G. Yelle for his assistance in recording the spectra. This work was partially supported by Army Grant No. DAAG 29-75-G-0096.

References

1. R. DEPAPE, *Compt. Rend. H.* 260, 4527 (1965).
2. A. MAGNÉLI, *Ark. Kemi* 1, 213 (1949).
3. A. HARDY, A. HADDY AND G. FEREY, *Acta Crystallogr. Sect. B* 29, 1654 (1973).
4. D. M. E. BUCHANAN, M. ROBBINS, H. J. GUGGENHEIM, G. K. WERTHEIM, AND V. G. LAMBRECHT, JR., *Solid State Commun.* 9, 583 (1971).
5. N. N. GREENWOOD, F. MENIL, AND A. TRESSAUD, *J. Solid State Chem.* 5, 402 (1972).
6. E. BANKS, J. A. DELUCA, AND O. BERKOOZ, *J. Solid State Chem.* 6, 569 (1973).
7. E. BANKS, O. BERKOOZ, AND J. A. DELUCA, *Mater. Res. Bull.* 6, 659 (1971).
8. E. RHODES, A. POLINGER, J. J. SPIKERMAN, AND B. W. CHRIST, "Parabola-Lorentzian Least Squares Analysis of Mössbauer Data Program," National Bureau Standards, Washington, D.C.

THE CRYSTAL STRUCTURE OF $K_{0.54}(Mn,Fe)F_3$ AT ROOM TEMPERATURE*†

by

Ephraim Banks, Shigeo Nakajima
Department of Chemistry
Polytechnic Institute of New York
Brooklyn, New York 11201

and

Graheme J. B. Williams
Department of Chemistry
Brookhaven National Laboratory
Upton, L.I., N. Y. 11973

Acta Cryst. B.
RECEIVED
IUCr No. 51645F
6-19-78

Abstract

A specimen of flux-grown $K_{0.54}(Mn,Fe)F_3$ was studied at room temperature by single crystal X-ray diffractometry. The crystal has a structure of the tetragonal tungsten bronze type with a doubled c axis. The unit cell parameters are a = 12.765(1) Å, c = 8.002(1) Å, and the space group is $P4_2bc$. Least-squares refinement was carried out with 2395 symmetry-independent reflections collected with an automatic diffractometer (Mo-Kα radiation). The final R value ($\Sigma \left| F_o^2 - kF_c^2 \right| / \Sigma \left| F_o^2 \right|$) is 0.049, with anisotropic thermal parameters. In the structure, potassium atoms fully occupy pentagonal (CN = 15) sites and partially occupy tetragonal (CN = 12) sites. The transition metal ions occupy three different kinds of octahedra. The mean M-F distances in

*Research carried out in part at Brookhaven National Laboratory under contract with the U.S. Dept. of Energy and supported in part by its Office of Basic Energy Sciences.

†Research at Polytechnic Institute of New York supported by the U.S. Army Research Office (Durham, N.C.) Grant No. DAAG 29-75-G-0096 and the Joint Services Electronic Program under Contract No. F44620-69-C-0047.

each octahedron are: 2.100 Å for M(1)-F, 1.939 Å for M(2)-F, and 1.995 Å for M(3)-F. These distances indicate that the M(1) sites are mainly occupied by bivalent ions, chiefly Mn^{2+}, the M(2) sites by Fe^{3+} and the M(3) sites by Mn^{2+} and Fe^{3+}.

Introduction

In recent years, considerable attention has been focused on ternary metal fluorides of the general type $A_xM^{II}_xM^{III}_{(1-x)}F_3$, where A is an alkali metal and M^{II} and M^{III} may be the same or different transition metal ions (Babel, Pausewang and Viebahn (1967), Babel (1972), and DePape (1965)). Interest in these compounds has been from the viewpoint of studying the nature of magnetic ordering, and, in the case where the bivalent and tervalent ions are of the same element, the possibility of metallic conductivity by delocalization of the electrons over the crystallographic sites. No such cases have yet been discovered.

The potassium compounds in these series all show a phase having the "tetragonal bronze" structure in the homogeneity range $0.4 \leq x \leq 0.6$, which has been studied, in the system K_xFeF_3, by DePape (1965). The only single crystal X-ray study yet reported was by Hardy, Hardy and Férey (1973) who proposed a structure for $K_{0.6}FeF_3$ based on an orthorhombic cell of dimensions a = 12.750 Å, b = 12.637 Å, c = 3.986 Å. This is a slightly distorted version of the tetragonal cell found in K_xWO_3 (Magnéli (1950a)).

In the tetragonal bronze type structure, potassium ions are distributed over sites which lie in the pentagonal and

tetragonal tunnels formed by a network of corner-sharing octahedra centered on the transition metal ions (Figure 1). The coordination number of anions about the potassium ions is 15 for the pentagonal tunnel site and 12 for the site in the tetragonal tunnel, the latter environment being the same as is found in the perovskite structure for the large cations. Férey (1977) has found that the potassium ions in $K_{0.5}FeF_3$ completely occupy the pentagonal sites and half fill the tetragonal sites.

Experimental

The crystals were grown from molten potassium chloride flux, (Perez 1972) using a powdered sample of $KMnFeF_6$ previously prepared by solid state reaction of the simple fluorides in a sealed platinum capsule in an argon atmosphere. The flux mixture was heated to 900°C in a Pt crucible under argon and cooled at 5°C/hr to 300°C. After cooling, dark brown and transparent crystals were recovered by washing out the flux. Powder samples of $KMnFeF_6$ and melts prepared in sealed graphite crucibles were much less deeply colored. We believe the color is due to the reduction of some Fe^{3+} to Fe^{2+} by chloride ions in the flux, thereby increasing the ratio of bivalent to tervalent ions in the melt, causing the increased value of x determined in the X-ray refinement. A suitable crystal was selected and mounted on a goniometer. Precession photographs (Mo-Kα radiation) showed these crystals to have a superstructure of the tetragonal bronze

unit cell, with the tetragonal $\underset{\sim}{a}$ axis unchanged, but doubling the $\underset{\sim}{c}$ axis.

A crystal of parallelepiped shape 0.11 x 0.11 x 0.35 mm was mounted on an Enraf-Nonius CAD-4 automatic diffractometer. Three dimensional intensity data for a total of 7088 reflections, using Mo Kα radiation up to $\sin\theta/\lambda = 0.90$ were collected from the quadrant with $h \geq 0$ and $\ell \geq 0$. Data were corrected for Lorentz, polarization and absorption effects and symmetry equivalent points were merged, $R_m = .03$, to yield 2397 unique intensities. The unit cell parameters and their estimated standard deviations were obtained by the least-squares method, using the 2θ values of 12 high angle reflections. These are shown with other crystal data in Table 1.

Table 1 - Crystal Data for $K_{0.54}(Mn,Fe)F_3$

Space group $P4_2bc$

$a_o = 12.765(1)$ Å

$c_o = 8.002(1)$ Å

$Z = 20$; $\bar{\mu}_{MoK_\alpha} = 62.75\ cm^{-1}$

Structure Determination and Refinement

From the systematic extinctions (hhℓ, $\ell \neq 2n$; h0ℓ, $h \neq 2n$; h00, $h \neq 2n$; 00ℓ, $\ell \neq 2n$), the crystal has a space group of $P4_2bc$ or $P4_2/mbc$. Starting with the atomic coordinates determined for $K_{0.6}WO_3$ by Magnéli (1950a) least-squares refinements were carried out for both space groups, using mean values of the scattering

factors for iron and manganese (Doyle and Turner, 1968), with fixed isotropic temperature factors of 1.5 $\mathring{A}^2$ for K, 0.4 $\mathring{A}^2$ for Mn and Fe and 2.0 $\mathring{A}^2$ for fluorine. This calculation yielded R factors of 0.151 for $P4_2bc$ and 0.248 for $P4_2/mbc$. Parallel refinements in both groups were conducted and the eventual selection (see below) was for $P4_2bc$. The function minimized was $\Sigma w \left| F_o^2 - k^2 F_c^2 \right|^2$, where k is a scale factor and $w^{-1} = \sigma_c^2 + (0.01\ F_o^2)^2 + [0.01\ (F_o^2 - F_o^2/A)]^2$. In this expression σ_c^2 is the counting statistics variance corrected for Lp and absorption; A is the transmission coefficient. Using the atomic coordinates from the initial refinements, electron-density and difference electron-density syntheses were calculated to determine the potassium site occupancy. Finally, a full-matrix least-squares refinement was done, varying atomic coordinates, multiplicities of potassium atoms, anisotropic thermal parameters for all atoms, and an extinction parameter.

The refinement (in $P4_2bc$) converged to a final R value $(\Sigma \left| F_o^2 - F_c^2 \right| / \Sigma \left| F_o^2 \right|) = 0.049$ for 2395 reflections (002 and 004 reflections showed exceptionally poor agreement, which could not be accommodated by refining an isotropic extinction term and they were therefore excluded). The final weighted R factor $R_w = (\Sigma\ w \left| F_o^2 - k^2 F_c^2 \right|^2 / \Sigma\ w \left| F_o^2 \right|^2)^{\frac{1}{2}}$ was 0.054.

Trial least-squares refinements in space group $P4_2/mbc$ were conducted, resulting in values of R = 0. 65 and R_w = 0.098.

According to a standard significance test (Hamilton, 1965) the non-centric group ($P4_2bc$) is the most probable at the 0.995 acceptance level.

A tabulation of calculated and observed structure factors and of anisotropic thermal parameters is available‡. Final atomic coordinates are listed in Table 2.

Results and Discussion

Figure 1 is a projection along the c axis of half the unit cell, having the familiar "tetragonal bronze" structure. The manganese and iron atoms are in octahedral sites surrounded by fluoride ions. There are three different octahedral sites, designated M(1), M(2) and M(3) (see Table 4). The latter sites are stacked above each other along the c axis, while the M(1) and M(2) sites alternate along that axis, giving rise to the observed doubling of the c axis (Fig. 2). The potassium atoms occupy two kinds of sites (Table 3); K(1) atoms are in tetragonal holes in an environment like that in the perovskite structure (CN - 12) while K(2) atoms are in pentagonal holes (CN - 15) (Fig. 3). The occupancy factor for the K(1) sites was 0.70 in the refinement and in the K(2) sites it was 1.0. On the basis of these occupancy numbers, the chemical composition is suggested to be $K_{0.54}(Mn,Fe)F_3$. The observed preferential filling of the

‡A tabulation of structure factors and anisotropic thermal parameters has been deposited as Supplementary Publication No. SUP00000 (13 pp.) with the British Library Lending Division. Copies may be obtained from the Executive Secretary, International Union of Crystallography, 13 White Friars, Chester CH1 1NZ, England.

pentagonal sites has previously been found in $PbNb_2O_6$ (Labbe, Frey and Allais, 1973) where the Pb atoms were found to occupy all the pentagonal sites and half the tetragonal sites. It would appear that it is necessary to fill the pentagonal sites in order to stabilize this structure type; this may account for the lower limit of $x = 0.4$ which is found for the homogeneity range of this phase in systems as diverse as the potassium tungsten bronzes and the mixed potassium transition metal fluorides of the type under present discussion. One apparent exception to this rule is the homogeneity range ($0.28 \leq x \leq 0.38$) found for this structure in Na_xWO_3 (Ribnick, Post and Banks, 1963; Magnéli, (1950b). Equilibrium preparations of Na_xWO_3 have a cubic perovskite structure above $x \cong 0.4$. Crystals have been prepared electrolytically which retain the tetragonal structure at higher sodium content. With such crystals, Takusagawa and Jacobson (1976) studied the structures of $Na_{0.22}WO_3$ and $Na_{0.48}WO_3$, reporting that sodium atoms preferentially occupy the pentagonal sites, which are completely filled at $x = 0.48$, the remaining atoms partially occupying the tetragonal (perovskite-like) sites. As noted in the Introduction, Férey (1977) has found a similar situation in $K_{0.5}FeF_3$. The only exception known to the authors to preferential occupancy of the pentagonal sites in this structure is the report by Brusset, Gillier-Pandraud and Mahé (1970) on the structure of $Pb_{0.7}Ba_{0.3}Nb_2O_6$, where the tetragonal sites

are preferentially occupied.

The potassium-fluorine distances in the "tetragonal" K(1) sites (Table 3) average to 2.832 Å, which compares reasonably to the sum of ionic radii (Shannon and Prewitt, 1969) for 12-coordinate potassium and 4-coordinate fluorine (each fluorine in this structure has two transition metal and two potassium neighbors). In the pentagonal positions, K(2)- there are seven K-F distances less than 3.10 Å, as shown in Figure 2. The distances from K(2) to fluorine F(2), F(3), F(6) and F(7) range from 3.215 to 3.579 Å, much larger than the maximum sum of ionic radii, even with allowance for 15- coordination. The coordination polyhedron about K(2) is therefore a trigonal prism with one rectangular face capped. This was also found in $K_{0.6}FeF_3$ by Hardy, et al. (1973).

The distances in the three octahedral sites permit some conclusions about the distribution of bivalent and tervalent transition metal ions in the structure. The mean M-F distances are 2.100 Å for the M(1) site, 1.939 Å for the M(2) site, and 1.995 Å for the M(3) site. Radius sums for 6-coordinate high-spin Mn^{2+} and Fe^{3+} with 2-coordinate F^- give values of 2.105 Å and 1.930 Å, respectively, and the mean radius of Mn^{2+} and Fe^{3+} gives a value of 2.018 Å. These agree remarkably well with the observed distances and we therefore postulate that the M(1) site is primarily occupied by bivalent ions, M(2) by tervalent ions

(Fe^{3+}) and the M(3) site is occupied by a mixture of bivalent and tervalent ions. A recent Mössbauer study of site preferences of Mn^{2+} and Fe^{2+} in a series of tetragonal bronze type fluorides (Banks, Torre, DeLuca, 1977) showed that Fe^{2+} strongly preferred the 2c site (in P4/mbm, corresponding to the present M(3) site) in competition with Mn^{2+}, in $K_{0.5}Fe^{2+}_{0.2}Mn^{2+}_{0.3}Fe^{3+}_{0.5}F_3$. If this site preference is present here, the presence of Fe^{2+} on these sites in preference to Mn^{2+} may explain the shorter M(3)-F distance and the longer M(2)-F distance, relative to the distances calculated using Mn^{2+} and Fe^{3+} radii.

The z parameters of the atoms in Table 2 indicate that the substance is probably ferroelectric. With the M(3) atom fixed at z = 0, the other metal atoms show negligible displacements from that value, whereas five fluorine atoms show average displacements of about 0.008 Å in the positive z direction, two (F(1) and F(8)) show no significant displacement and only one (F(3)) has a significant negative displacement. The resulting net charge displacement should produce a spontaneous polarization. We have not yet been able to test for ferroelectricity, and the strong light absorption of the material makes it impossible to test for second harmonic generation.

References

Babel, D. (1972) Z. anorg. allgem. Chem., 387, 161-178.

Babel, D., Pausewang, G. and Viebahn, W. (1967) Z. Naturforsch., 226, 1219-1220.

Banks, E., Torre, G. and De Luca, J.A. (1977), J. Solid State Chem., 32, 95-100.

Brusset, H., Gillier-Pandraud, H. and Mahé, R. (1970) C. R. Acad. Sci. Paris, 270, 302-305.

De Pape, R. (1965) C. R. Acad. Sci. Paris, 260, 4527-4530.

Doyle, P.A. and Turner, P.S. (1968) Acta Cryst., A24, 390-397.

Férey, G. (1977) Thèse de Docteur ès Sciences Physique, Univ. P. et M. Curie, Paris (VI).

Hamilton, W.C. (1965) Acta Cryst., 18, 502-510.

Hardy, A., Hardy, A.M. and Férey, G. (1973) Acta Cryst., B 29, 1654-1658.

Labbe, P., Frey, M. and Allais, G. (1973) Acta Cryst., B29, 2204-2210.

Magnéli, A. (1950a) Arkiv Kemi 1, 213-221.

Magnéli, A. (1950b) Arkiv Kemi 1, 269-272.

Perez, I. (1972) M.S. Thesis, Polytechnic Institute of New York.

Ribnick, A., Post, B. and Banks, E. (1963) Non-stoichiometric Compounds, Advances in Chemistry Series, No. 39, pp. 246-253, Washington, D.C.

Shannon, R.D. and Prewitt, C.T. (1969) Acta Cryst., B 25, 925-946.

Takusagawa, F. and Jacobson, R.A. (1976) J. Solid State Chem., 18, 163-174.

Table 2.

Final Atomic Coordinates for $K_{0.54}(Mn,Fe)F_3$

Estimated Standard Deviations Given in Parentheses Refer to the Last Significant Digit

	Position	x	y	z
K-1*	4a	0.0000	0.0000	0.2503(8)
K-2	8c	0.1695(2)	0.6728(2)	0.2501(7)
M-1	8c	0.0758(0)	0.2144(0)	-0.0004(4)
M-2	8c	0.2901(0)	0.4244(0)	0.0000(4)
M-3	4b	0.0000	0.5000	0.0000
F-1	4b	0.0000	0.5000	0.2509(15)
F-2	8c	0.0783(4)	0.2099(5)	0.2620(13)
F-3	8c	0.9221(5)	0.7949(4)	0.7416(13)
F-4	8c	0.9827(2)	0.3462(2)	0.0074(12)
F-5	8c	0.3430(2)	0.9962(2)	0.0066(14)
F-6	8c	0.1483(2)	0.0650(2)	0.0059(13)
F-7	8c	0.0704(2)	0.8650(1)	0.0075(12)
F-8	8c	0.2732(1)	0.7842(1)	-0.0007(10)

*Occupies 0.7 of 4a sites. All other sites fully occupied.

Table 3.

The K(1)-F Distances in Tetragonal Site

2x	K(1)-F(7)	2.748(6) Å
2x	K(1)-F(7')	2.830(7)
2x	K(1)-F(6)	2.845(6)
2x	K(1)-F(6')	2.908(7)
2x	K(1)-F(2)	2.861(5)
2x	K(1)-F(3)	2.801(4)
Mean	K(1)-F	2.832 Å

The K(2)-F Distances in Pentagonal Site

	K(2)-F(4)	2.867(5) Å
	K(2)-F(4')	2.758(5)
	K(2)-F(5)	2.984(6)
	K(2)-F(5')	3.025(7)
	K(2)-F(8)	2.792(6)
	K(2)-F(8')	2.786(7)
	K(2)-F(1)	3.090(4)
Mean	K(2)-F	2.900 Å
	K(2)-F(6)	3.335(6) Å
	K(2)-F(6')	3.344(6)
	K(2)-F(7)	3.375(5)
	K(2)-F(7')	3.490(5)
	K(2)-F(2)	3.256(7)
	K(2)-F(2')	3.501(3)
	K(2)-F(3)	3.215(6)
	K(2)-F(3')	3.579(8)
Mean	K(2)-F	3.387

Table 4.

The M-F Distances in Octahedral Site

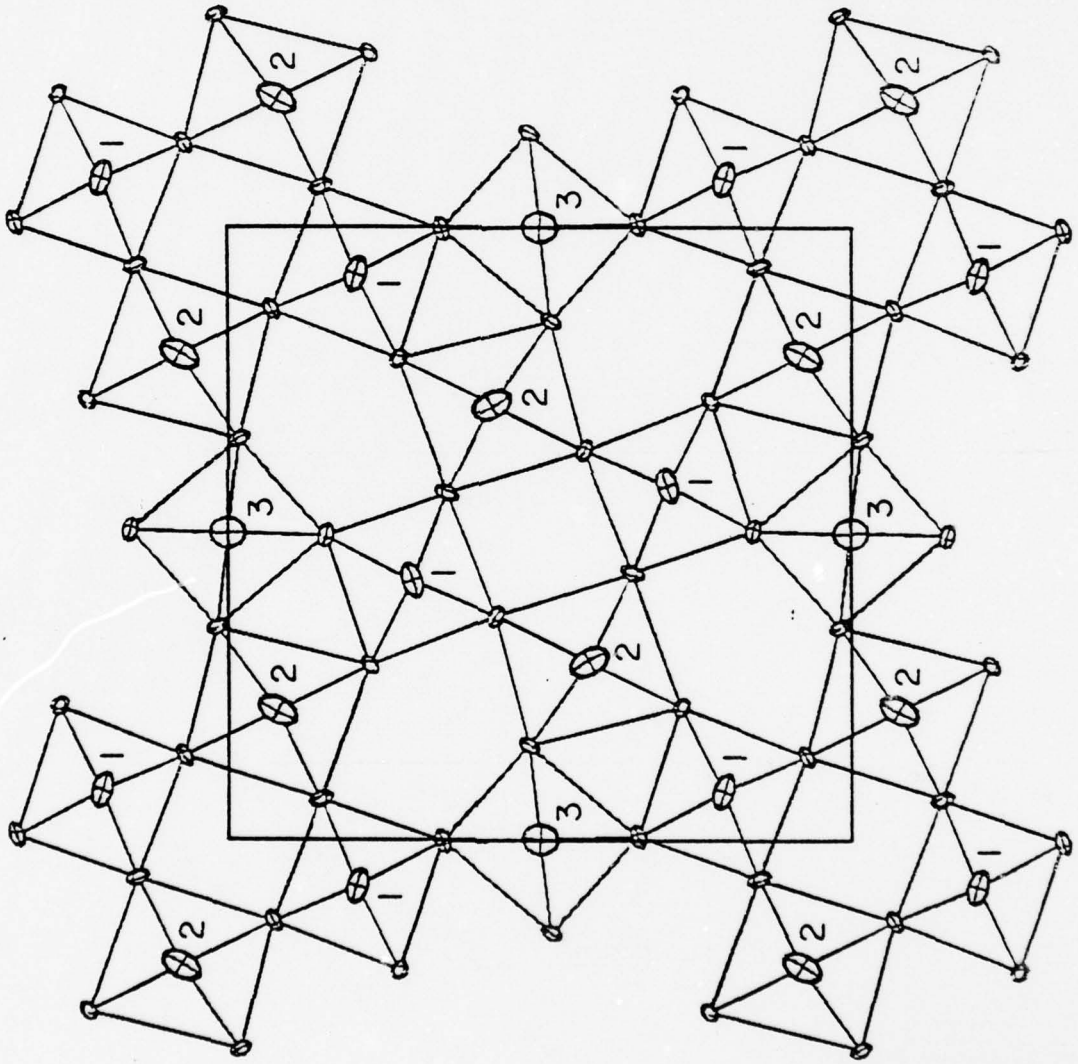
M(1) Octahedra		
	M(1)-F2	2.101(8) Å
	M(1)-F3	2.068(8)
	M(1)-F4	2.061(2)
	M(1)-F6	2.120(2)
	M(1)-F7	2.125(2)
	M(1)-F8	2.124(2)
Mean	M(1)-F	2.100 Å
M(2) Octahedra		
	M(2)-F2	1.905(8) Å
	M(2)-F3	1.934(7)
	M(2)-F5	1.931(2)
	M(2)-F6	1.960(2)
	M(2)-F7	1.937(2)
	M(2)-F8	1.964(2)
Mean	M(2)-F	1.939 Å
M(3) Octahedra		
	M(3)-F1	2.007(10) Å
	M(3)-F1	1.994(10)
2x	M(3)-F4	1.977(2)
2x	M(3)-F5	2.006(2)
Mean	M(3)-F	1.995 Å

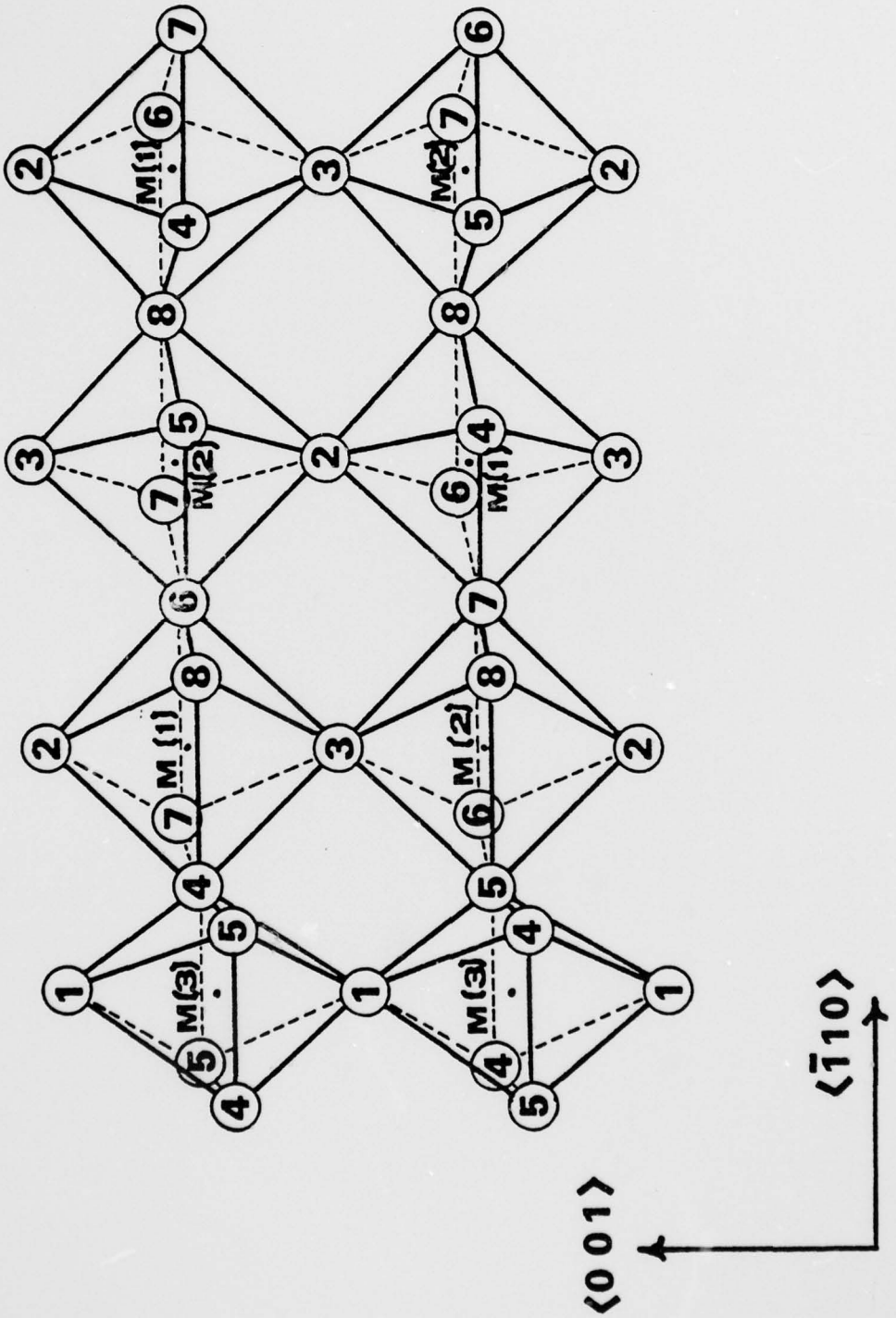
Figure Captions

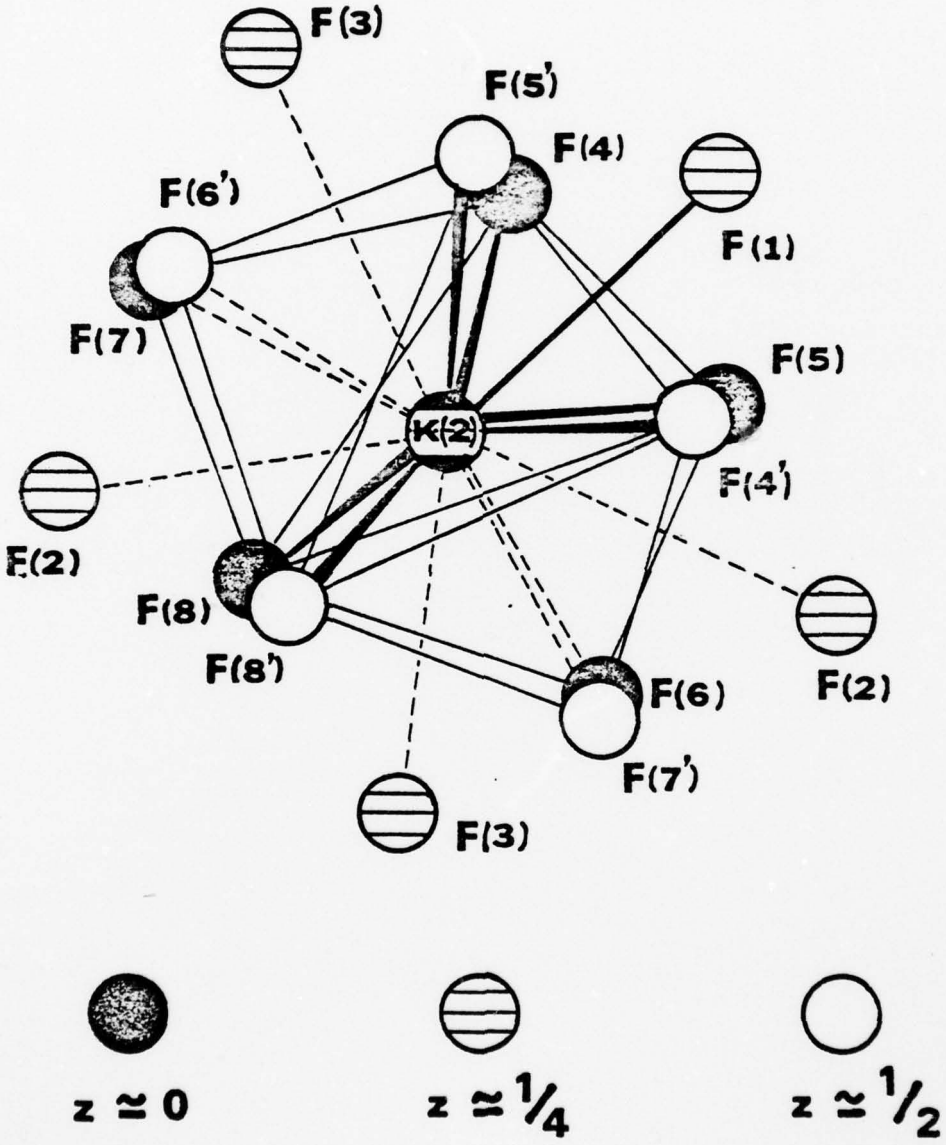
Figure 1 - One layer of connected octahedra viewed in the c direction. Transition metal sites 1, 2 and 3 are indicated. Sites 1 and 2 alternate in successive layers, sites 3 stack above one another. Potassium ions K(1) are in the square tunnels and K(2) in the pentagonal tunnels. Probability ellipsoids are drawn at the 30% level.

Figure 2 - An illustration of two chains of connected octahedra viewed along a < 110 > direction. The fluorine atoms are numbered.

Figure 3 - A view along c of the first and second neighboring fluorine ions for a K(2) ion.


1
2
3


M(1)
M(2)
M(3)
M(1)
M(2)
M(3)
⟨0 0 1⟩
⟨1̄ 1 0⟩


F(3)
F(5')
F(4)
F(6')
F(1)
F(7)
F(5)
K(2)
F(4')
F(2)
F(8)
F(8')
F(2)
F(6)
F(7')
F(3)
z ≃ 0
z ≃ 1/4
z ≃ 1/2

Material for Deposition under supplementary publication scheme

The Crystal Structure of $K_{0.54}(Mn,Fe)F_3$ at Room Temperature

by

Ephraim Banks, Shigeo Nakajima

Department of Chemistry
Polytechnic Institute of New York
Brooklyn, New York 11201

and

Graheme J. B. Williams
Department of Chemistry
Brookhaven National Laboratory
Upton, L. I., New York 11973

The quantities tabulated are h, k, F_o^2, $\sigma_{F_o}{}^2$, and F_c^2. The amplitudes are on the absolute scale.

This table comprises 13 pages.

*** L= 0 ***

1	1	-15	12	13
2	0	1360	23	1174
2	1	2549	27	2326
2	2	2607	43	2487
3	124592	18322927		
3	247335	34048144		
3	318886	20618633		
4	025906	20323659		
4	173226	53769617		
4	230309	22629424		
4	3	113	14	116
4	4	1628	56	1585
5	1	910	20	896
5	217455	13817111		
5	331919	23931983		
5	413272	11013552		
5	590865	91997021		
6	0	3968	57	3702
6	1	2685	35	2485
6	278963	57978379		
6	375467	54878621		
6	4	614	20	600
6	5	1891	31	1867
6	637440	41339327		
7	177036	58173621		
7	2	646	21	582
7	3	4823	54	4827
7	4	2245	35	2314
7	5	9669	91	9807
7	6	160	18	135
7	7	9324	157	9548
8	0	7117	87	6845
8	1	7418	76	7082
8	236206	28634576		
8	356148	42656619		
8	4	6678	84	6937
8	5	4529	57	4529
8	6	9090	92	9215
8	7	3201	49	3296
8	810735	16310835		
9	1	3085	45	2918
9	2	1645	34	1597
9	3	1388	40	1590
9	426264	21626542		
9	511213	10911558		
9	6	3941	56	4113
9	7	2999	49	2979
9	8	1469	25	1578
9	9	9979	163	10251
10	018311	18617876		
10	1	5224	64	5238
10	2	8059	87	7832
10	3	91	15	59
10	4	680	27	667
10	5	9415	102	9543
10	6	5	17	20
10	7	301	18	355
10	8	264	25	305
10	9	8632	99	8611
10	10	1360	85	1437
11	1	6965	80	7011
11	211588	11611602		
11	3	2094	43	1927
11	4	177	16	114
11	5	3701	41	3685
11	616012	15216584		
11	7	1911	43	1948
11	813394	13513531		
11	9	4177	65	4256
11	10	978	44	1022
11	11	2348	86	2520
12	0	7366	76	7432
12	1	2800	35	2747
12	2	2873	36	2872
12	3	2924	54	3115
12	412771	13112822		
12	5	15	25	153
12	626117	23326591		
12	7	38	10	50
12	8	6297	84	6288
12	9	76	13	91
12	10	5790	84	5878
12	11	447	35	472
12	12	857	68	861
13	1	183	24	199
13	2	8074	94	8219
13	3	6773	84	6580
13	4	1821	44	1729
13	5	194	25	172
13	6	99	17	104
13	7	6096	89	6359
13	8	280	29	255
13	9	189	19	238
13	10	3504	67	3596
13	11	2958	62	2761
13	12	760	31	716
13	13	-30	79	50
14	046734	43247698		
14	1	946	36	947
14	2	1562	42	1500
14	3	6	10	17
14	4	4884	73	4851
14	5	413	31	449
14	6	856	36	823
14	7	388	59	414
14	8	229	31	173
14	9	273	30	277
14	10	5773	87	5865
14	11	72	9	61
14	12	556	53	528
14	13	787	60	849
14	1414656	33715062		
15	1	1554	44	1604
15	2	762	35	712
15	3	2635	53	2841
15	4	5719	83	5927
15	5	46	15	85
15	6	904	39	857
15	7	5493	85	5554
15	8	118	17	72
15	9	3	14	2
15	10	3838	109	4141
15	11	235	54	218
15	12	614	59	490
15	13	99	34	78
15	14	571	66	619
15	15	-165	127	118
16	0	-162	85	17
16	1	1299	46	1468
16	2	9	11	2
16	3	5441	83	5598
16	4	1135	41	1142
16	5	15	11	7
16	6	5942	89	5980
16	7	350	29	388
16	8	4668	71	4372
16	9	19	20	34
16	10	370	59	470
16	11	2914	94	2867
16	12	10	22	39
16	13	944	67	829
16	14	148	40	159
16	15	88	24	57
16	16	147	70	67
17	1	2955	64	3107
17	2	1965	52	1989
17	3	23	15	21
17	4	60	12	73
17	5	54	13	52
17	6	3386	101	3519
17	7	1652	75	1647
17	8	3993	116	4331
17	9	71	16	40
17	10	45	21	52
17	11	649	59	660
17	12	1199	79	1066
17	13	2111	92	2098
17	14	-6	52	9
17	15	737	68	668
18	0	983	89	1172
18	1	1949	80	2087
18	2	4210	107	4154
18	3	126	43	144
18	4	296	46	266
18	5	3179	96	3088
18	6	725	59	841
18	7	23	20	17
18	8	891	61	802
18	9	3528	112	3442
18	10	216	52	194
18	11	-57	37	22
18	12	3655	117	3577
18	13	770	72	764
18	14	32	48	123
19	1	50	21	52
19	2	-37	29	5
19	3	170	47	212
19	4	395	50	415
19	5	7338	154	7681
19	6	160	39	182
19	7	319	55	231
19	8	55	22	24
19	9	3624	117	3674
19	10	50	32	37
19	11	375	55	316
19	12	83	22	53
19	13	450	64	394

20	0	91	24	102
20	1	660	59	748
20	2	6011	137	6400
20	3	1660	81	1810
20	4	130	30	130
20	5	738	59	653
20	6	937	62	805
20	7	-29	54	3
20	8	1340	75	1462
20	9	1057	76	972
20	10	106	27	49
20	11	703	63	691
21	1	2527	95	2525
21	2	523	63	470
21	3	58	17	32
21	4	-21	23	12
21	5	152	48	148
21	6	189	43	236
21	7	1820	82	1749
21	8	385	62	412
21	9	378	57	456
22	0	293	57	304
22	1	360	59	305
22	2	554	67	649
22	3	2669	97	2645
22	4	382	61	461
22	5	18	33	43
22	6	1370	78	1262
23	1	91	24	76

*** L= 1 ***

2	0	322	16	262
2	1	269	12	231
3	1	169	15	160
3	2	-3	10	3
4	0	18	6	27
4	1	104	13	85
4	2	-9	9	7
4	3	363	16	450
5	1	211	15	205
5	2	372	16	418
5	3	26	6	29
5	4	127	18	172
6	0	125	15	93
6	1	315	16	278
6	2	332	17	366
6	3	11	4	8
6	4	4	4	15
6	5	-1	12	8
7	1	2	6	11
7	2	334	18	338
7	3	164	15	123
7	4	650	21	632
7	5	491	21	402
7	6	-245	36	17
8	0	272	21	290
8	1	-9	9	8
8	2	675	22	623
8	3	86	13	79
8	4	160	18	116
8	5	540	23	506
8	6	409	22	418
8	7	21	13	51
9	1	50	6	54
9	2	578	24	565
9	3	80	13	73
9	4	-2	6	5
9	5	143	19	191
9	6	123	20	154
9	7	299	21	275
9	8	-9	6	25
10	0	7	12	6
10	1	32	8	41
10	2	156	20	146
10	3	16	7	1
10	4	129	13	108
10	5	-7	8	6
10	6	61	7	62
10	7	14	11	3
10	8	41	10	28
10	9	247	29	362
11	1	212	22	233
11	2	35	13	26
11	3	118	20	103
11	4	533	19	522
11	5	70	10	74
11	6	12	11	0
11	7	63	12	96
11	8	196	23	141
11	9	11	8	23
11	10	476	31	456
12	0	-5	7	32
12	1	370	18	367
12	2	-7	13	4
12	3	210	22	205
12	4	68	13	79
12	5	24	10	36
12	6	91	17	70
12	7	139	21	108
12	8	292	27	294
12	9	-1	22	11
12	10	28	9	36
12	11	139	21	149
13	1	18	10	31
13	2	163	23	149
13	3	9	20	18
13	4	64	12	50
13	5	9	12	6
13	6	4	10	8
13	7	379	28	288
13	8	5	11	3
13	9	3	14	19
13	10	111	18	109
13	11	243	27	190
13	12	-38	23	7
14	0	93	13	102
14	1	43	10	39
14	2	53	11	55
14	3	212	25	202
14	4	-15	12	10
14	5	867	36	861
14	6	45	17	86
14	7	-22	27	12
14	8	17	19	20
14	9	244	29	204
14	10	9	16	24
14	11	1	10	3
14	12	26	14	10
14	13	-73	44	0
15	1	172	25	165
15	2	4	13	12
15	3	11	13	10
15	4	-12	25	7
15	5	28	11	24
15	6	28	15	14
15	7	59	12	45
15	8	-29	28	10
15	9	-14	21	14
15	10	18	19	17
15	11	-25	21	1
15	12	350	49	236
15	13	203	47	201
15	14	50	32	55
16	0	26	11	28
16	1	324	31	376
16	2	-50	27	3
16	3	175	21	153
16	4	0	13	7
16	5	-17	15	1
16	6	131	24	95
16	7	3	11	5
16	8	36	14	30
16	9	209	45	200
16	10	-11	41	5
16	11	50	20	27
16	12	51	30	5
16	13	66	21	99
16	14	-76	53	34
16	15	65	45	183
17	1	208	21	168
17	2	88	21	42
17	3	-11	23	10
17	4	79	10	70
17	5	2	11	28
17	6	-36	38	8
17	7	237	38	225
17	8	173	34	173
17	9	-11	20	0
17	10	186	44	70
17	11	-63	49	6
17	12	-10	23	1
17	13	129	51	161
17	14	56	40	85
17	15	4	25	26
18	0	135	21	108
18	1	-14	19	3
18	2	13	18	4
18	3	-32	41	3
18	4	111	33	41
18	5	15	27	69
18	6	3	44	46
18	7	74	41	84
18	8	42	21	3
18	9	61	16	71
18	10	103	37	145
18	11	84	22	120
18	12	108	23	87
18	13	-31	24	3
18	14	-28	52	2
19	1	68	27	116

19	2	135	33	99
19	3	4	20	20
19	4	145	34	91
19	5	33	42	1
19	6	29	21	4
19	7	214	25	238
19	8	-107	45	2
19	9	24	22	29
19	10	88	19	90
19	11	50	24	20
19	12	66	25	39
20	0	79	16	89
20	1	-50	45	27
20	2	149	23	60
20	3	-10	21	2
20	4	8	21	6
20	5	-77	50	9
20	6	183	39	167
20	7	59	41	21
20	8	251	43	244
20	9	-1	23	5
20	10	14	18	27
20	11	-19	24	11
21	1	75	43	2
21	2	1	44	10
21	3	-96	46	3
21	4	212	41	259
21	5	39	23	47
21	6	17	23	8
21	7	-1	22	16
21	8	79	27	26
21	9	27	27	14
22	0	174	33	144
22	1	10	23	19
22	2	123	41	132
22	3	-64	46	2
22	4	56	23	52
22	5	-28	18	5
22	6	83	25	120

*** L= 2 ***

1	1	942	25	874
2	0	2480	35	2219
2	122926		17222662	
2	217999		19518439	
3	141140		30540121	
3	212616		10112394	
3	3	1037	30	1016
4	0	7422	80	6678
4	1	810	20	783
4	2	2947	35	3000
4	3	12	5	8
4	4	2717	50	2723
5	1	3264	39	3132
5	2	444	17	485
5	3	152	14	183
5	425448		19826658	
5	539689		42142146	
6	017940		17217063	
6	1	33	5	33
6	236262		27936075	
6	327177		21227418	
6	4	165	17	162
6	5	2405	37	2483
6	6	790	34	823
7	144157		34442582	
7	2	2270	36	2173
7	3	698	22	685
7	4	1631	30	1577
7	5	6238	68	6362
7	6	179	18	134
7	7	96	22	113
8	0	752	28	770
8	1	-12	13	23
8	2	4085	53	4016
8	323063		19222958	
8	4	674	24	621
8	5	57	14	58
8	6	4404	58	4703
8	7	133	19	119
8	8	1212	33	1084
9	1	1760	36	1670
9	2	2361	41	2243
9	3	4704	61	4592
9	410101		10210287	
9	525877		21626523	
9	6	4001	57	4126
9	7	7020	58	7311
9	8	4310	63	4394
9	9	4663	95	4933
10	0	2908	54	2926
10	110808		10810548	
10	2	25	8	42
10	3	45	13	55
10	4	-3	9	3
10	5	851	29	854
10	6	703	20	654
10	7	367	26	427
10	8	1206	37	1279
10	9	6651	83	6603
10	10	299	39	361
11	1	7015	82	7163
11	2	2602	47	2471
11	310384		7710180	
11	4	1211	24	1220
11	5	960	32	978
11	6	7767	91	7757
11	7	1672	41	1754
11	810035		11010132	
11	9	-1	8	7
11	10	12	14	3
11	11	5723	116	5020
12	0	51	15	54
12	1	1101	33	990
12	2	2236	46	2266
12	3	4037	62	3935
12	4	4951	70	4856
12	5	1093	36	1033
12	6	4781	71	4510
12	7	127	20	72
12	8	4544	71	4735
12	9	737	35	645
12	10	1686	47	1668
12	11	1622	47	1603
12	12	4002	104	4229
13	1	1589	39	1479
13	2	1653	41	1705
13	311417		12211092	
13	4	3738	62	3599
13	5	103	14	97
13	6	-1	14	13
13	713941		14713514	
13	8	1382	42	1283
13	9	92	17	66
13	10	701	37	660
13	11	2591	59	2678
13	12	915	59	936
13	13	1717	98	1689
14	033853		32732925	
14	1	1377	39	1455
14	2	80	19	77
14	3	385	29	401
14	4	338	29	345
14	5	287	26	177
14	6	777	33	694
14	7	-13	19	7
14	8	1463	47	1502
14	9	747	37	719
14	10	1288	37	1151
14	11	70	25	70
14	12	418	48	390
14	13	408	50	271
14	14	9178	253	8507
15	1	3	12	21
15	2	141	21	138
15	3	3189	61	2966
15	4	4997	77	4988
15	5	622	35	696
15	6	360	30	311
15	7	8222	107	7807
15	8	107	23	88
15	9	108	18	78
15	10	3262	98	3037
15	11	2828	91	2728
15	12	8	45	51
15	13	61	31	62
15	14	84	31	96
15	15	103	28	18
16	0	385	36	371
16	1	662	34	532
16	2	701	37	701
16	3	3983	70	3758
16	4	392	31	263
16	5	215	29	226
16	6	2416	57	2385
16	7	17	13	2
16	8	608	57	723
16	9	34	19	26
16	10	276	46	203
16	11	3799	109	3581
16	12	765	65	724
16	13	1642	79	1535
16	14	136	27	108
16	15	159	19	149
16	16	3	79	47
17	1	3865	72	3891
17	2	2136	46	2232
17	3	1528	39	1542
17	4	332	27	309
17	5	213	42	198

17	6	4323	110	3994
17	7	545	56	557
17	8	4774	119	4267
17	9	740	58	720
17	10	-4	47	7
17	11	1288	75	1215
17	12	276	54	335
17	13	2785	105	2589
17	14	15	19	1
17	15	2240	96	2169
18	0	30	27	23
18	1	2202	83	2102
18	2	2179	78	2159
18	3	236	41	108
18	4	29	20	39
18	5	1666	76	1710
18	6	-31	32	5
18	7	-39	21	0
18	8	348	54	379
18	9	2443	89	2206
18	10	-3	18	7
18	11	15	23	17
18	12	1696	83	1389
18	13	612	66	535
18	14	-42	58	52
19	1	327	52	258
19	2	94	23	118
19	3	-35	20	21
19	4	239	51	188
19	5	9287	176	9052
19	6	190	47	158
19	7	1320	71	1259
19	8	27	21	77
19	9	5102	131	4918
19	10	243	54	239
19	11	107	26	73
19	12	8	25	13
20	0	716	59	618
20	1	468	58	514
20	2	3161	102	3150
20	3	1842	79	1727
20	4	91	23	64
20	5	493	58	510
20	6	432	55	423
20	7	108	24	51
20	8	576	53	414
20	9	516	60	504
20	10	254	51	158
20	11	780	68	720
21	1	3906	121	4109
21	2	198	53	238
21	3	63	22	28
21	4	30	17	14
21	5	1048	67	942
21	6	359	55	320
21	7	858	67	753
21	8	544	60	536
22	0	867	67	829
22	1	334	64	392
22	2	248	48	142
22	3	2555	99	2538
22	4	135	30	79
22	5	48	27	67
22	6	317	60	358
***		L= 3	***	
2	0	50	12	104
2	1	13	7	5
3	1	28	4	26
3	2	-1	7	8
4	0	63	11	114
4	1	9	4	5
4	2	0	7	2
4	3	701	20	832
5	1	21	7	30
5	2	302	17	339
5	3	-31	15	16
5	4	119	16	143
6	0	2	9	5
6	1	38	7	37
6	2	322	18	371
6	3	-2	11	13
6	4	20	7	38
6	5	-18	17	34
7	1	21	11	30
7	2	135	18	176
7	3	17	7	5
7	4	388	20	359
7	5	152	18	83
7	6	-29	23	15
8	0	154	21	175
8	1	54	10	66
8	2	351	21	307
8	3	26	8	23
8	4	29	8	23
8	5	249	21	233
8	6	295	23	324
8	7	-6	10	25
9	1	92	17	92
9	2	362	22	333
9	3	55	11	57
9	4	8	6	2
9	5	149	20	143
9	6	107	9	127
9	7	222	22	226
9	8	13	8	43
10	0	23	23	6
10	1	22	9	32
10	2	132	19	121
10	3	5	9	15
10	4	36	7	52
10	5	7	6	2
10	6	31	8	39
10	7	-12	9	2
10	8	12	10	20
10	9	253	28	299
11	1	195	15	221
11	2	7	8	22
11	3	98	11	93
11	4	247	26	263
11	5	35	12	45
11	6	25	17	2
11	7	68	14	100
11	8	75	12	98
11	9	24	10	23
11	10	325	30	313
12	0	-7	21	50
12	1	232	23	234
12	2	0	10	9
12	3	192	23	149
12	4	45	18	50
12	5	63	10	68
12	6	65	9	57
12	7	65	12	64
12	8	176	27	201
12	9	-5	26	9
12	10	-7	13	30
12	11	119	14	123
13	1	59	17	32
13	2	65	15	100
13	3	2	10	11
13	4	39	9	36
13	5	3	13	5
13	6	2	9	8
13	7	251	28	226
13	8	9	14	3
13	9	-17	27	3
13	10	81	12	82
13	11	209	23	157
13	12	4	40	3
14	0	84	14	70
14	1	3	17	25
14	2	39	13	24
14	3	165	23	147
14	4	2	12	6
14	5	719	34	682
14	6	43	11	56
14	7	-36	28	11
14	8	10	22	19
14	9	163	23	161
14	10	-19	12	19
14	11	9	14	6
14	12	-15	43	8
14	13	10	21	2
15	1	108	15	139
15	2	8	18	11
15	3	6	14	2
15	4	6	11	2
15	5	13	12	20
15	6	2	27	4
15	7	34	13	42
15	8	-6	15	4
15	9	-23	42	7
15	10	-16	46	13
15	11	-37	42	1
15	12	168	48	184
15	13	182	40	186
15	14	67	24	48
16	0	-23	31	23
16	1	270	28	286
16	2	5	12	6
16	3	119	16	111
16	4	27	14	15
16	5	-6	12	2
16	6	136	21	95
16	7	-2	38	4
16	8	20	17	26
16	9	195	45	182
16	10	-86	46	2
16	11	6	17	19

16	12	-11	32	3
16	13	67	23	84
16	14	39	26	24
16	15	113	49	156
17	1	156	20	133
17	2	40	12	50
17	3	-2	12	8
17	4	43	18	47
17	5	64	21	27
17	6	-15	18	9
17	7	271	42	191
17	8	152	34	124
17	9	-9	39	0
17	10	86	23	67
17	11	14	22	5
17	12	-16	24	1
17	13	113	25	145
17	14	82	23	74
18	0	125	26	94
18	1	10	15	15
18	2	-21	19	7
18	3	42	22	2
18	4	33	21	28
18	5	15	20	55
18	6	42	27	44
18	7	-27	48	64
18	8	-13	40	3
18	9	44	17	57
18	10	122	24	115
18	11	85	27	111
18	12	30	52	78
18	13	-36	52	3
19	1	81	28	95
19	2	108	21	81
19	3	17	28	11
19	4	161	34	85
19	5	-9	16	2
19	6	10	21	3
19	7	170	45	202
19	8	2	44	9
19	9	10	17	20
19	10	126	23	81
19	11	-30	48	17
19	12	44	48	39
20	0	41	22	81
20	1	25	21	26
20	2	88	35	47
20	3	-70	51	1
20	4	-21	45	6
20	5	51	25	10
20	6	120	22	137
20	7	36	18	16
20	8	130	54	225
20	9	-14	23	3
20	10	13	49	27
21	1	-9	17	1
21	2	-39	46	10
21	3	-13	23	6
21	4	198	47	234
21	5	17	24	43
21	6	-50	50	5
21	7	-17	38	14
21	8	7	24	23

22	0	100	26	124
22	1	10	24	18
22	2	115	27	113
22	3	-26	33	2
22	4	21	24	48

*** L= 4 ***

1	1	32	8	24
2	0	496	21	440
2	1	1607	32	1615
2	2	1213	36	1223
3	112512		11012388	
3	224790		19526033	
3	312172		15112868	
4	013742		14113128	
4	141947		32542303	
4	221480		17422370	
4	3	135	16	146
4	4	1419	42	1434
5	1	74	14	79
5	2	6260	67	6193
5	313407		11913667	
5	4	7317	76	7538
5	552127		55455474	
6	0	849	30	815
6	1	1309	30	1249
6	240140		31540128	
6	339280		30540827	
6	4	212	21	236
6	5	1359	32	1437
6	621925		26222876	
7	140437		32340157	
7	2	286	22	271
7	3	2360	42	2391
7	4	1234	37	1306
7	5	5267	66	5427
7	6	163	20	147
7	7	9516	10110120	
8	0	4865	72	4759
8	1	4218	58	4010
8	221661		18921339	
8	332596		26733358	
8	4	4231	59	4224
8	5	2919	49	3003
8	6	6288	54	6378
8	7	2176	44	2238
8	8	7719	128	8400
9	1	2151	43	2006
9	2	602	28	610
9	3	365	25	384
9	417112		11217402	
9	5	8069	65	8420
9	6	2828	50	2892
9	7	2040	44	2137
9	8	1064	34	1051
9	9	8024	135	8016
10	013723		10813526	
10	1	4339	44	4402
10	2	6923	59	6843
10	3	39	7	32
10	4	742	44	715
10	5	6687	84	6779
10	6	35	9	18
10	7	203	26	266

10	8	251	26	275
10	9	6252	84	6268
10	10	1301	58	1308
11	1	4597	66	4517
11	2	8535	98	8683
11	3	1464	40	1487
11	4	71	14	41
11	5	2384	50	2392
11	611156		12211367	
11	7	1427	48	1405
11	8	9661	111	9722
11	9	2745	55	2803
11	10	680	36	771
11	11	1729	70	2043
12	0	4814	80	4787
12	1	1886	44	1939
12	2	2240	47	2243
12	3	2238	47	2256
12	4	9776	112	9757
12	5	63	22	49
12	618195		17818676	
12	7	-9	16	41
12	8	4609	74	4625
12	9	-19	14	41
12	10	4799	79	4821
12	11	357	28	454
12	12	748	88	839
13	1	149	19	94
13	2	5927	81	5875
13	3	4664	71	4577
13	4	1508	43	1569
13	5	192	29	274
13	6	95	11	106
13	7	4564	75	4705
13	8	232	30	264
13	9	264	26	266
13	10	2929	52	3078
13	11	2268	80	2150
13	12	603	54	595
13	13	-8	68	41
14	033107		32633907	
14	1	760	34	709
14	2	1161	39	1125
14	3	28	11	11
14	4	3936	69	3897
14	5	299	31	358
14	6	739	39	727
14	7	238	33	272
14	8	234	31	168
14	9	249	27	236
14	10	4707	116	4982
14	11	38	21	51
14	12	517	53	421
14	13	593	62	675
14	1412148		30212251	
15	1	990	40	1074
15	2	608	35	573
15	3	2045	51	2283
15	4	4947	79	4952
15	5	43	20	72
15	6	740	38	702
15	7	4589	65	4649
15	8	67	22	62

15	9	-15	20	6
15	10	3525	105	3540
15	11	300	42	190
15	12	533	55	397
15	13	44	25	56
15	14	578	60	519
15	15	81	38	86
16	0	-4	33	40
16	1	1112	42	1227
16	2	20	13	15
16	3	4377	62	4643
16	4	1043	36	1221
16	5	18	42	28
16	6	4828	115	4901
16	7	225	37	309
16	8	3890	110	3650
16	9	98	41	21
16	10	469	54	541
16	11	2359	91	2465
16	12	27	23	31
16	13	819	68	729
16	14	165	42	136
16	15	92	37	58
17	1	2623	84	2646
17	2	1802	74	1694
17	3	31	15	44
17	4	51	18	70
17	5	14	22	28
17	6	2674	94	2833
17	7	1152	66	1273
17	8	3260	103	3496
17	9	44	20	14
17	10	20	18	46
17	11	641	60	582
17	12	966	68	880
17	13	1751	88	1801
17	14	-22	25	8
18	0	772	57	900
18	1	1796	75	1894
18	2	3264	102	3520
18	3	196	35	139
18	4	274	47	205
18	5	2533	89	2449
18	6	478	58	657
18	7	-20	44	17
18	8	606	61	637
18	9	3006	103	2882
18	10	267	43	154
18	11	7	24	11
18	12	3062	108	3078
19	1	131	31	76
19	2	-3	21	5
19	3	97	34	198
19	4	256	54	353
19	5	6196	141	6334
19	6	117	30	155
19	7	230	44	173
19	8	70	38	28
19	9	2999	108	3152
19	10	-19	53	42
19	11	318	57	286
20	0	15	50	99
20	1	543	61	613
20	2	4645	123	5211
20	3	1506	75	1476
20	4	49	24	85
20	5	502	66	577
20	6	727	66	660
20	7	-247	60	5
20	8	1206	72	1219
20	9	875	69	871
21	1	2095	90	2187
21	2	270	60	403
21	3	46	18	18
21	4	56	19	12
21	5	133	25	147
21	6	180	53	227
21	7	1557	83	1625
22	0	230	49	231
22	1	241	55	270
22	2	645	61	594

*** L= 5 ***

2	0	407	40	350
2	1	315	20	285
3	1	240	19	216
3	2	1	6	12
4	0	111	22	128
4	1	52	16	65
4	2	19	11	10
4	3	34	8	29
5	1	282	20	227
5	2	15	8	37
5	3	-27	18	9
5	4	81	13	94
6	0	150	25	153
6	1	219	23	215
6	2	17	8	23
6	3	54	15	47
6	4	-16	9	16
6	5	35	6	21
7	1	-3	9	11
7	2	41	9	40
7	3	169	21	117
7	4	275	24	306
7	5	456	19	436
7	6	-2	7	3
8	0	118	25	112
8	1	56	9	27
8	2	353	25	354
8	3	53	6	48
8	4	116	12	94
8	5	182	22	163
8	6	197	23	259
8	7	40	9	44
9	1	14	6	7
9	2	344	17	338
9	3	27	14	25
9	4	-5	10	29
9	5	43	11	42
9	6	10	12	7
9	7	43	8	39
9	8	-35	13	8
10	0	89	27	122
10	1	-7	11	8
10	2	105	14	89
10	3	-13	12	17
10	4	67	14	66
10	5	-7	23	8
10	6	43	8	57
10	7	-5	17	14
10	8	52	12	35
10	9	168	29	214
11	1	69	16	68
11	2	-9	12	2
11	3	17	8	11
11	4	443	30	458
11	5	64	12	62
11	6	-2	22	5
11	7	46	10	41
11	8	57	10	63
11	9	-13	15	4
11	10	238	31	268
12	0	24	21	46
12	1	150	23	151
12	2	0	8	16
12	3	118	21	123
12	4	41	12	37
12	5	7	12	12
12	6	11	19	10
12	7	40	9	27
12	8	196	31	223
12	9	4	20	3
12	10	36	9	51
12	11	-11	41	106
13	1	32	12	33
13	2	121	20	101
13	3	-9	14	26
13	4	47	13	48
13	5	29	23	1
13	6	-19	15	1
13	7	235	31	254
13	8	-9	21	7
13	9	1	11	11
13	10	55	20	74
13	11	172	47	114
13	12	-4	45	18
14	0	59	12	47
14	1	66	15	44
14	2	68	11	59
14	3	144	21	152
14	4	-15	15	10
14	5	372	32	407
14	6	25	23	71
14	7	3	12	14
14	8	8	30	10
14	9	189	30	121
14	10	-8	15	32
14	11	23	45	17
14	12	-7	46	1
14	13	-9	47	1
15	1	135	18	113
15	2	15	13	7
15	3	17	25	13
15	4	2	12	14
15	5	13	15	56
15	6	-14	19	26
15	7	63	16	61
15	8	3	21	8
15	9	-18	24	3

15	10	-28	29	7
15	11	-8	16	4
15	12	146	27	115
15	13	143	41	164
15	14	75	18	45
16	0	6	11	12
16	1	211	26	252
16	2	-14	40	5
16	3	239	40	120
16	4	-17	31	2
16	5	12	24	9
16	6	17	33	31
16	7	-79	49	3
16	8	21	46	16
16	9	189	45	193
16	10	-13	49	5
16	11	-11	23	15
16	12	35	25	0
16	13	50	20	68
16	14	-3	25	20
17	1	186	36	142
17	2	16	17	31
17	3	-69	49	6
17	4	29	21	34
17	5	42	21	30
17	6	41	21	10
17	7	209	23	174
17	8	111	24	108
17	9	-57	23	2
17	10	16	43	38
17	11	-119	57	0
17	12	-18	24	0
17	13	170	28	137
18	0	99	24	79
18	1	0	19	3
18	2	12	41	11
18	3	21	21	12
18	4	36	23	29
18	5	70	21	66
18	6	52	30	38
18	7	71	28	59
18	8	6	25	1
18	9	91	33	41
18	10	24	38	85
18	11	32	42	111
19	1	89	20	107
19	2	33	23	64
19	3	-18	17	15
19	4	74	47	86
19	5	-40	53	1
19	6	-26	48	5
19	7	128	30	174
19	8	-20	53	1
19	9	7	26	15
19	10	90	22	78
20	0	-104	55	91
20	1	22	17	17
20	2	59	19	39
20	3	-34	51	2
20	4	-9	49	10
20	5	8	32	18
20	6	170	34	123
20	7	42	23	15
20	8	194	44	184
21	1	7	25	1
21	2	24	18	20
21	3	-115	54	4
21	4	137	41	202
21	5	-50	51	37

*** L= 6 ***

0	0	35727	54639	008
1	1	285	31	291
2	0	501	28	531
2	1	7616	83	7811
2	2	5567	94	5721
3	1	16364	17316	119
3	2	6620	75	6816
3	3	193	32	227
4	0	3671	62	3576
4	1	676	26	691
4	2	221	21	211
4	3	37	15	16
4	4	485	34	414
5	1	316	24	318
5	2	19	9	26
5	3	428	25	517
5	4	10020	10410	501
5	5	18530	16619	804
6	0	9631	119	9349
6	1	14	14	25
6	2	12684	12612	769
6	3	9924	74	9970
6	4	8	7	19
6	5	1466	38	1547
6	6	287	34	273
7	1	18072	33717	988
7	2	1102	23	1052
7	3	567	20	587
7	4	742	28	754
7	5	2678	50	2774
7	6	141	18	135
7	7	675	44	806
8	0	780	35	760
8	1	-21	8	2
8	2	2070	45	2074
8	3	9826	106	9896
8	4	233	27	314
8	5	46	11	67
8	6	2675	51	2686
8	7	68	17	60
8	8	970	52	943
9	1	701	31	706
9	2	564	30	551
9	3	837	38	755
9	4	5266	75	5386
9	5	14867	14915	277
9	6	2209	50	2329
9	7	4272	68	4359
9	8	2359	52	2224
9	9	3656	96	3616
10	0	2403	58	2516
10	1	7221	90	6990
10	2	280	27	325
10	3	31	10	29
10	4	59	10	41
10	5	572	31	598
10	6	499	30	409
10	7	263	26	223
10	8	698	35	638
10	9	3751	69	3818
10	10	328	47	348
11	1	3772	64	3733
11	2	1879	48	1834
11	3	6270	86	6196
11	4	508	31	482
11	5	335	29	336
11	6	4093	69	3953
11	7	1083	40	1116
11	8	5618	85	5705
11	9	58	12	55
11	10	-2	12	11
11	11	3358	136	3388
12	0	-11	12	25
12	1	594	33	543
12	2	1681	45	1593
12	3	2370	55	2260
12	4	3281	64	3131
12	5	442	32	358
12	6	2367	55	2251
12	7	59	14	45
12	8	2550	60	2631
12	9	311	27	272
12	10	1225	67	1250
12	11	1161	67	1183
12	12	3257	141	3117
13	1	789	37	758
13	2	959	40	951
13	3	6551	92	6243
13	4	2665	59	2649
13	5	-5	13	2
13	6	26	13	30
13	7	8358	91	8160
13	8	868	59	905
13	9	-8	14	9
13	10	766	62	652
13	11	1772	81	1794
13	12	645	56	636
13	13	1279	102	1074
14	0	18145	21117	693
14	1	762	39	862
14	2	57	21	47
14	3	234	31	211
14	4	257	28	302
14	5	145	21	132
14	6	642	52	595
14	7	6	27	13
14	8	1075	65	1070
14	9	541	53	473
14	10	1033	66	1022
14	11	60	23	44
14	12	186	45	231
14	13	240	51	194
14	14	6615	213	5857
15	1	48	10	57
15	2	114	12	114
15	3	2276	81	2078
15	4	3694	102	3610
15	5	406	49	497
15	6	277	51	248

5532	3	1	-17	10	4	12	5	77	14	57
40	3	2	8	6	8	12	6	25	10	7
89	4	0	25	7	49	12	7	17	15	5
2314	4	1	1	6	3	12	8	60	15	85
1785	4	2	10	10	1	12	9	4	19	2
43	4	3	184	15	188	12	10	14	28	27
56	5	1	-9	11	13	12	11	102	22	66
93	5	2	54	11	51	13	1	27	20	34
194	5	3	-15	11	11	13	2	30	12	32
433	5	4	65	9	61	13	3	26	11	17
345	6	0	-11	15	1	13	4	-3	15	20
2720	6	1	-4	15	4	13	5	-9	20	1
417	6	2	89	11	69	13	6	26	37	2
81	6	3	2	9	7	13	7	170	45	128
1707	6	4	14	8	30	13	8	-81	49	2
1	6	5	1	12	18	13	9	-1	20	1
600	7	1	-9	15	9	13	10	15	16	38
10	7	2	14	9	12	13	11	158	37	69
278	7	3	-31	20	7	13	12	-64	47	4
2583	7	4	72	16	77	14	0	15	12	19
456	7	5	-10	23	4	14	1	21	14	11
1091	7	6	8	13	5	14	2	12	38	9
2875	8	0	29	10	32	14	3	77	17	67
1623	8	1	25	8	39	14	4	7	20	4
1133	8	2	71	10	66	14	5	243	46	238
222	8	3	16	12	1	14	6	30	20	22
180	8	4	16	10	0	14	7	-37	34	9
2619	8	5	-5	24	16	14	8	3	43	9
317	8	6	165	22	145	14	9	-7	36	66
2859	8	7	2	14	7	14	10	30	22	18
587	9	1	47	8	42	14	11	29	23	17
2	9	2	119	18	107	14	12	5	51	8
914	9	3	25	10	18	14	13	-2	33	2
260	9	4	-25	16	1	15	1	111	20	72
39	9	5	35	12	32	15	2	-1	15	2
1696	9	6	20	11	12	15	3	-92	47	0
1630	9	7	29	9	36	15	4	-18	46	2
99	9	8	18	13	8	15	5	47	21	30
31	10	0	5	16	8	15	6	-13	21	3
1122	10	1	-11	12	1	15	7	51	26	38
7	10	2	44	14	55	15	8	11	21	0
1	10	3	19	11	15	15	9	-5	23	0
237	10	4	-29	25	10	15	10	-0	23	2
1623	10	5	-2	14	1	15	11	-56	52	1
5	10	6	4	11	23	15	12	67	22	59
108	10	7	1	15	8	15	13	120	25	132
46	10	8	15	18	13	16	0	24	30	8
12	10	9	144	15	135	16	1	67	36	128
167	11	1	97	14	79	16	2	17	16	10
6317	11	2	5	11	6	16	3	63	22	51
122	11	3	34	12	20	16	4	7	30	11
775	11	4	53	12	78	16	5	28	40	10
61	11	5	17	15	15	16	6	44	22	39
477	11	6	9	10	2	16	7	-13	23	4
359	11	7	64	16	47	16	8	-7	25	11
2181	11	8	22	12	23	16	9	169	32	146
1159	11	9	53	37	10	16	10	-16	24	0
68	11	10	76	16	100	16	11	48	26	6
406	12	0	29	12	13	16	12	-10	27	0
297	12	1	38	19	39	17	1	45	21	74
*	12	2	0	10	12	17	2	96	32	38
154	12	3	53	15	57	17	3	-25	22	4
15	12	4	35	16	14	17	4	15	22	9

17	5	5	24	26
17	6	24	18	11
17	7	114	22	110
17	8	-12	51	42
17	9	-49	53	1
17	10	82	26	33
18	0	76	20	43
18	1	-1	23	17
18	2	10	17	14
18	3	2	24	9
18	4	35	23	9
18	5	-15	32	34
18	6	68	24	33
18	7	80	47	29
18	8	58	46	2
18	9	8	35	23
19	1	46	31	62
19	2	48	23	37
19	3	7	18	3
19	4	108	23	67
19	5	21	33	1
19	6	30	26	2
20	0	78	33	73
20	1	-45	51	16
20	2	41	25	20

*** L= 8 ***

0	0	8915	413	94106460
1	1	45	14	19
2	0	96	8	91
2	1	558	28	511
2	2	242	38	241
3	1	3333	58	3296
3	2	7406	104	7681
3	3	4795	99	4892
4	0	4224	66	4101
4	1	15268	153	15061
4	2	9932	112	10086
4	3	105	16	77
4	4	833	48	753
5	1	72	18	105
5	2	953	36	905
5	3	2886	55	2954
5	4	2224	48	2209
5	5	16971	235	17653
6	0	25	9	41
6	1	362	29	349
6	2	11317	146	11029
6	3	11128	123	11157
6	4	28	9	45
6	5	661	34	725
6	6	7556	139	7721
7	1	12239	134	11919
7	2	138	28	65
7	3	672	34	647
7	4	479	30	413
7	5	1597	45	1641
7	6	104	14	107
7	7	7399	141	7368
8	0	2028	53	1971
8	1	1336	44	1222
8	2	8018	102	7820
8	3	11139	129	11123
8	4	1610	48	1506
8	5	1204	42	1224
8	6	2862	59	2920
8	7	889	40	916
8	8	4247	104	4484
9	1	950	39	894
9	2	60	15	56
9	3	-1	12	0
9	4	7088	97	6977
9	5	3852	71	3967
9	6	1360	44	1334
9	7	1000	44	1032
9	8	460	29	436
9	9	4356	157	4180
10	0	6815	96	6872
10	1	2755	60	2605
10	2	4141	74	4050
10	3	6	20	11
10	4	556	37	527
10	5	3106	64	3095
10	6	-18	16	10
10	7	131	14	121
10	8	152	35	156
10	9	3089	96	3060
10	10	941	93	904
11	1	1808	52	1718
11	2	4291	77	4365
11	3	933	41	795
11	4	6	17	5
11	5	989	35	908
11	6	4645	67	4775
11	7	582	57	663
11	8	4537	116	4569
11	9	1027	67	999
11	10	318	54	385
11	11	1168	103	1212
12	0	1816	43	1823
12	1	850	34	856
12	2	1235	38	1205
12	3	1123	38	1067
12	4	5182	123	5103
12	5	-48	46	1
12	6	8146	161	8268
12	7	6	20	25
12	8	2283	86	2310
12	9	-14	21	5
12	10	2964	97	2850
12	11	340	56	392
12	12	803	95	709
13	1	42	15	22
13	2	2806	86	2641
13	3	2063	81	2088
13	4	1064	68	1168
13	5	330	49	341
13	6	8	48	88
13	7	2336	93	2492
13	8	235	33	247
13	9	261	52	242
13	10	1943	86	1972
13	11	1188	77	1187
13	12	409	59	364
13	13	-67	75	36
14	0	1561	824	61561
14	1	444	50	381
14	2	546	57	556
14	3	36	20	6
14	4	2135	97	2171
14	5	159	49	204
14	6	461	56	460
14	7	104	40	89
14	8	151	46	144
14	9	144	42	164
14	10	3288	107	3132
14	11	11	19	33
14	12	319	57	254
14	13	414	58	367
15	1	442	49	397
15	2	284	47	331
15	3	1033	74	1290
15	4	3304	104	3106
15	5	38	32	44
15	6	423	60	427
15	7	3130	99	2967
15	8	75	21	43
15	9	12	48	11
15	10	2294	101	2311
15	11	254	55	142
16	0	100	24	52
16	1	784	57	757
16	2	22	39	37
16	3	2595	99	2874
16	4	1047	71	1086
16	5	64	24	42
16	6	2783	101	2894
16	7	243	36	170
16	8	2355	95	2196
16	9	-5	50	5
16	10	486	63	529
17	1	1701	82	1742
17	2	1220	73	1086
17	3	7	53	65
17	4	19	47	56
17	5	3	24	5
17	6	1514	84	1663
17	7	684	68	673
17	8	1826	92	2031
18	0	449	55	448
18	1	1155	79	1390
18	2	2371	95	2275
18	3	109	27	117
18	4	61	41	100
18	5	1378	77	1345
18	6	320	54	346
19	1	118	34	86
19	2	3	19	9

*** L= 9 ***

2	0	163	35	231
2	1	159	38	151
3	1	141	29	104
3	2	18	14	8
4	0	161	37	102
4	1	45	36	26
4	2	-17	24	5
4	3	198	36	177
5	1	111	22	136
5	2	10	15	1
5	3	-30	33	5

| | | |

21	7	511	68	537
22	0	228	53	240
22	1	180	39	176
22	2	134	27	138
22	3	1111	78	1113
22	4	-1	46	58

*** L= 11 ***

2	0	96	14	43
2	1	6	18	7
3	1	2	23	1
3	2	7	23	3
4	0	-8	45	16
4	1	18	44	1
4	2	7	43	0
4	3	14	18	27
5	1	-3	20	6
5	2	-65	46	5
5	3	-34	20	5
5	4	-0	24	22
6	0	-10	16	2
6	1	-10	46	3
6	2	-23	47	9
6	3	-75	48	2
6	4	-22	46	7
6	5	7	21	5
7	1	-25	50	2
7	2	-13	50	4
7	3	-22	33	2
7	4	29	46	15
7	5	-0	45	2
7	6	-26	22	2
8	0	-22	21	4
8	1	-39	47	11
8	2	-30	29	17
8	3	-32	31	0
8	4	13	22	0
8	5	-36	46	1
8	6	83	18	51
8	7	-0	45	2
9	1	33	20	8
9	2	51	21	38
9	3	-24	49	6
9	4	7	46	0
9	5	-17	22	7
9	6	-54	50	2
9	7	-13	38	1
9	8	-74	33	0
10	0	16	26	3
10	1	-12	50	2
10	2	33	24	20
10	3	-58	37	3
10	4	-8	23	2
10	5	-2	53	0
10	6	8	25	16
10	7	-41	54	8
10	8	31	26	10
10	9	55	25	46
11	1	39	18	18
11	2	-3	23	5
11	3	-218	61	2
11	4	12	25	32
11	5	-46	57	4
11	6	24	22	1
11	7	-5	26	11
11	8	-44	53	3
11	9	28	26	5
11	10	-15	26	32
12	0	5	24	11
12	1	10	55	2
12	2	-17	24	4
12	3	50	49	20
12	4	-28	25	3
12	5	42	25	25
12	6	-91	56	1
12	7	-41	54	3
12	8	55	25	40
12	9	20	29	0
12	10	-0	27	18
12	11	55	26	31
13	1	19	18	26
13	2	-26	52	9
13	3	-12	25	13
13	4	-3	35	10
13	5	5	26	1
13	6	-22	26	1
13	7	-7	44	63
13	8	-17	52	4
13	9	-17	27	2
13	10	-34	61	19
13	11	-23	28	21
13	12	14	28	2
14	0	-11	42	5
14	1	-40	53	3
14	2	-18	25	7
14	3	81	25	29
14	4	-1	26	3
14	5	18	55	59
14	6	9	23	11
14	7	-14	55	5
14	8	-32	57	3
14	9	33	20	20
14	10	44	27	14
14	11	4	29	22
14	12	-14	27	26
14	13	-85	62	1
15	1	-38	26	31
15	2	34	25	0
15	3	-94	57	2
15	4	52	20	2
15	5	-14	57	31
15	6	-30	28	3
15	7	38	22	19
15	8	-84	63	3
15	9	4	57	5
15	10	-123	64	0
15	11	20	22	2
15	12	-18	26	10
15	13	-27	64	76
15	14	-28	24	14
16	0	25	27	4
16	1	2	26	54
16	2	-2	26	6
16	3	-17	57	20
16	4	-11	26	4
16	5	-47	58	13
16	6	23	20	7
16	7	-27	27	3
16	8	5	28	3
16	9	68	34	100
16	10	-69	59	1
16	11	-31	65	1
16	12	19	27	1
16	13	17	28	23
17	1	44	26	35
17	2	14	40	19
17	3	-12	42	2
17	4	-4	27	1
17	5	13	55	23
17	6	6	28	12
17	7	6	60	52
17	8	8	28	12
17	9	-45	57	3
17	10	11	23	8
17	11	34	28	1
17	12	8	27	1
18	0	-1	27	8
18	1	-10	55	7
18	2	60	39	14
18	3	47	50	27
18	4	-22	24	2
18	5	2	43	19
18	6	-10	57	17
18	7	-22	27	12
18	8	9	51	1
18	9	37	25	8
18	10	3	52	16
18	11	46	26	67
19	1	52	20	36
19	2	64	20	11
19	3	-57	48	2
19	4	66	43	41
19	5	-21	26	0
19	6	-30	26	1
19	7	37	27	71
19	8	16	20	3
19	9	-37	28	1
20	0	89	21	60
20	1	-16	43	9
20	2	-3	43	4
20	3	-34	26	8
20	4	20	27	2
20	5	13	27	9
20	6	23	53	26
21	1	-14	25	1
21	2	41	27	13

*** L= 12 ***

0	0	25747	53825	113
1	1	-40	76	8
2	0	57	21	45
2	1	240	57	206
2	2	65	59	89
3	1	1059	68	1054
3	2	2504	97	2416
3	3	1528	117	1491
4	0	1351	81	1359
4	1	5037	132	5013
4	2	4031	120	3777
4	3	45	51	29
4	4	256	84	264

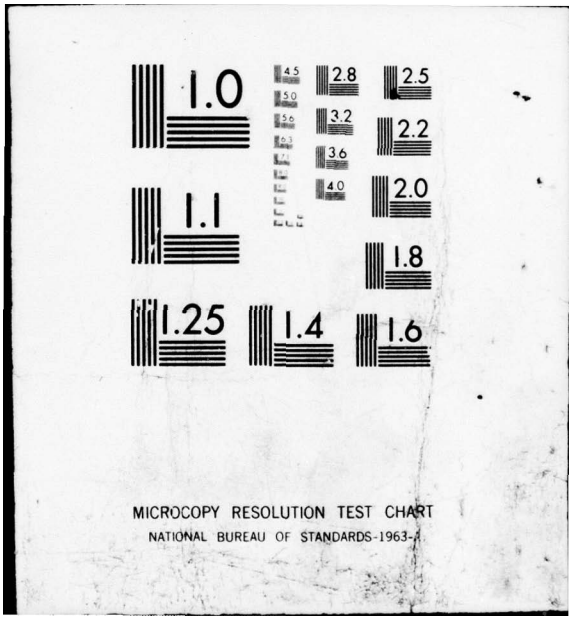
AD-A065 237 POLYTECHNIC INST OF NEW YORK BROOKLYN F/G 7/4
COMPOUNDS WITH DEFECT LATTICE STRUCTURES.(U)
NOV 78 E BANKS DAAG29-75-G-0096

UNCLASSIFIED ARO-12613.1-C NL

2 OF 2
AD
A065237



END
DATE
FILMED
4-79
DDC


1.0
1.1
1.25
1.4
1.6
1.8
2.0
2.2
2.5
2.8
3.2
3.6
4.0
4.5
5.0
5.6
MICROCOPY RESOLUTION TEST CHART
NATIONAL BUREAU OF STANDARDS-1963-A

5	1	103	37	98
5	2	81	53	120
5	3	467	63	650
5	4	778	68	800
5	5	5690	206	5837
6	0	28	17	6
6	1	106	23	109
6	2	3369	115	3447
6	3	3196	107	3236
6	4	-56	48	12
6	5	282	58	357
6	6	2115	153	2371
7	1	3990	120	3901
7	2	8	24	5
7	3	246	54	158
7	4	119	28	90
7	5	491	60	554
7	6	77	22	60
7	7	3906	173	3648
8	0	719	65	703
8	1	285	63	306
8	2	2883	103	2659
8	3	3858	120	3684
8	4	542	65	442
8	5	419	66	437
8	6	1447	78	1299
8	7	317	61	296
8	8	2001	125	1982
9	1	298	61	299
9	2	13	54	3
9	3	11	22	18
9	4	2646	104	2645
9	5	2118	91	1832
9	6	635	64	601
9	7	620	66	521
9	8	265	55	192
9	9	2112	131	1773
10	0	3101	113	3008
10	1	1584	85	1402
10	2	2020	89	1777
10	3	-74	57	5
10	4	296	39	248
10	5	1267	86	1212
10	6	29	20	7
10	7	36	27	34
10	8	132	31	43
10	9	1236	88	1362
10	10	527	94	480
11	1	842	103	640
11	2	1896	130	1883
11	3	346	105	439
11	4	69	30	2
11	5	284	41	302
11	6	1666	96	1775
11	7	373	57	286
11	8	2009	100	1944
11	9	243	49	253
11	10	103	24	156
11	11	705	94	620
12	0	650	94	596
12	1	332	80	324
12	2	652	105	566
12	3	556	95	456
12	4	2382	146	2303
12	5	3	30	2
12	6	3331	166	3143
12	7	-22	84	13
12	8	1113	116	1045
12	9	-102	93	1
12	10	1633	124	1353
12	11	265	59	276
13	1	-57	87	12
13	2	1060	115	994
13	3	883	117	951
13	4	731	114	742
13	5	218	97	232
13	6	-87	95	51
13	7	1206	129	1304
13	8	112	64	188
13	9	87	63	142
13	10	790	130	998
13	11	435	107	574
14	0	6554	231	6505
14	1	194	79	199
14	2	218	81	217
14	3	-59	90	7
14	4	944	127	937
14	5	113	31	97
14	6	261	89	217
14	7	-88	91	18
14	8	105	31	108
14	9	114	31	102
14	10	1583	125	1538
14	11	-124	94	19
15	1	-3	85	106
15	2	194	72	155
15	3	524	100	604
15	4	1748	132	1628
15	5	3	30	25
15	6	200	68	224
15	7	1478	129	1611
15	8	0	32	25
15	9	-65	86	11
15	10	1297	134	1229
15	11	137	33	99
16	0	-28	84	35
16	1	420	91	374
16	2	-39	29	34
16	3	1392	127	1486
16	4	751	110	668
16	5	3	29	26
16	6	1228	132	1374
16	7	-59	102	73
16	8	1134	120	1022
16	9	-73	85	1
16	10	364	91	345
16	11	1138	109	945
17	1	955	105	965
17	2	392	105	562
17	3	61	33	60
17	4	16	30	36
17	5	11	80	5
17	6	597	120	829
17	7	253	92	299
17	8	911	119	980
17	9	30	53	28
17	10	35	84	15
18	0	95	54	168
18	1	1029	101	810
18	2	1201	117	1204
18	3	95	61	78
18	4	68	44	36
18	5	576	102	604
18	6	99	31	142
18	7	-6	29	9
18	8	314	81	173
19	1	112	29	49
19	2	5	29	9
19	3	61	51	74
19	4	16	65	124
19	5	2193	134	2068

CdF_2:YbF_3:ErF_3—An Efficient Infrared to Visible Upconverting System

Martha Greenblatt

Department of Chemistry, Rutgers University, New Brunswick, New Jersey 08903

and E. Banks*

Department of Chemistry, Polytechnic Institute of New York, Brooklyn, New York 11201

ABSTRACT

Single crystals of CdF_2 doubly doped with YbF_3 and ErF_3 efficiently convert infrared radiation (~0.93 μm) from a Si:GaAs diode to red and green light. By varying the Yb concentration, phosphors have been made which produce a red or green visual response. For the series of crystal samples of CdF_2:1% ErF_3:1-10% YbF_3 studied: at YbF_3 concentrations below 3%, only red Er^{3+} emission peaks were observed (6450-6600 Å); at 3% YbF_3, red and green spectra (5300-5700 Å) were observed, the green bands being much less intense; the most intense phosphor contained 10 mole percent (m/o) Yb^{3+}, and the green intensity was an order of magnitude higher than the red. Charge compensation by NaF of the rare earth ions in CdF_2:1% ErF_3:10% YbF_3 greatly reduces the intensity of emission bands, as well as the intensity of the absorption band at 976 nm, in agreement with previous studies of the absorption spectra properties of the YbF_3:CdF_2 system (1). Recent results of ^{19}F NMR of single crystals of CdF_2 containing high concentrations of YbF_3 and ErF_3, respectively, indicate that most of the rare earth ions and their associated interstitial fluorides are found in $(M^{3+}$-$F^-)_2$ dimers in the crystal (2). The intense absorption band observed at 976 nm in Yb^{3+}-doped CdF_2 can be assigned to this dimer, which is destroyed by the use of Na^+ as a charge compensator in place of interstitial fluoride, the native charge compensating defect. Similarly, as the accepted mechanism of the infrared-to-visible conversion in the Yb^{3+} sensitized Er^{3+} activated systems involves the transfer of two infrared photons from Yb^{3+} to Er^{3+}, phosphor emission by diode excitation will decrease when the $(M^{3+}$-$F^-)_2$ complex is destroyed by NaF substitution. The 976 nm strong absorption band was also observed in samples (10% Yb, 1% Er) prepared with 1-30 m/o of CaF_2 substituted for CdF_2 without appreciable decrease in the intensity; however the emission intensities of both green and red bands were significantly enhanced for all of the samples codoped with CaF_2. There appears to be a plateau for the compositions 1.5-3% CaF_2 and a decrease in the 4.5 and 10% CaF_2 samples. Of all the materials investigated to date, YF_3 and $BaYF_5$ codoped with Yb^{3+} and Er^{3+} are reported to be the most efficient upconverting systems with a quantum efficiency between 10^{-4} and 10^{-5} ($\lambda = 0.97$ μm). The quantum efficiency of CdF_2:10% YbF_3:1% ErF_3 is found to be 0.23% and that of CdF_2:10% YbF_3:1% ErF_3:2.5% CaF_2, 0.70%. These values were obtained under intense excitation with a GaAs diode. Lower values might be found at lower excitation densities.

Infrared excited visible fluorescence has attracted considerable attention in recent years (1-5). In combination with GaAs:Si diodes emitting in the near infrared (0.91-1 μm), phosphor materials capable of converting infrared to visible light are potential display or infrared detecting devices.

All the known phosphors of this class use trivalent rare earth ions. The systems which produce the brightest visible light use Yb^{3+} as the sensitizer with Er^{3+}, Ho^{3+}, or Tm^{3+} as the activator. The host crystals in which the most efficient upconversion has been obtained are YF_3, $BaYF_5$, LaF_3, and α-$NaYF_4$, doped with Yb^{3+} and Er^{3+}. The Yb^{3+} ions can absorb the GaAs infrared emission and are able to transfer most of the energy to Er^{3+} ions, both in their ground state and excited state, which then emit the green or red depending on concentration and the host crystal. Similarly, Yb^{3+} in combination with Ho^{3+} upconverts in the green or red and Yb^{3+} with Tm^{3+} in the appropriate host crystals upconverts in the blue.

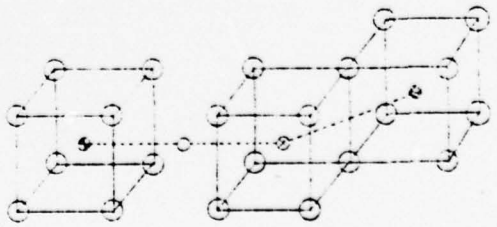
In the first part of this paper a brief review of the spectroscopic properties of CdF_2 doped with small concentrations of YbF_3 is presented. The infrared visible upconverting properties of CdF_2:Yb:Er system are then discussed in detail.

* Electrochemical Society Active Member.

Key words: infrared-visible upconversion, rare earth luminescence, CdF_2:Yb^{3+},Er^{3+}.

CdF_2:YbF_3—The 976 nm Band

CdF_2 has the fluorite structure ($Fm3m$) of CaF_2 shown in Fig. 1. This may be visualized as a cubic lattice of fluoride ions in which every other body center position is occupied by divalent cadmium. Rare earth



○ F^-

⊗ $R.E.^{3+}$ Ion Substitutionally in a Cd^{2+} Position

○ Nearest Neighbor Interstitial Position (100 Direction)

● Nearest Neighbor Cd^{2+} Position (110 Direction)

● Next Nearest Neighbor Cd^{2+} Position (100 Direction)

Fig. 1. The symmetry of sites in the CdF_2 (RE) system

ions can enter the lattice substitutionally at the Cd^{2+} sites. Compensation for the excess charge of the tripositive rare earth ions in CdF_2 has been shown to occur by the incorporation of fluoride ions into the interstitial sites (6). The interstitial fluoride ion is either a nearest neighbor of RE^{3+}, an electrostatically favorable arrangement, in which case the symmetry around the rare earth is reduced to tetragonal, or the interstitial fluorides may be at a distance from the rare earth ion, thus preserving the cubic symmetry of the RE site. Charge compensation can also be attained by the introduction of univalent ions, such as Na^+, for each trivalent ion. The nearest neighbor Cd^{2+} sites are in [110] directions, and if the compensating Na^+ goes into one of these positions the symmetry around the RE is reduced to orthorhombic.

The absorption spectrum of CdF_2:0.1 Yb^{3+} single crystals was found to be unusual (7); the spectrum consists of an intense band at 976 nm and a less intense broad band absorption extending to about 900 nm. As NaF was added to the CdF_2:Yb^{3+} system the intensity of the 976 nm band decreased. A sample containing sufficient sodium for complete charge compensation showed a spectrum which resembled that of Yb^{3+} in other solids, *e.g.*, yttrium gallium garnet, $YbCl_3 \cdot 6H_2O$, or CeF_3. This spectrum consists mainly of a sharp line at 968 nm and a broader absorption at 920 nm (8). In Fig. 2, the energy level diagram of Yb^{3+} in CdF_2 and CaF_2 is shown (9). On the basis of the oscillator strength of the absorption bands as well as the expected crystal field splitting of states in a cubic environment, Abbruscato *et al.* assigned the 962 nm band to the $\Gamma_7 \rightarrow \Gamma_7'$ and the 920 band as due to $\Gamma_7 \rightarrow \Gamma_8'$ transitions. They showed that the 976 nm band cannot be part of a cubic or noncubic spectrum of isolated Yb^{3+} ions in CdF_2. In addition, ESR measurements of CdF_2:Yb^{3+} showed only sites of cubic symmetry, while the ESR of CdF_2:Yb^{3+}:Na^+ indicated Yb^{3+} in both cubic and orthorhombic sites. The ESR of CaF_2:Yb^{3+} showed Yb^{3+} in cubic and tetragonal environments in the crystal (9).

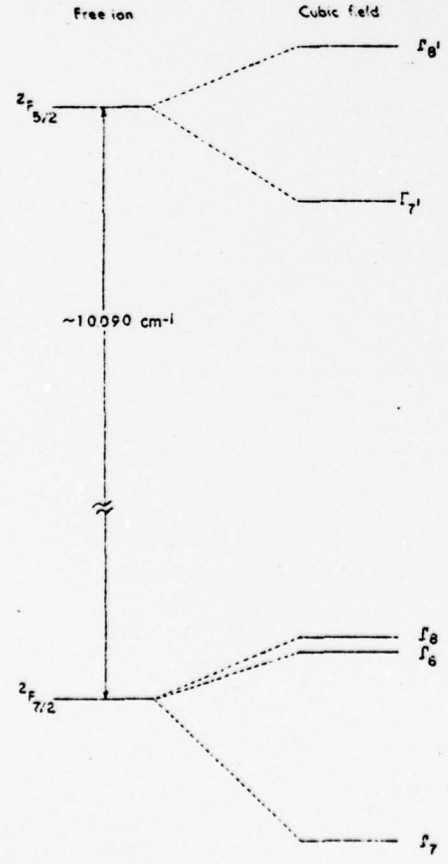


Fig. 2. Energy levels of the Yb^{3+} ion, free and in a cubic crystal field.

The main difference between the optical absorption of Yb^{3+} in CdF_2 and in CaF_2 has been the absence of the intense 976 nm absorption in CaF_2. Weller has shown that as little as 0.1% CaF_2 in the CdF_2:0.1 YbF_3 system decreased the intensity of the 976 nm band drastically and at about 7% CaF_2 content, the 976 nm band disappeared completely (10). Prener and Kingsley have shown that when CdF_2 crystal doped with Yb^{3+} or other RE ion is heated in Cd vapor to 500°C, the insulating transparent crystal becomes semiconducting and colored. Apparently the interstitial fluorides migrate to the surface and oxidize Cd. The liberated electrons do not reduce the rare earth (except Eu) but remain in a diffuse state over the 12 nearest neighbor Cd^{2+} ions. If Ca^{2+} is added the semiconducting property decreases until at 8% CaF_2, it disappears completely (11). On the basis of the above evidence Abbruscato *et al.* postulated that the 976 nm band in CdF_2:Yb^{3+} is not an *f-f* transition but might be due to some center involving Yb^{3+} and interstitial F^-, Yb^{3+}-Yb^{3+} interactions via interstitial F^- or some similar defect.

^{19}F NMR in CdF_2:Yb^{3+}

The ^{19}F NMR measurement of CdF_2 doped with Er^{3+} and Yb^{3+} was undertaken in the hope of finding further evidence for the mechanism responsible for the unusual properties of CdF_2 doped with rare earth ions. In addition to the main resonance from the bulk of the lattice fluorides, weaker anisotropic resonances for two types of fluoride ions were detected (12, 13); one having axial symmetry about the [111] axes and the other one with its symmetry axis along the [100] axis. The [111] resonances were identified as the lattice fluorides adjacent to one rare earth ion. The [100] resonance can only arise from the interstitial fluorides (see Fig. 1) and their intensity indicates that this resonance accounts for nearly all the interstitial fluorides in the crystal. It has been shown that the anisotropy of the [100] ^{19}F resonance can only be explained by assuming each interstitial fluoride must have two rare earth ions at adjacent Cd^{2+} sites in which the RE^{3+}-F^--RE^{3+} angle is 90°. This is most readily explained by assuming that most of the rare earth ions and their associated interstitial fluorides are found in $(Re^{3+}\text{-}F^-)_2$ dimers as shown in Fig. 3. The [100] NMR spectrum could also be explained by zigzag chains of rare earth-interstitial fluoride along the (110) direction.

The ^{19}F NMR results appear to offer an explanation of the above-described ESR and optical spectra of Yb^{3+}-doped CdF_2 which showed only cubic ESR and additional bands not attributable to cubic sites. The additional bands can be assigned to this dimer; the lack of any ESR signal from these dimers can probably be attributed to spin exchange interactions between the two metal ions in the dimer. This would be equally true for the chain model.

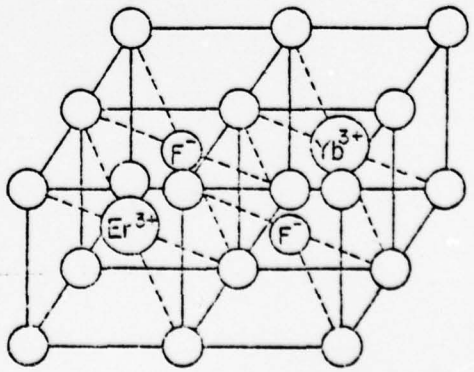


Fig. 3. Orthorhombic cluster site, showing unlike ion pairing

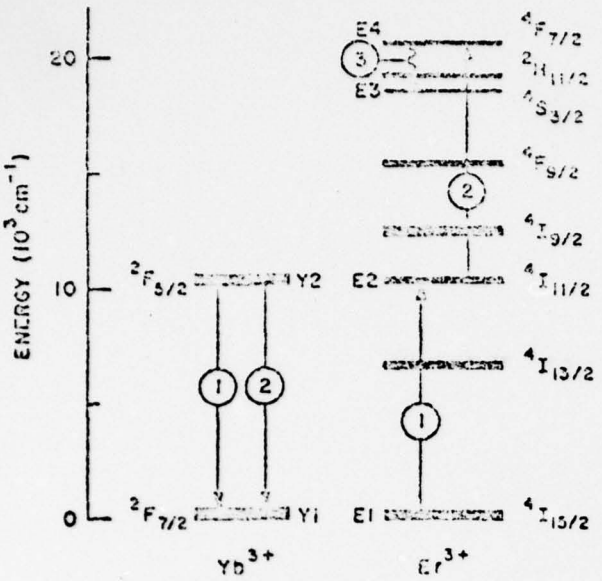


Fig. 4. Energy level diagram for Yb^{3+} and Er^{3+} showing the upconversion process.

CdF_2:Yb^{3+}:Er^{3+}—Infrared Visible Phosphor

The intense absorption band observed in CdF_2:Yb^{3+} at 976 nm suggested that efficient infrared-visible upconversion might be enhanced in CdF_2 crystals doped with Yb^{3+} and Er^{3+} if the primary absorption process is more efficient compared with other systems.

Figure 4 is an energy level diagram of Yb^{3+} and Er^{3+} showing the upconversion process in the green (14). Ytterbium ions absorb infrared radiation in the 0.91-1 μm range; an excited ytterbium ion transfers its energy to an erbium ion which is excited to the $^4I_{11/2}$ manifold; a second transfer of infrared quantum excites the $^4I_{11/2}$ to the $^4F_{7/2}$ level. The erbium then decays nonradiatively to the $^4S_{3/2}$ level, followed by visible fluorescence from $^4S_{3/2}$ in the region of 540 nm. In this process, two quanta of infrared are absorbed for every quantum of visible light emitted, and the intensity of green emission is found to increase as the square of the infrared exciting power (15). The conversion of infrared into red can take place by various routes, by the absorption of two or three quanta. In fluoride hosts, excitation spectra in the 350-500 nm range show that the most important path for red emission in Yb^{3+}-Er^{3+} samples is excitation of Er^{3+} to the $^4I_{11/2}$ level (by the transfer of energy from infrared-excited Yb^{3+}) followed by rapid nonradiative decay to the $^4I_{13/2}$ manifold; a second quantum of energy excites the electron from $^4I_{13/2}$ to $^4F_{9/2}$ from which red fluorescence is observed (16). The three quantum process for red emission has also been observed at high rare earth ion concentrations, with excitation of Er^{3+} by two quanta to ($^4I_{15/2} \rightarrow {}^4I_{11/2} \rightarrow {}^4F_{7/2}$), followed by nonradiative transition to $^4S_{3/2}$; from $^4S_{3/2}$ transition to $^4I_{13/2}$ accompanied by the back transfer of an infrared quantum to Yb^{3+}; a third quantum excites the Er^{3+} from $^4I_{13/2}$ to $^4F_{9/2}$ followed by transition to the ground state and red emission.

The complexity of the mechanism for upconversion implies that many factors affect the efficiency of the process. The purity of the samples is extremely important (17).

Experimental

CdF_2 was prepared from 99.999% pure cadmium metal (American Smelting and Refining Company) by precipitation with hydrofluoric acid. ErF_3, YbF_3, of purity > 99.9% (Lindsay Division of the American Potash and Chemical Corporation), NaF and CaF_2 of 99.99% purity were used. The CdF_2 single crystals doped and codoped with various concentrations of YbF_3, ErF_3, NaF, and CaF_2 were grown by the Bridgman technique: a graphite crucible was slowly lowered through a temperature gradient in the work coil of an rf generator, the crucible being maintained in an argon atmosphere. The weights were measured accurately before and after crystal growth; weight loss was attributed to CdF_2, hence the concentration of dopants reported is the minimum concentration possible. The crystals were cut to a uniform thickness of 1.7 mm and polished. Absorption spectra of samples were recorded on a Cary Model 14 spectrophotometer at room temperature. For the emission measurements, a thin disk (1.7 mm) of a polished single crystal was placed near the dome of a GaAs:Si diode (Texas Instruments Model TIXL 16) operated at 2A. The infrared radiation (~ 0.93 μm) emitted by the diode is absorbed by the phosphor which then emits visible light. The fluorescent output of the crystal was analyzed with the monochromator of a Spex spectrometer and detected with an (ITT-F-W-130-Products for Research) photomultiplier S20.

Results and Discussion

Figure 5 shows the emission spectrum of CdF_2:10% YbF_3:1% ErF_3 [all percent concentrations represent mole percent (m/o)] the most efficient phosphor in the series CdF_2:1-10% YbF_3:1% ErF_3 studied. A complex spectrum of three stronger bands at 532.3, 543.6, and 552.5 nm and two weaker broad bands at ~ 522 and 530 nm are observed in the green region, and several peaks at 623.3, 652.0, 656.5, and 666.5 nm in the red. The intensity of emission bands in the 550 nm region is an order of magnitude greater than the intensity of the red bands and the crystal displays a bright green visible fluorescence. Samples of CdF_2:1-2% YbF_3:1% ErF_3 showed fluorescence bands only in the red; CdF_2:3% YbF_3:1% ErF_3 emitted in the green and the red, but bands in the green were much weaker than bands in the red. The effect of increasing the concentration of Yb^{3+} on the intensity of several of the emission bands is shown in Fig. 6. The intensity of both green and red emission increases with increasing concentration of Yb^{3+}; apparently the optimum concentration of Yb^{3+} is ~ 20% in the CdF_2:Yb:Er system for green emission.

One of the objects of studying the infrared-to-visible upconverting properties of CdF_2:YbF_3:ErF_3 system was to shed further light on the origin of the 976 nm absorption band. The intensity of the emission bands is greatly reduced when NaF is introduced to replace interstitial F^- charge compensation by substitutional Na^+ which in effect destroys the $(M^{2+}$-$F_{int.}^-)_2$ clusters, and reduces the intensity of the 976 nm band. The emission spectrum of CdF_2:3.5% NaF:10% Yb:1% ErF_3 is shown in Fig. 7. The increased structure in

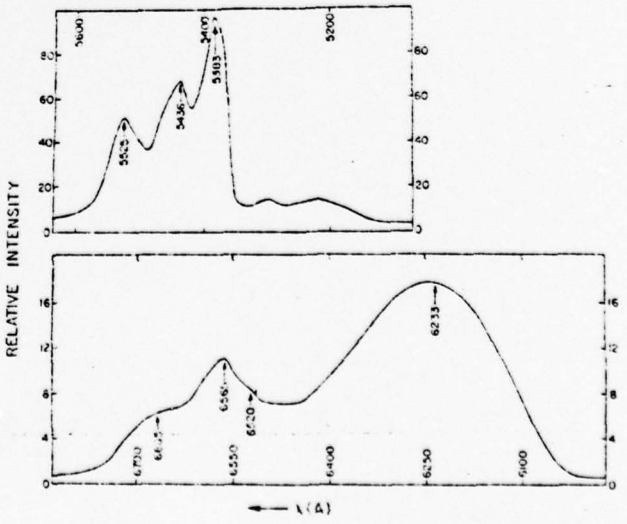


Fig. 5. Emission spectrum of CdF_2:10% YbF_3:1% ErF_3 (room temperature). Excitation by Si:GaAs diode (λ = 0.93 μm).

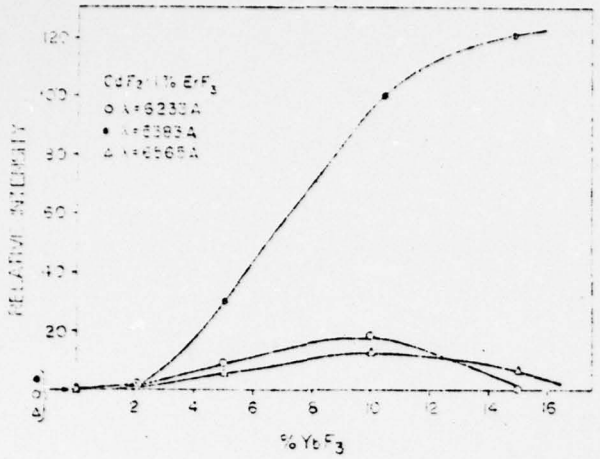


Fig. 6. Variation of relative intensity of various bands vs. Yb^{3+} concentration (Er^{3+} constant at 1 m/o).

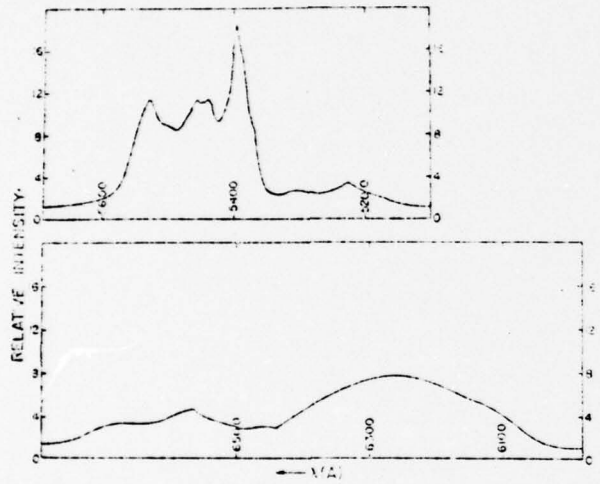


Fig. 7. Emission spectrum of CdF_2:10% YbF_3:1% ErF_3:3.3% NaF (diode excitation).

the emission bands observed is in agreement with the decreased site symmetry of the rare earth ion when Na^+ enters the lattice substitutionally, lifting the degeneracy of the excited states of the rare earth ion giving rise to the emission. The absorption spectra of Yb^{3+}-doped samples charge compensated with NaF show similar decreases in the intensity of the 976 nm band with increasing NaF concentration (7).

The results of CaF_2 substitution into the CdF_2:Yb:Er phosphor were unexpected. In Fig. 8 the variation with

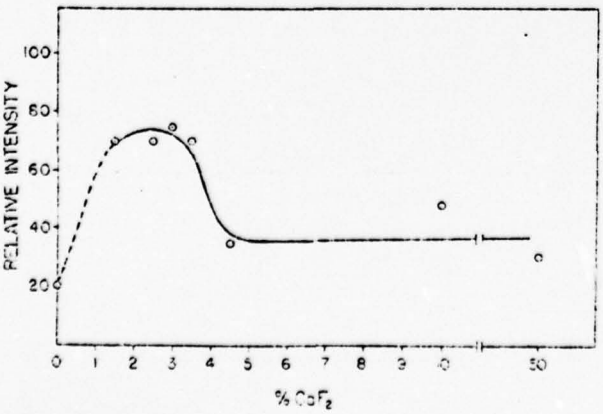


Fig. 8. Variation of relative intensity of 5203 Å peak with CaF_2 concentration in $(CdF_2)_{1-x}(CaF_2)_x$:10% YbF_3:1% ErF_3

CaF_2 concentration of intensity of the strongest green emission band (5203.2 nm.) is shown. For all the compositions CdF_2:10% YbF_3:1% ErF_3:1.5-10% CaF_2 studied, the intensity of the emission bands is significantly enhanced both in the green and red regions of the spectra; however the increase in intensity is not very sensitive to the CaF_2 concentration. There appears to be a plateau for the composition range 1.5-3.5% CaF_2 and a decrease in intensity of the emission bands for the 4.5 and 10% CaF_2-doped samples. The absorption spectra of CdF_2:10% YbF_3:1% ErF_3 doped with 1-10% CaF_2, respectively, show no appreciable diminution in the 976 band intensity, with increasing concentration of CaF_2 at these high Yb^{3+} concentrations. In the light of the results on ^{19}F NMR with the proposed $(M^{3+}$-$F^-)_2$ dimers, it is tempting to propose that the effect of CaF_2 may be enhancement of the formation of mixed pair complexes (Er^{3+}-$F_{int.}^-$-Yb^{3+}) over pure complexes (Er^{3+}-$F_{int.}^-$-Er^{3+}) or (Yb^{3+}-$F_{int.}^-$-Yb^{3+}). Such centers would provide the most efficient energy transfer path for upconversion. Previous work has shown that the 976 nm band does not decrease appreciably in intensity when a second rare earth ion is present (8).

Efficiency.—The quantum efficiency of CdF_2:10% YbF_3:1% ErF_3 and CdF_2:10% YbF_3:1% ErF_3:2.5% CaF_2 crystals, respectively, was measured as follows: the crystal was placed near the dome of the GaAs:Si diode and the fluorescent output was measured by a Clairex-CL-603 cadmium selenide photocell in conjunction with a Keithley 149 micromillivoltmeter. The voltage reading of the meter with diode alone (= A = total infrared emission), the diode plus phosphor (= B = total infrared transmitted and visible emitted), and the diode + phosphor + filter (= C = visible emitted and transmitted by the filter) was measured, and the quantum efficiency calculated from the formula

$$\eta = \frac{C \times f}{A - B}$$

where f = attenuation factor of the filter (Corning No. 1-57). The formula, although approximate, is valid when $Cf << (A - B)$, which is true in this case. Determined in this way, the quantum efficiency of CdF_2:10% YbF_3:1% ErF_3 is 0.23% and that of CdF_2:10% YbF_3:1% ErF_3:2.5% is 0.70%. The efficiency of green emitting GaP diode is about 0.1% (18). The quantum efficiency of the most efficient upconverting systems is between 10^{-2} and 10^{-1}% (λ_{ex} = 0.97 μm) (19). These values are difficult to compare due to differences in the condition of measurement. Our measurements were on single crystals, and well-known upconverting phosphors are available as powders. Grinding our samples would expose them to the well-known degradation of luminescence efficiency by crystal damage. Since our measurements were made at high excitation densities, the reported high efficiency compared to other materials may be attributable to this, at least in part. On the other hand, preliminary excitation studies on this phosphor system indicate that the quantum efficiency would most likely be improved with 976 nm excitation. These studies show a major excitation peak near 976 nm, corresponding to the "dimer" absorption band. A complete study of the excitation spectra is now in progress.

Conclusion

A new efficient infrared to visible upconverting system CdF_2:YbF_3:ErF_3:CaF_2 in single crystal form has been prepared. At the optimum concentrations of the rare earth ions (10 Yb:1 Er) and codoped with ~3.5% CaF_2, in combination with a GaAs:Si diode emitting at ~0.93 μm the phosphor fluoresces a bright green. Quantum efficiency measurements indicate this system to be a highly efficient upconverting phosphor.

The upconverting properties of the system codoped with NaF are in agreement with previously measured spectroscopic properties of the CdF_2:Yb system and

support the existence of $(M^{3+}$-$F_{int.}^-)_2$ dimers, or similar complex centers.

The enhancement of the upconversion upon introducing CaF_2 into the system is contrary to predictions based on previously reported spectral data in the CdF_2:CaF_2:Yb system, which showed quenching of the intense 976 nm absorption band. The quantum efficiency of the most efficient phosphor system CaF_2: 10% YbF_3:1% ErF_3:2.5% CaF_2 studied is 0.70%.

Acknowledgments

The authors thank G. DeLhery of the U.S. Army Signal Research and Development Laboratory for quantum efficiency measurements. This research was supported by Grants DA-ARO-D-31-124-G-1056, DA-ARO-D-31-124-72-G-7, and DAAG-29-75-G-0096 from the Army Research Office, Durham, North Carolina, and contract No. F44620-74-C-0056, Joint Services Electronics Program.

Manuscript submitted Aug. 16, 1976; revised manuscript received Oct. 30, 1976.

Any discussion of this paper will appear in a Discussion Section to be published in the December 1977 JOURNAL. All discussions for the December 1977 Discussion Section should be submitted by Aug. 1, 1977.

REFERENCES

1. N. Bloembergen, *Phys. Rev. Lett.*, **2**, 84 (1959).
2. F. Auzel, *Compt. Rend.*, **262**, 1016 (1966).
3. F. W. Ostermeyer, Jr., *Metall. Trans.*, **2**, 747 (1971).
4. R. A. Logan *et al.*, *Appl. Phys. Lett.*, **13**, 139 (1968).
5. L. G. Van Uitert *et al.*, *Mater. Res. Bull.*, **4**, 777 (1969).
6. M. Rubenstein and E. Banks, *This Journal*, **106**, 104 (1959).
7. E. Banks and P. Wagner, *J. Chem. Phys.*, **44**, 713 (1966).
8. V. Abbruscato, E. Banks, and B. R. McGarvey, *ibid.*, **49**, 903 (1968).
9. M. T. Weber and R. W. Bierig, *Phys. Rev.*, **134**, A1492 (1963).
10. P. Weller, *Inorg. Chem.*, **5**, 736 (1966).
11. J. S. Prener and J. D. Kingsley, *J. Chem. Phys.*, **38**, 667 (1963).
12. E. Banks, M. Greenblatt, and B. R. McGarvey, *ibid.*, **58**, 4707 (1973).
13. Mustafa *et al.*, *ibid.*, **62**, 2700 (1975).
14. G. H. Dieke, "Spectra and Energy Levels of Rare Earth Ions in Crystals," p. 142, Interscience, New York (1968).
15. L. F. Johnson *et al.*, *J. Appl. Phys.*, **43**, 1125 (1972).
16. J. L. Sommerdijk and A. Bril, *Philips Tech. Rev.*, **34**, 24 (1974).
17. Y. Sekiguchi and Y. Furukawa, *Jpn. J. Appl. Phys.*, **10**, 891 (1971).
18. L. F. Johnson *et al.*, *Appl. Phys. Lett.*, **15**, 48 (1969).
19. A. Bril *et al.*, *This Journal*, **122**, 660 (1975).

Reprinted from JOURNAL OF THE ELECTROCHEMICAL SOCIETY
Vol. 124, No. 3, March 1977
Printed in U.S.A.
Copyright 1977

Detection of dimers by ^{19}F NMR in CdF_2 doped with ErF_3 and YbF_3

M. R. Mustafa, W. E. Jones*, and B. R. McGarvey

Department of Chemistry, University of Windsor, Windsor, Ontario, Canada

M. Greenblatt† and E. Banks

Department of Chemistry, Polytechnic Institute of New York, Brooklyn, New York
(Received 25 November 1974)

The ^{19}F NMR of single crystals of CdF_2 containing large concentrations of ErF_3 or YbF_3 has been studied at 30 and 46.5 MHz from 190° to 373°K. In addition to the main resonance, two types of weaker resonances were detected: one type displaying symmetry about the [111] axis and the other displaying symmetry about the [100] axis. The 111 lines are attributed to the lattice fluorides adjacent to one rare earth ion while the 100 lines are attributed to the interstitial fluoride. It is shown that the anisotropy of the interstitial fluoride resonance can only be explained by the presence of two rare earth ions at 90° angles and therefore the bulk of rare earth ions and interstitial fluorides must be present as $(RE^{3+} - F_i^-)_2$ dimers. The anisotropic portion of the NMR shifts is shown to be entirely due to the dipolar contribution of spin residing on the rare earth ion. Further it is shown that the isotropic shift is of opposite sign to that predicted by the equation currently used to explain contact shift of lanthanide ions.

I. INTRODUCTION

Extensive studies have been made on rare earth ions doped into a fluorite lattice, principally CaF_2. The fluorite lattice consists of fluoride ions at the corners of a cube with every other body centered position being occupied by an alkaline earth ion. If a rare earth fluoride is used as a dopant, the trivalent rare earth ion (RE^{3+}) enters the lattice substitutionally at the alkaline earth ion site and charge compensation occurs by incorporation of interstitial fluoride ions in empty body centered positions. If the interstitial fluoride ion occupies the nearest neighbor position forming a dipolar $RE^{3+} - F_i^-$ unit referred to as an ion-defect pair, the local symmetry of the rare earth ion is tetragonal. If such a pair is not formed the symmetry is cubic. ESR and optical studies at low concentrations of RE^{3+} have shown that both types of sites are present.

Cadmium fluoride also has a fluorite lattice and ESR and ENDOR studies[1–4] have shown only a cubic site for the rare earth at low concentrations. Optical studies[1,5] of Yb^{3+} in CdF_2 have found an intense peak at 10 250 cm^{-1} that is not attributable to f-f transitions in an isolated Yb^{3+} ion in either a cubic or tetragonal site.

Some recent studies[6–12] have been concerned with higher concentrations of rare earth ions to determine any differences in the environment of the ion as the concentration of the dopant increases. Makovsky[6] noticed the appearance of additional lines in the optical spectrum of calcium fluoride doped with Gd^{3+} ions as the concentration increased. These were referred to as the "ambiguous lines" and were attributed to the substitution of three gadolinium ions for two calcium ions. O'Hare[9] proposed the formation of a separate phase at higher concentrations while Naberhuis and Fong[3] carried out a detailed calculation for such systems which showed that ion-defect pairs dimerize to form clusters. Fenn *et al.*[10] also proposed the formation of dimers and higher order clusters in their optical study of the ErF_3–CaF_2 system.

Although the size of the rare earth ion is comparable to the size of the divalent cation it replaces, the increased charge of the RE^{3+} ion and the larger size of the interstitial fluoride ion should cause an appreciable distortion in the fluoride ion lattice in the vicinity of the rare earth ion. Cheetham *et al.*[13,14] have tried to measure this distortion by neutron diffraction studies on single crystals of CaF_2 containing large concentrations of YF_3. It was found that the interstitial fluorides were displaced from the normal body centered position along the [110] direction while some of the lattice fluorides were displaced along the [111] direction. Although the positions of the Y^{3+} ions were not determined, it was postulated that the ion-defect pairs formed dimeric clusters. Catlow[15] calculated the formation energy of such a cluster and by minimization of the energy calculated a set of coordinates for the nearby lattice fluorides, as well as those of the atoms forming the dimer.

With the exception of the neutron diffraction studies, most studies on doped fluorite systems have determined the environment in the vicinity of the rare earth ion by measuring magnetic or optical properties of the rare earth ion. Recently Banks, Greenblatt, and McGarvey[16] and Wolfe and Markiewicz[17] have shown that the NMR of the fluoride ions in the vicinity of the rare earth ions can be detected, thus allowing the determination of the environment of the fluoride ion. Wolfe and Markiewicz[17] measured the ^{19}F NMR of CaF_2 single crystals containing only 0.05% Yb^{3+} at liquid He temperatures. They were able to detect the lattice fluorides for the cubic site and the lattice and interstitial fluoride for the tetragonal site. At this concentration no dimers or clusters were detected or expected. Although the actual distances of the fluorides from the rare earth ion cannot be determined from the NMR shifts, it was possible to determine that considerable distortion of the lattice

Copyright © 1975 American Institute of Physics

fluorides occurs in the tetragonal site.

Banks *et al.*[16] measured the ^{19}F NMR of single crystals of CdF_2 containing 10% ErF_3 and YbF_3 at room temperature and were able to identify resonances from the lattice fluorides adjacent to a rare earth ion in the case of the Er^{3+} doped crystal. They showed that the anisotropy in the shift was determined only by the distance between the rare earth ion and molar susceptibility of the ion, and therefore, the shift could be used to measure fluoride–rare earth distances. No definite conclusions could be drawn, however, regarding interstitial ions or cluster formation due to limited resolution and signal to noise at the frequencies of measurement (8 and 16 MHz). Measurement of NMR at room temperatures has two drawbacks in comparison to the type of NMR done by Wolfe and Markiewicz[17] at 4 °K: it is much less sensitive and the resolution of signals from different fluoride ions is much poorer. Its main advantage, other than the obvious one of easily achievable temperatures, is that the shift is determined by a thermal average over all crystal field states of the lowest J manifold and this average can be related to the molar magnetic susceptibility, which can be measured for the sample being studied. As will be shown in this article, this allows meaningful distances to be calculated from measured NMR shifts. A similar analysis of shifts measured at 4 °K requires a knowledge of the wavefunction of the lowest crystal field state in the J manifold and this is often either not available or readily obtainable.

It was apparent that the work of Banks *et al.*[16] should be extended to higher frequencies which would give both better resolution and better sensitivity for detecting signals from less abundant species in the crystal. It was also hoped that lowering the temperature might improve resolution since the shifts should vary inversely with the absolute temperature. We have, therefore, constructed a NMR spectrometer operating at 30 and 46 MHz with a variable temperature Dewar big enough to hold the large crystals used in this study.

II. EXPERIMENTAL

The NMR spectra were obtained using a broad line spectrometer constructed in our laboratory using mostly the components in our Varian E-12 ESR spectrometer to which were added an rf transmitter, a bridge, and an rf amplifier. The transmitter was a Logimetric Signalock 925 operating between 0.5 and 80 MHz, rf amplifiers for 30 and 46 MHz were designed and constructed in our electronic shop. The bridge circuit was a bridged-T null circuit (No. 2) described by Tuttle.[18] This circuit has the advantage of delivering maximum rf signal to the sample for a given output of the transmitter since it is basically a series resonant tuned circuit. Its main disadvantage was impedance matching to the rf amplifier. The samples studied here have very short T_1's and the higher power available in this bridge made it easier to achieve acceptable signal to noise ratios. For some very weak resonances it was found necessary to use sweep times of up to 30 min to plot the spectrum. In these cases it was found difficult to keep the bridge tuned to display only the absorption mode signal. This problem was rectified by adding an automatic frequency control circuit which kept the transmitter tuned to the bridge.

The crystals were the same as those used in an earlier study.[15] They were cylinders approximately 1 cm in diameter and were mounted on a perspex rod which had a hole drilled into it at the desired angle with a diameter equal to that of the crystal. For room temperature rotation studies a coil was wound directly around the rod and crystal to obtain a maximum filling factor. Rotation studies at room temperature were done by rotating the magnet through 180° when the crystals were mounted with either the [100] axis or the [110] axis parallel to the axis of rotation.

The resonance was studied at different temperatures by using a specially constructed dewar (with the coil wound around the outside) that connected to the Varian ESR variable temperature accessory. The temperature of the sample was measured by means of a thermocouple touching the top of the crystal. By this means it was possible to follow the temperature dependence of the paramagnetic shift from 190° to 373 °K. The lower temperature limit was determined by the fact that the satellite lines observed became too broad for detection at temperatures lower than 190 °K.

The magnetic susceptibility and its temperature dependence were determined by Professor Lever of York University, on powder samples obtained from the crystals studied.

III. RESULTS

Single crystals of CdF_2 containing ≃10 mole percent ErF_3 and ≃6 mole percent YbF_3 were mounted such that the magnetic field could be rotated in the (100) and (110) planes. Typical spectra for both crystals are given in Fig. 1. The large resonance is due to the bulk of lattice fluorides that are not close to a rare earth ion. This resonance is used as an internal reference for measuring the shift of other lines to avoid any corrections for

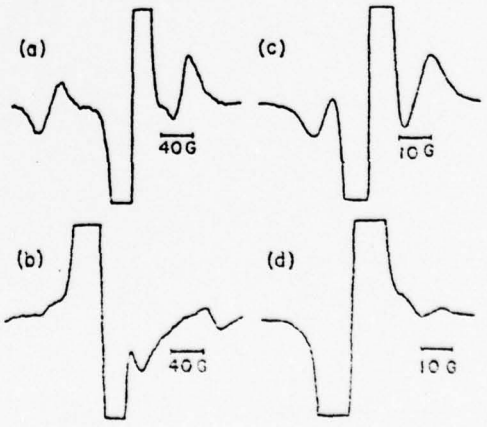


FIG. 1. Typical ^{19}F NMR spectra at 46.8 MHz of cadmium fluoride crystals doped with Er^{3+} and Yb^{3+} ions. (a) CdF_2–ErF_3 at orientation along [111] axis. (b) CdF_2–ErF_3 at orientation along [100] axis. (c) CdF_2–YbF_3 at orientation along [111] axis. (d) CdF_2–YbF_3 at orientation along [100] axis.

the large demagnetization fields present inside the crystal. The spectra recorded for the magnetic field along the [111] axis are given in Fig. 1(a), (c). The two small resonances on either side of the main resonance are those previously seen[18] at lower frequencies for the CdF_2–ErF_3 crystal which had been identified as being from lattice fluorides adjacent to one rare earth ion. When the magnetic field is close to a [100] axis a new weaker resonance was found upfield from the main resonance peak. This resonance can be seen in Fig. 1(b), (d). The other resonances are not seen in this orientation because they occur under the main resonance. This resonance maximizes its shift along the [100] axis and will be called the 100 line while the other resonance lines will be called the 111 lines since they are symmetrical about the [111] direction.

Increasing the frequency of the NMR spectrometer does not increase the resolution and sensitivity as much as expected, because the linewidth of all lines was found to increase with frequency. For pure CdF_2 the second moment[19] of the ^{19}F resonance is 2.40 G^2 when the magnetic field is along the [111] axis and this should give a linewidth of 3.1 G in the derivative of the absorption curve. Experimentally we find that the linewidth of all lines increases linearly with frequency from this value. At 46.6 MHz the width of the central line is 15 G in the ErF_3 crystal and 6 G in the YbF_3 crystal while the 111 lines are 25 G and 9 G, respectively. The extra widths for corresponding lines are roughly in the ratio of the rare earth ion's susceptibility indicating the extra broadening is caused by the magnetic ions. The width of the 111 lines increases almost twofold as the magnetic field moves away from the [111] axis.

In Figs. 2 and 3 are plotted the shifts ΔH of the various lines relative to the center main resonances as a function of orientation. The angle ω is a laboratory angle of the magnetic field and is approximately the angle of the [110] axis of the crystal. The solid lines in Figs. 2 and 3 are obtained by fitting the experimental

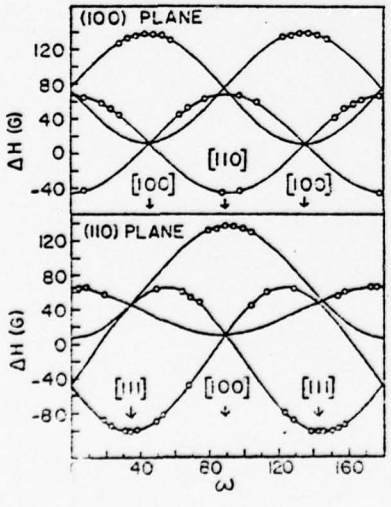


FIG. 2. Orientation dependence of various ^{19}F NMR lines at 46.6 MHz for CdF_2–ErF_3 crystal. The circles indicate experimental points while the solid lines are curves fitted to Eq. (1).

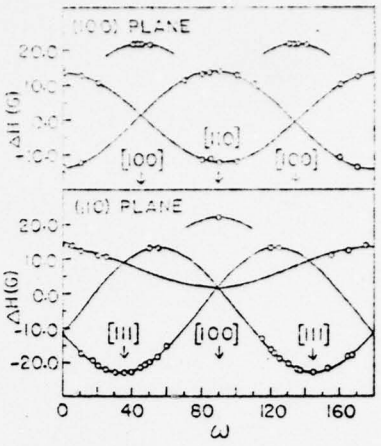


FIG. 3. Orientation dependence of various ^{19}F NMR lines at 46.6 MHz for CdF_2–YbF_3 crystal. The circles indicate experimental points while the solid lines are curves fitted to Eq. (1).

points to the equation.

$$\Delta H = (\Delta H_{max} - \Delta H_{min}) \cos^2(\omega - \omega_{max}) + \Delta H_{min} \tag{1}$$

by a least squares refinement. In these plots we have only included data from those spectra in which the resolution was sufficient to accurately determine the line centers. The existence of the satellite lines is apparent at smaller shifts but it is difficult to determine the center due to overlap with the large resonance from the bulk lattice fluorides.

It is clear from Figs. 2 and 3 that the 111 lines are from fluoride ions in sites of axial symmetry with the symmetry axis along a [111] crystal axis. The shift is down field when the magnetic field is along the [111] axis and upfield when perpendicular to the [111] axis. For the 100 lines in CdF_2–ErF_3 the fitted curves predict a minimum shift of 12 ± 15 G for the rotation of magnetic field in the (100) plane and 7 ± 15 G for the rotation in the (110) plane. Since these extrapolated values are the same within experimental error we must conclude that the 100 resonance displays axial symmetry around the [100] axis. Unlike the 111 resonance lines, however, these lines have a large upfield shift when the magnetic field is parallel to the symmetry axis.

The basic theory for paramagnetic shifts in the ^{19}F NMR of single crystals of transition metal fluorides[20–24] predicts the shift to be given by the equation

$$\Delta H/H = -[a_s + (a_p + a_M)(3\cos^2\theta - 1)] \tag{2}$$

in which θ is the angle between the magnetic field and the axis between the fluoride ion and the magnetic ion, a_s is the isotropic contribution from the Fermi contact interaction, a_p is the dipolar contribution of an unpaired spin in the fluorine $2p$ orbital, and a_M is the direct dipolar contribution from unpaired spin on the metal ion. Values of a_s and $(a_p + a_M)$ at 25 °C are tabulated in Table I for the different frequencies at which they have been measured. The values for the 100 line in CdF_2–YbF_3 could not be determined directly because it was not possible to observe the line over more than a 10°

TABLE I. Values of a_s and (a_p+a_d) at 25 °C for the 111 and 100 NMR lines observed in CdF_2 crystals doped with ErF_3 or YbF_3.

Crystal	Line	NMR frequency (MHz)	Percent of fluorides	$a_s\times10^3$	$(a_p+a_d)\times10^3$
CdF_2–ErF_3	111	16.0	30±4[a]	−1.0±0.1[a]	4.85±0.10[a]
		46.6	28±4	−0.9±0.1	4.85±0.09
	100	46.6	6±3	−4.6±0.9	−3.7±0.5
CdF_2–YbF_3	111	30.0	–	−0.2±0.1	1.1±0.1
		46.6	20±4	−0.12±0.07	1.06±0.04
	100	46.6	6±3	−0.3±0.1[b]	−0.81±0.02[b]

[a]See Ref. 16.
[b]Estimated by procedure given in text.

interval. These values have been estimated by assuming that the ratio of the (a_p+a_d) terms for the 100 lines is the same as for the 111 lines in the two crystals. This assumption is justified in the discussion and allows us to assign a value to a_s from the observed shift of this line in the [100] direction.

An attempt has been made to estimate the percentage of fluoride ions giving rise to each type of resonance by numerical integration of experimental curves to determine relative areas. The values obtained are also included in Table I. In the case of the 111 lines, the area of the downfield 111 line was determined when the magnetic field was along the [111] direction. This was then compared to the total integrated area of all lines in the spectrum. Since this line represents only one fourth of the fluoride ions giving rise to the 111 lines, the resulting value was multiplied by four. A similar measurement was made for the 100 line in the [100] orientation and this value multiplied by three. Since this double integration depends strongly upon good determinations of the curve in the wings, it was checked by estimating the area ratios from the values of (derivative peak heights)×(linewidth)^2 for each line in the spectrum. The ratios of these values should be proportional to areas if the shape of all resonance lines are similar. This method of estimation gave values in reasonable agreement with those given in Table I.

The temperature dependence of a_s and (a_p+a_d) for the 111 lines was determined by mounting the crystal in an orientation that gave two resolved 111 lines, one upfield and one downfield from the main line. The value of θ in Eq. (2) for each line was determined from the room temperature plot and data in Table I. a_s and (a_p+a_d) could then be calculated from the measured shift of the two lines. The data are given in Table II. The linewidths of the 111 lines increased as the temperature went down to values of 85 G for ErF_3 and 17 G for YbF_3 at 190 °K for the downfield lines.

It is expected on theoretical grounds, that a_s and (a_p+a_d) are proportional to the magnetic susceptibility χ of the rare earth ion. To check this, sections of both crystals were sliced and powdered and the susceptibility was measured from 80° to 460 °K. After correction for diamagnetic contributions, the susceptibility was found to follow the Curie law

$$\chi = C/(T+T_c), \tag{3}$$

with Curie temperatures $T_c = 15\pm1$ °K for the ErF_3 doped crystal and $T_c = 44\pm1$ °K for the YbF_3 doped crystal.

IV. DISCUSSION

In the previous study[16] of the CdF_2–ErF_3 crystal at lower frequencies, the 111 lines were attributed to the lattice fluorides adjacent to one rare earth ion. This is the only reasonable assignment since these are the closest fluorides and should have the largest shifts as well as a symmetry about the [111] axis. The a_d term in Eq. (2) can be calculated[25,26] from

$$a_d = \chi/R^3, \tag{4}$$

where χ is the magnetic susceptibility per ion and R is the distance between the fluoride and the rare earth ion. The values of a_d at 25 °C calculated from experimental values of χ and assuming $R = 2.333$ Å (the $Cd^{2+}-F^-$ distance in CdF_2) are 4.34×10^{-3} and 1.14×10^{-3} for the CdF_2-ErF_3, and CdF_2-YbF_3, respectively. These values are close to the experimental values of (a_p+a_d). Since the concentration of rare earth ion is known only approximately for these crystals, it might be better to calculate χ in Eq. (4) from

$$\chi = g_J^2 J(J+1)\beta_e^2/3kT. \tag{5}$$

This gives for a_d the values 3.04×10^{-3} for CdF_2-ErF_3 and 1.13×10^{-3} for CdF_2-YbF_3 which are in even better agreement with the experimental values of (a_p+a_d). Thus it appears that $a_p \simeq 0$ in these crystals.

The 100 lines must originate from the interstitial

TABLE II. Values of a_s and (a_p+a_d) for the 111 NMR lines at different temperatures.

	CdF_2–ErF_3			CdF_2–YbF_3	
°K	$a_s\times10^3$	$(a_p+a_d)\times10^3$	°K	$a_s\times10^3$	$(a_p+a_d)\times10^3$
193	−1.2±0.2	5.2±0.2	193	−0.15±0.05	1.20±0.05
203	−1.2±0.2	5.1±0.2	213	−0.15±0.05	1.18±0.05
223	−1.1±0.2	5.0±0.2	233	−0.13±0.05	1.15±0.05
243	−1.1±0.2	4.9±0.2	253	−0.13±0.05	1.13±0.05
253	−1.0±0.1	4.8±0.2	273	−0.11±0.05	1.11±0.05
273	−1.1±0.1	4.8±0.2	293	−0.11±0.04	1.09±0.04
293	−0.90±0.05	4.65±0.15	313	−0.12±0.03	1.07±0.03
313	−0.80±0.05	4.52±0.15	333	−0.11±0.03	1.07±0.03
333	−0.72±0.05	4.40±0.15	353	−0.12±0.03	1.06±0.03
353	−0.64±0.05	4.31±0.15	373	−0.11±0.03	1.06±0.03
373	−0.61±0.05	4.24±0.15	393	−0.12±0.03	1.06±0.03

fluorides because the interstitial site is the only one that can have axial symmetry along the [100] axis relative to the metal ions. This is confirmed by the intensity measurements. The percentage of interstitial fluorides in CdF_2–ErF_3 and CdF_2–YbF_3 are 4.8 percent and 5.9 percent, respectively, and these are equal (within experimental accuracy) to the percentage of fluorides giving the 100 lines. The resonance cannot come from an ion defect pair, however. If we assume a_p is negligible, as for the 111 lines, then a_M for an ion defect pair is given by Eq. (4) which predicts a value of $(a_p + a_M)$ opposite in sign to that found for the ErF_3 doped crystal (see Table I). This interstitial fluoride then must be associated with more than one rare earth ion in some sort of cluster.

The most obvious arrangement that will both have axial symmetry about a [100] axis and predict a_M values of opposite sign to that given by Eq. (4) is a planar cluster in which each interstitial fluoride is surrounded by four rare earth ions occupying the adjacent metal ion sites. This cluster will have a symmetry axis perpendicular to the plane of the five ions and will give an a_M value of

$$a_M = -2\chi/R^3. \tag{6}$$

A check of this model can be made by noting that χ is the same for both the 111 resonances and the 100 resonances so that we can obtain the ratio of R_{100}/R_{111} from the experimental ratio of a_M's for the two lines. Using data from Table I for CdF_2–ErF_3 and Eqs. (4) and (6) we obtain $R_{100}/R_{111} = 1.38$. If the CdF_2 lattice is not distorted this ratio should be 1.15. Although we cannot expect the lattice to remain undistorted it is unlikely that we would find this great a difference in the ratio of R_{100}/R_{111}. Although rather unlikely on other grounds, it is possible to explain a larger value of this ratio by assuming the four rare earth ions occupy the nearest interstitial sites rather than the nearest metal ion sites. For an undistorted lattice R_{100}/R_{111} would equal 1.63 which again agrees poorly with the value 1.38 found from experiment.

A third model can also explain the [100] symmetry and negative sign of a_M. If we assume that only two adjacent metal ion sites are occupied by rare earth ions and that these sites are 90° apart in direction from the interstitial fluoride, we find that we get accidental axial symmetry in the magnetic shifts, even though the true symmetry is not axial. As long as the angle is 90°, the shift will be the same everywhere in the plane of the three ions. In this case a_M will be exactly half that given by Eq. (6) and experiment predicts a value of $R_{100}/R_{111} = 1.09$ which is very close to the expected value of 1.15 for an undistorted lattice.

Since the percentage of fluoride ions giving rise to the 100 lines is equal to the percentage of interstitial fluorides in the lattice which are in turn equal to the number of rare earth ions in the lattice, our analysis indicates that the bulk of the rare earth ions in CdF_2 are associated in either dimer clusters

$$\begin{array}{ll} RE^{3+} & -F_i^- \\ | & | \\ F_i^- & -RE^{3+} \end{array}$$

or in extended chains of alternating rare earth ions and interstitial fluorides with right angle bends at each interstitial fluoride. We searched in vain for interstitial fluoride resonances from either a single ion defect pair or a linear RE^{3+}–F_i^-–RE^{3+} cluster. These fluorides should have a downfield shift when the magnetic field is along the [100] direction and should be easily resolvable if the intensity were great enough. We estimate from our search that such interstitial fluorides must be present at concentrations of less than 0.5 percent in the lattice since we could not detect them. There should also be a third type of fluoride resonance in these clusters, namely, those lattice fluorides which are adjacent to both rare earth ions. There should be six of these lines each with an intensity equal to that of one of the 100 lines. Unfortunately these lines could not be observed, although we tried. The best orientation for detection would be with the [110] axis parallel to the field but at this orientation the stronger 111 lines are also shifted in the same direction making resolution difficult.

The frequency dependent linewidth of the main line is undoubtedly due to magnetic broadening by the rare earth ions in the lattice. We have estimated this broadening by using Van Vleck's[19] second moment equation and assuming $\mu = \chi H$ and find that the experimental linewidths are of the expected order of magnitude. The greater breadth of the 111 lines is probably due to distortions of the lattice fluorides from normal lattice sites when they are adjacent to a rare earth ion. Wolfe and Markiewicz[17] have shown that such distortions exist for the ion defect pair in CaF_2. Catlow[16] has calculated these distortions for the dimer in CaF_2–YF_3 crystals. We have calculated the expected spectrum for CdF_2–ErF_3 using Catlow's coordinates and find it impossible to fit to our results and conclude that distortions of both lattice fluorides and interstitial fluorides from normal lattice sites is much less in CdF_2 than Catlow estimated for the CaF_2–YF_3 system.

If $a_p = 0$, as seems to be the case, then Eq. (4) predicts that a plot of $(a_p + a_M)/\chi$ versus temperature should give a straight line of zero slope. The generally accepted theory[27,28] for a_s predicts the same for a_s/χ. Both of these values are plotted in Fig. 4. Within experimental error a_s/χ and $(a_p + a_M)/\chi$ are seen to be in-

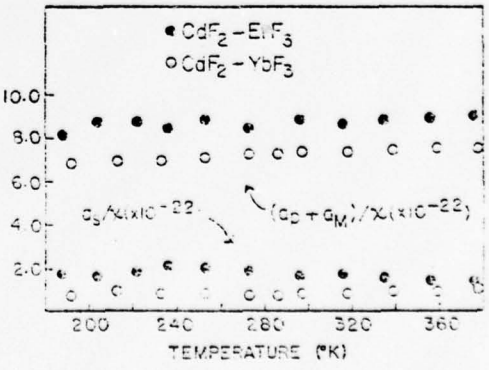


FIG. 4. a_s/χ and $(a_p + a_M)/\chi$ vs absolute temperature T. χ is the atomic susceptibility.

dependent of temperature. Further the value of a_s/χ like that of $(a_z - a_x)/\chi$ is approximately the same for both Er^{3+} and Yb^{3+}. Any differences noted in Fig. 4 are not significant since the value of χ used depended on our knowledge of the concentration of rare earth ion in the crystal and this was known only approximately.

V. CONCLUSIONS

This work has conclusively established that at high doping concentrations of rare earth fluorides in CdF_2, the main species is an ion defect pair dimer of the type postulated by several workers[3,10,12,13-15] for CaF_2 and not the cubic phase postulated by O'Hare.[9,11] It is anticipated that the same will be found for CaF_2 crystals but a similar study should be undertaken on them to confirm this fact. Further the results of this work suggest a ready explanation for the unusual optical bands found[1,5] in CdF_2–YbF_3 crystals at lower concentrations. If we suppose that some dimer is formed at these lower concentrations then the bands can be attributed to it. The fact that only the ESR of Yb^{3+} in cubic sites[1,2] was observed is then explained by assuming that spin exchange interactions in the dimer made ESR detection of the rare earth ions in the dimers impossible.

The fact that the anisotropy in the NMR shifts is due entirely to a_s, and our use of this to establish the existence of dimers in the lattice suggest that similar NMR studies on rare earth single crystals is potentially useful for determining the position of magnetic nuclei near a rare earth ion. ENDOR studies on Yb^{3+} in CdF_2[2] and CaF_2[29] as well as a low temperature NMR study of Yb^{3+} in CaF_2[17] have found that the anisotropy in the ^{19}F hyperfine interaction for lattice fluorides in the cubic sites is much larger than can be accounted for by a dipolar interaction between the spin on the rare earth ion and the fluorine nucleus. This at first appears contradictory to our observation that $a_p = 0$. However, these low temperature measurements are of only the hyperfine interaction in the lowest crystal field state of the ion while our measurements reflect a thermal average over all crystal field states of the lowest J manifold. It would appear that the extra anisotropy is averaged out. Preliminary calculations show that this would be unlikely if the extra anisotropy in the ground state resulted from partial occupation of fluorine p orbitals by the unpaired f electron. Rather our calculations show that this situation would result if the extra anisotropy was an anisotropic Fermi contact term produced by an indirect polarization mechanism.

The values of a_s are all negative and the values for the interstitial ions are more than triple in magnitude to those for the closer lattice ions. It has been customary for researchers studying NMR shifts in lanthanide complexes to assume that the shift for atoms adjacent to rare earth ions is Fermi contact in nature and that a_s is given by the equation[27,23,30]

$$a_s = -\frac{\langle S_z \rangle_{J,z}}{g_N \beta_N H} A_s = \frac{(g_J - 1)\chi}{g_J g_N \beta_e \beta_N} A_s , \qquad (7)$$

where $\langle S_z \rangle_{J,z}$ is a thermal average of spin in z direction over the J manifold, A_s is the isotropic hyperfine interaction term, β_e and β_N are electronic and nuclear magnetons, and χ is the susceptibility per ion. Implicit in the derivation of Eq. (7) is the assumption that A_s is the same for all crystal states of the J manifold. It appears that our results show this assumption to be false. ENDOR studies of Yb^{3+} in CdF_2[2] and CaF_2[29] show that A_s is positive for the ground state of Yb^{3+} in cubic sites. Thus by Eq. (7) a_s should also be positive rather than the observed negative value. Wolfe and Markiewicz[17] have also found that A_s is positive for Yb^{3+} in cubic sites and have shown that it is large and positive for one set of lattice fluorides next to the ion defect pair and small and negative for the second set. The average A_s (which is all we would observe in our experiments) would however still be positive. Further, although they find A_s to be negative for the interstitial fluoride ion, consistent with our value of a_s, its magnitude is smaller than that of the fluorides adjacent to the rare earth ion contrary to what we observed for the a_s values. These arguments strongly suggest that Eq. (7) is incorrect and any conclusions based on its use must be carefully reexamined.

ACKNOWLEDGMENTS

The support of this research by the National Research Council of Canada and the National Science Foundation, U.S.A. is gratefully acknowledged.

*Present address: Department of Chemistry, Howard University, Washington, D.C.

†Present address: Department of Chemistry, Rutgers University, New Brunswick, NJ.

[1] V. Abbruscato, E. Banks, and B. R. McGarvey, J. Chem. Phys. 49, 903 (1968).
[2] T. Chang, M. I. Cohen, and W. R. Hosler, J. Chem. Phys. 54, 4278 (1971).
[3] T. C. Ensign, J. Chem. Phys. 54, 5188 (1971).
[4] R. Valentin, Phys. Lett. A 30, 344 (1969).
[5] E. Banks and P. Wagner, J. Chem. Phys. 44, 713 (1966).
[6] J. Makovsky, Phys. Lett. 19, 647 (1966).
[7] M. R. Brown, K. G. Roots, J. M. Williams, W. A. Shand, C. Grater, and H. F. Kay, J. Chem. Phys. 50, 891 (1969).
[8] S. L. Naberhuis and F. K. Fong, J. Chem. Phys. 56, 1174 (1972).
[9] J. M. O'Hare, J. Chem. Phys. 57, 3836 (1972).
[10] J. B. Fenn, Jr., J. C. Wright, and F. K. Fong, J. Chem. Phys. 59, 5591 (1973).
[11] J. M. O'Hare, T. P. Graham, and G. T. Johnston, J. Chem. Phys. 61, 1602 (1974).
[12] F. K. Fong, J. Chem. Phys. 61, 1604 (1974).
[13] A. K. Cheetham, B. E. F. Fender, D. Steele, R. J. Taylor, and B. T. M. Willis, Solid State Commun. 8, 171 (1970).
[14] A. K. Cheetham, B. E. F. Fender, and M. J. Cooper, J. Phys. C 4, 3107 (1971).
[15] C. R. A. Catlow, J. Phys. C 6, L64 (1973).
[16] E. Banks, M. Greenblatt, and B. R. McGarvey, J. Chem. Phys. 58, 4787 (1973).
[17] J. P. Wolfe and R. S. Markiewicz, Phys. Rev. Lett. 30, 1105 (1973).
[18] W. N. Tuttle, Proc. IRE 28, 23 (1940).
[19] J. H. Van Vleck, Phys. Rev. 74, 1168 (1948).
[20] B. Bleaney, Phys. Rev. 104, 1190 (1956).
[21] R. G. Shulman and V. Jaccarino, Phys. Rev. 103, 1126 (1956); 108, 1219 (1957).
[22] V. Jaccarino and R. G. Shulman, Phys. Rev. 107, 1196 (1957).

[3]A. J. Stillman, Phys. Rev. 141, 127 (1966).
[4]V. Jaccarino, R. C. Stillman, and J. W. Stout, Phys. Rev. 130, 924 (1957).
[5]R. J. Kurland and B. R. McGarvey, J. Mag. Reson. 2, 286 (1970).
[6]E. Blearney, J. Mag. Reson. 9, 91 (1973).
[7]W. E. Lewis, J. H. Jackson, B. F. Lemons, and H. Taube, J. Chem. Phys. 36, 694 (1962).
[8]W. E. Lewis, S. W. Rabideau, N. H. Krikorian, and W. G. Witteman, Phys. Rev. 170, 455 (1968).
[9]U. Ranon and J. S. Hyde, Phys. Rev. 141, 259 (1966).
[10]R. D. Fischer in *NMR of Paramagnetic Molecules*, edited by G. N. LaMar, W. DeW. Horrocks, Jr., and R. H. Holm (Academic, New York, 1973), Chap. 13, pp. 521-552.

[Reprinted from Inorganic Chemistry 15, 2317 (1976).]
Copyright 1976 by the American Chemical Society and reprinted by permission of the copyright owner.

Contribution from the Department of Inorganic and Structural Chemistry, University of Leeds, Leeds LS2 9JT, England, and the Deparment of Chemistry, Polytechnic Institute of New York, Brooklyn, New York, 11201

The Defect Model and Oxidation State of Europium and Molybdenum in Eu_xMoO_4

Norman N. Greenwood,*[1a] Francisca Viegas,[1a] Ephraim Banks,[1b] and Michael Nemiroff[1b]

Received March 26, 1976 AIC60239Y

A new series of tetragonal scheelite-type compounds with stoichiometry Eu_xMoO_4 ($0.67 \leq x \leq 1.00$) was recently reported by Banks[2] and the scheelite solid-solution series $EuMO_4$–$Eu_2(MO_4)_3$ (M = Mo, W) have also been studied by McCarthy.[3] Unit cell parameters and density measurements suggest a cation vacancy model leading to the formulation $Eu^{II}_{1-y}Eu^{III}_{2y}\square MoO_4$ where $y = 1 - x$ and x is the stoichiometric amount of europium in Eu_xMoO_4 (i.e., $Eu^{II}_{3-2x}Eu^{III}_{2x-2}\square_{1-x}MoO_4$). There is some uncertainty though, concerning the oxidation state of molybdenum, and the possible presence of Mo^V has been postulated.[2] We sought to resolve this uncertainty by determining the area ratios of Eu^{II} and Eu^{III} Mössbauer resonance peaks as previously employed by Greenwood et al.[4] for the related phases Eu_xWO_4. Our results allow us to rule out the presence of $[Mo^VO_4]^{3-}$ tetrahedra in the series Eu_xMoO_4, though when gadolinium is also present, as in the two-phase mixture of overall composition "$Gd_{0.5}Eu_{0.5}MoO_4$", then the observed Eu^{II}/Eu^{III} ratio can only be explained by the simultaneous partial reduction of molybdenum(VI) or the much less likely reduction of gadolinium(III).

Experimental Section

Samples were prepared as previously described.[2] The material listed as "$Gd_{0.5}Eu_{0.5}MoO_4$" was, in fact, an equimolar mixture of $Gd_{0.85}Eu_{0.15}MoO_4$ and $Gd_{0.15}Eu_{0.85}MoO_4$.

Mössbauer spectra were obtained using Elscint equipment as previously described,[5] with both source and absorber at 4.2 K. The source was 300 mCi $^{151}SmF_3$ and the resonance line widths were in the range 2.4–3.5 mm s^{-1} for Eu^{III} and 4.3–5.7 mm s^{-1} for Eu^{II}. Samples were mounted with a thickness of 10–20 mg of $^{151}Eu/cm^2$ except for "$Gd_{0.5}Eu_{0.5}MoO_4$" which had 6.7 mg of $^{151}Eu/cm^2$. Acceptable spectra were obtained with about 3×10^6 counts per channel.

Results and Discussion

Typical spectra are shown in Figure 1. The most obvious features are the complete lack of any magnetic hyperfine interaction at 4.2 K and the presence of substantial amounts of Eu^{II}. The relative proportions of Eu^{II} and Eu^{III} in the various samples are shown in the Table I. Experimental values were calculated from the areas of the computer-fitted reso-

Table I. Mössbauer Data and Proportions of Eu^{II} and Eu^{III} in Eu_xMoO_4

Material	$\delta(Eu^{II})$,[a] mm s^{-1}	Percentage Eu^{II} Exptl	Percentage Eu^{II} Theor	$\delta(Eu^{III})$,[a] mm s^{-1}	Percentage Eu^{III} Exptl	Percentage Eu^{III} Theor
$Eu_{0.9}MoO_4$	−11.7	73 ± 2	77.8	+0.6	27 ± 1	22.2
$Eu_{0.7}MoO_4$	−12.1	15 ± 2	14.3	+0.6	85 ± 2	85.7
$Eu_{0.5}MoO_4$		0 ± 0.1	0	+0.7	100 ± 0.1	100
"$Gd_{0.5}Eu_{0.5}MoO_4$"	−12.0	55 ± 0.8	See text	+0.9	45 ± 00.7	See text

[a] Chemical isomer shifts δ are quoted relative to EuF_3 as zero.

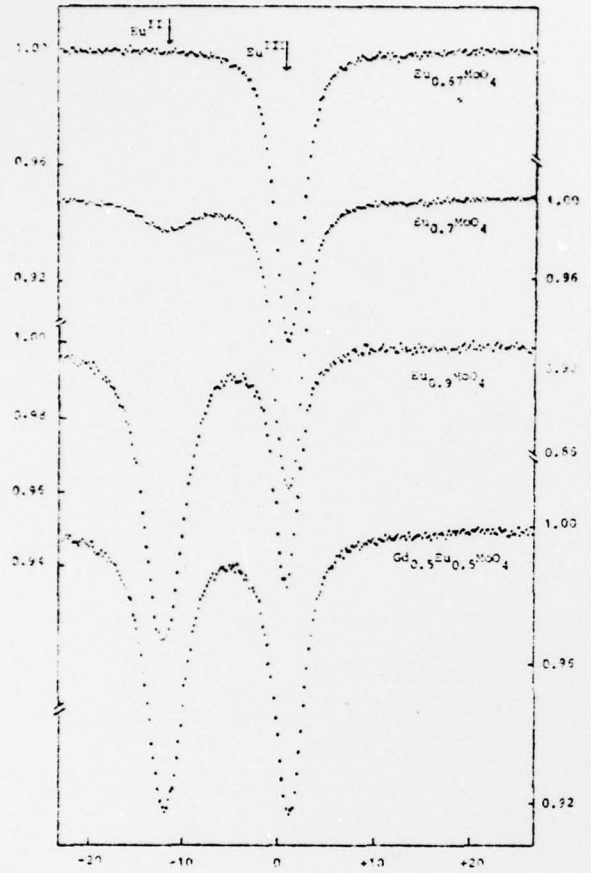


Figure 1.

nances on the assumption that both species have the same Mössbauer recoil-free fraction. The theoretical values were calculated according to the cation vacancy defect model with no contribution from Mo^V. Since saturation effects will tend to decrease the intensity of stronger peaks,[6] the concentration of Eu^{II} in $Eu_{0.9}MoO_4$ will be slightly greater than the uncorrected experimental value of 73% and the concentration of Eu^{III} in $Eu_{0.7}MoO_4$ will be slightly greater than 85%. The close agreement of these values with those calculated on the basis of the cation vacancy model rules out the possibility of any significant reduction of molybdenum to Mo^V and the presence of $[Mo^VO_4]^{3-}$ ions in these phases since this would substantially reduce the concentration of Eu^{II} required for charge balance.

In the case of "$Gd_{0.5}Eu_{0.5}MoO_4$", the two-phase mixture of limiting solid solutions was studied because no samples of the single-phase materials remained from previous work. Table I shows that 45% of all the europium is Eu^{III}. The phase $Gd_{0.85}Eu_{0.15}MoO_4$ contained predominantly $[Mo^VO_4]^{3-}$ ions, implying that both gadolinium and europium are in the 3+ state; this accounts for one-third of the Eu^{III} resonance area. The second phase ($Gd_{0.15}Cu_{0.85}MoO_4$) contains the other two-thirds of the Eu^{III} (i.e., $Eu^{III}_{0.30}$); charge balance then requires that part of the molybdenum in this phase is also present as Mo^V, the detailed formulation being $Gd^{III}_{0.15}Eu^{II}_{0.55}Eu^{III}_{0.30}Mo^V_{0.45}Mo^{VI}_{0.55}O_4$.

Acknowledgment. We thank the U.K. Science Research Council for financial support and Instituto de Alta Cultura (Portugal) for a grant (to F.V.). The work at Polytechnic was sponsored by the U.S. Army Research Office (Durham, N.C.), Grant No. DA-ARO-D-31-124-72-G-7, and the Joint Services Electronic Program under Contract No. F44620-69-C-0047.

Registry No. Eu_xMoO_4, 52322-41-5; $Gd_{0.5}Eu_{0.5}MoO_4$, 59753-15-0.

References and Notes

(1) (a) University of Leeds; (b) Polytechnic Institute of New York.
(2) E. Banks and M. Nemiroff, *Inorg. Chem.*, 13, 2715 (1974).
(3) R. G. Johnston and G. T. McCarthy, *J. Inorg. Nucl. Chem.*, 37, 1923 (1975).
(4) C. S. Dimbylow, I. J. McColm, C. M. P. Barton, N. N. Greenwood, and G. E. Turner, *J. Solid State Chem.*, 10, 128 (1974).
(5) T. C. Gibb, R. Greatrex, N. N. Greenwood, D. C. Puxley, and K. G. Snowdon, *J. Solid State Chem.*, 11, 17 (1974).
(6) N. N. Greenwood and T. C. Gibb, "Mössbauer Spectroscopy", Chapman and Hall, London, 1971.

Electron spin resonance of CrO_4^{3-} in fluoroapatite $Ca_5(PO_4)_3F$

M. Greenblatt and J. H. Pifer

Departments of Chemistry and Physics, Rutgers University, New Brunswick, New Jersey 08903

E. Banks

Department of Chemistry, Polytechnic Institute of New York, Brooklyn, New York 11201

(Received 8 September 1976)

Electron spin resonance spectra measured in CrO_4^{3-} doped fluoroapatite $Ca_5(PO_4)_3F$ single crystals at liquid helium temperature show the presence of three magnetically nonequivalent chromate (V) tetrahedra indicating that hexagonal ($P_{6_3/m}$) fluoroapatite similar to chloro- and hydroxyapatite undergoes a phase transition at low temperature to a phase of lower symmetry. Spin-Hamiltonian parameters determined by an analysis of the electron spin resonance spectra are presented. The ground state of the unpaired d^1 electron is found to be d_{z^2}.

INTRODUCTION

It has been established that both synthetic hydroxyapatite, $Ca_5(PO_4)_3OH$[1,2] and stoichiometric chloroapatite $Ca_5(PO_4)_3Cl$[3] have a monoclinic pseudohexagonal ($P_{2_1/b}$) crystal structure near room temperature and undergo a reversible transition to the hexagonal ($P_{6_3/m}$) structure near 200 °C.[4,5] The monoclinic cell is generated by the doubling of the hexagonal a axis due to the ordering of the hydroxide or chloride ions along the hexagonal c axis which changes the mirror plane of $P_{6_3/m}$ to the glide plane of $P_{2_1/b}$. The hexagonal c axis remains the unique axis. Structural investigations by x-ray diffraction show three crystallographically distinct sets of tetrahedra each considerably distorted from T_d symmetry in monoclinic hydroxyapatite and chloroapatite.[2,3] In hexagonal apatites all six PO_4^{3-} tetrahedra are crystallographically equivalent.

Recently we have confirmed the existence of the monoclinic ($P_{2_1/b}$) phase in synthetic chloroapatite single crystals doped with CrO_4^{3-} by electron spin resonance measurements at liquid helium temperature.[5] The ESR measurements showed three distinct paramagnetic ions, corresponding to the substitutional replacement of three nonequivalent PO_4^{3-} by CrO_4^{3-} tetrahedra.

Fluoroapatite, $Ca_5(PO_4)_3F$ has previously been observed only in the hexagonal ($P_{6_3/m}$) form[7,8,9] and attempts to detect the monoclinic form analogous to chloroapatite and hydroxyapatite by low temperature x-ray diffraction single crystal studies down to liquid N_2 temperature and by calorimetric differential thermal analysis have failed.

In this paper we present evidence on the basis of ESR measurements made at liquid helium temperature on single crystals of fluoroapatite doped with Cr^{5+} that, similar to chloro- and hydroxyapatite, fluoroapatite undergoes a phase transition from the hexagonal ($P_{6_3/m}$) to a lower symmetry most likely monoclinic ($P_{2_1/b}$) phase.

EXPERIMENTAL

Single crystals of $Ca_5(PO_4, CrO_4)_3F$ with small concentrations of Cr were grown from the melt using excess CaF_2 as flux. A typical composition used for growth of a 0.5% CrO_4^{3-} content was: 2.995 mole $Ca_3(PO_4)_2$, 0.005 mole Cr_2O_3, 0.015 mole $CaCO_3$, and 12 mole of CaF_2. The starting materials were thoroughly mixed and fired overnight in tightly covered platinum crucibles at 1400 °C in air and cooled to 1200 °C at 3°/h; from 1200 °C the crystals were rapidly cooled to room temperature in the furnace. The crystals were washed free of any adhering CaF_2 by boiling in water, and then they were mechanically separated from the powdery flux. Light green crystals in the shape of needlelike irregular hexagonal prisms of $Ca_5(PO_4, CrO_4)_3F$ were obtained this way. X-ray diffraction patterns confirmed the formation of $Ca_5(PO_4, CrO_4)_3F$ in the hexagonal phase.

ELECTRON SPIN RESONANCE SPECTRA

Electron spin resonance spectra were taken with an X-band coherent superheterodyne spectrometer operating in the absorption mode and using field modulation. The klystron frequency was ~ 9100 MHz. A single crystal of $Ca_5(PO_4, CrO_4)_3F$ with about 0.5% Cr content produced no ESR signal at room temperature, but a broad signal (~ 70 gauss) at about $g \cong 2$ was detected at liquid N_2 temperature. At liquid helium temperatures the broad line split into three sharp (~ 1 G width) signals as shown in Fig. 1. A single crystal of $Ca_5(PO_4, CrO_4)_3F$ was oriented by x-ray diffraction methods and rotational ESR spectra were recorded at liquid helium temperature about three orthogonal crystallographic axis a, a^* (direction perpendicular to ac in the hexagonal cell), and c (hexagonal c). The magnetic field was perpendicular to the axis of rotation. Absorption lines were observed at 10° intervals as the magnet was rotated about the crystal. Weak hyperfine lines corresponding to interaction between the magnetic moment of the electron and the nuclear magnetic moment of Cr^{53} ($I = \frac{3}{2}$) could be seen near the main resonance lines for certain orien-

 Copyright © 1977 American Institute of Physics

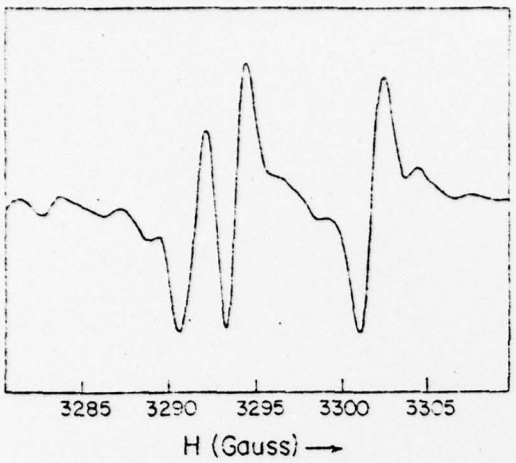


FIG. 1. First derivative of the electron spin resonance absorption curve for $Ca_5(PO_4, CrO_4)_3F$: rotation about a crystallographic axis.

tations of the crystal (Fig. 1). Due to the relatively small splitting of the spectra the hyperfine lines were poorly resolved and a meaningful analysis of them was not possible.

RESULTS AND PRELIMINARY ANALYSIS

It is reasonable to expect that the low temperature phase of fluoroapatite is pseudohexagonal monoclinic similar to the low temperature forms of chloro- and hydroxyapatite, and in CrO_4^{3-} doped $Ca_5(PO_4)_3F$ there will be at least three kinds of paramagnetic ions in the lattice as observed in chloroapatite. The CrO_4^{3-} ion with one unpaired electron has electronic spin $S=\frac{1}{2}$, hence the paramagnetic resonance spectrum for three crystallographically distinct chromate (V) ions will show three main resonance lines (each accompanied by four hyperfine lines if completely resolved. Such a pattern is seen in the data shown in Fig. 2(a)–2(c) in which are plotted the resonant magnetic fields for the main absorption peaks of the spectrum as a function of angular rotation. The three peaks are expected to split when the magnetic field is not along a symmetry direction since then the crystallographically equivalent tetrahedra do not all make the same angle with the magnetic field. Such a splitting is seen in Fig. 2(a)–2(c). However, it is rather small—much smaller than observed in the chloroapatite.[6] This indicates that the electric axes of each chromate tetrahedron are aligned nearly along symmetry axes.

We can qualitatively obtain the orientations of the electric axes by a closer examination of Fig. 2. Figure 2(b) shows a relatively small variation of the resonant magnetic fields for the peaks as a function of angular rotation for species A and B; the g values nearly superimpose when the crystal is rotated about the a crystallographic direction indicating that the electric axes for both A and B are oriented relatively close to the a axis. Similarly the angular variation of resonant magnetic field is almost constant for the peak corresponding to unique tetrahedron C, shown in Fig. 2(c), suggesting that the electric axis is nearly parallel with the a^* direction in this tetrahedron.

Each line in Fig. 2(a)–2(c) was least squares fitted to the function:

$$g^2=(g_{\max}^2-g_{\min}^2)\cos^2(\theta-\theta_{\max})+g_{\min}^2 . \tag{1}$$

In the case of the split lines the fit was made to the average. The results of the fits are plotted in Fig. 2(a)–2(c). $g_{\min}$ was the same for all of the rotations indicating axial symmetry. Thus the spectrum can be interpreted by the axial spin Hamiltonian:

$$\mathcal{H}=\beta_e g_\perp(H_x S_x+H_y S_y)+\beta_e g_\parallel H_z S_z . \tag{2}$$

From the fitting parameters in Eq. (1) we have made the identification of species A, B, and C shown in Fig. 2(a)–2(c) and obtained the spin Hamiltonian parameters given in Table I. The angles α and β give the orientation of the electric z axis relative to the crystal axes as shown in Fig. 3. The large errors in α arise because the ESR is insensitive to small changes in α when α is near 90°.

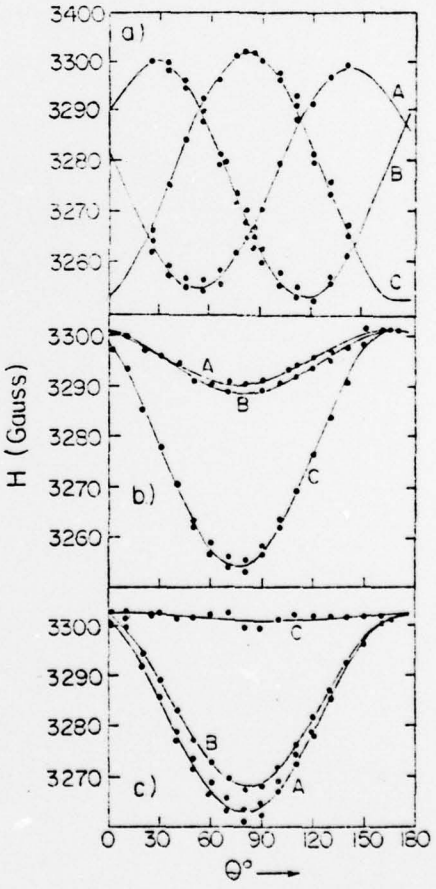


FIG. 2. Magnetic field H (gauss) at center of peak vs θ the angle between crystallographic axis and magnetic field. (a) Rotation about c axis, H parallel to a at $\theta=80$°. (b) Rotation about a axis, H parallel to c at $\theta=160$°. (c) Rotation about a^* axis, H parallel to a at $\theta=85$°. ● Experimental values. — Least-squares fit. The small difference in the maximum values of curve A and B indicates a small misalignment of the rotational axis.

TABLE I. Magnitude and orientation of the principal g values of the three tetrahedra in $Ca_5(PO_4)_3CrO_4F$.

	g_x	g_y	g_z	α
A	1.9824 ± 0.0005	1.9906 ± 0.0010	90 ± 15	−26.0 ± 3.9
B	1.9818 ± 0.0005	1.9906 ± 0.0010	90 ± 15	24.2 ± 2.5
C	1.9815 ± 0.0005	1.9911 ± 0.0010	90 ± 15	±25

DISCUSSION THEORY

The principal g values show axial symmetry of the electric axis in each of the three chromate tetrahedra A, B, and C, respectively, in fluoroapatite. Furthermore, the three sets of principal g values corresponding to the three different CrO_4^{3-} are the same, within experimental error. This indicates that the three distinct tetrahedra are distorted from the ideal T_d symmetry in a similar manner and differ primarily in the orientation of their electric axes, as far as our ESR [illegible] magnetic species A, B, and C with the corresponding tetrahedra in the structure of monoclinic fluoroapatite must wait for results of a detailed x-ray structure determination of the low symmetry phase of fluoroapatite.

The nature of the ground state of the d^1 electron was determined as follows: if we assume the distorted tetrahedra to have approximately C_{2v} symmetry as in the chloroapatite, the d^1 configuration will have either d_{z^2} or d_{xy} orbital as the ground state. From our results in Table I, $g_\parallel = 1.991$ and $g_\perp = 1.962$. Assuming pure atomic d orbitals and using second order perturbation theory, the spin–Hamiltonian parameters for a d_{xy} ground state[10] are:

$$g_\parallel = 2.0023 - \frac{8\lambda}{\Delta E_{(x^2-y^2)}} \tag{3}$$

and

$$g_\perp = 2.0023 - \frac{2\lambda}{\Delta E_{(xz,yz)}}, \tag{4}$$

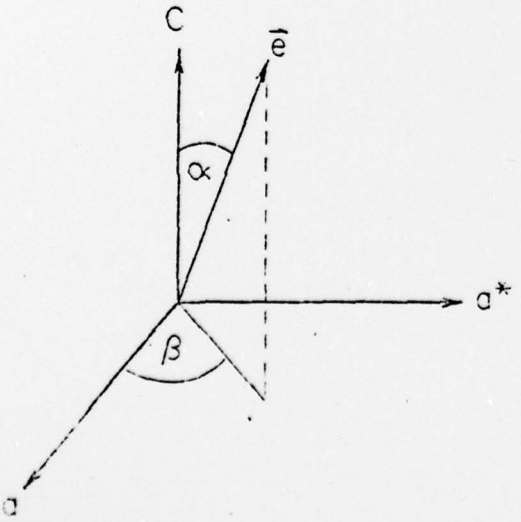


FIG. 3. Orientation of electric z axis with respect to crystallographic directions a, a^*, and c.

while for a d_{z^2} ground state the parameters are:

$$g_\parallel = 2.0023, \tag{5}$$

$$g_\perp = 2.0023 - \frac{6\lambda}{\Delta E_{(xz,yz)}}, \tag{6}$$

where λ is the spin–orbit coupling parameter, and $\Delta E_{(\gamma)}$ is the energy separation of the state γ above the ground state. Thus for a d_{xy} ground state $g_\parallel < g_\perp$ unless $\Delta E_{(xz,yz)}$ is much smaller than $\Delta E_{(x^2-y^2)}$. It has been established previously, that $\Delta E_{(x^2-y^2)}$ cannot possibly be four times greater than $\Delta E_{(xz,yz)}$.[6] For a d_{z^2} ground state $g_\parallel > g_\perp$. Thus the data indicate that the electron is in a d_{z^2} orbital in its ground state. $g_\perp = 1.962$ implies $\lambda/\Delta E_{(xz,yz)} = 0.0067$. Equation (5) indicates $g_\parallel$ must be close to 2.0023. We attribute the observed deviation ($g_\parallel = 1.991$) to third order effects in which the admixture of the higher $d_{(x^2-y^2)}$ state into the d_{z^2} ground state is taken into account[11]:

$$\psi_{z^2} = a d_{z^2} + b d_{x^2-y^2}, \tag{7}$$

[illegible] making $g_x \neq g_y$. We would presumably observe this effect with a more accurate determination of g or in the hyperfine lines if they could be resolved. An analysis including third order effects has been carried out for the ESR of CrO_4^{3-} in chloroapatite and spodiosite.[6,12] The results of such an analysis are given in Table II in comparison with chloroapatite and spodiosite. Since we observe axial symmetry and have no hyperfine data for the fluoroapatite, we are able to determine only the ratio $b^2/\Delta E_{(xy)}$.[13]

Comparison of the ESR linewidth which shows significantly broader lines for chloroapatite (~ 10 G) than for fluoroapatite (~ 1 G) provides evidence that $\Delta E_{(xy)}$ is considerably larger in fluoroapatite. The smaller value of $b^2/\Delta E_{(xy)}$ for fluoroapatite compared to chloroapatite (Table II) is in agreement with the above result. The effective distortion of tetrahedra in fluoroapatite appears to increase $\Delta E_{(xy)}$, resulting in a smaller mixing of $d_{(x^2-y^2)}$ into the d_{z^2} ground state, and the apparent axial symmetry of the electric axis.

The position of F^- ions at $z = \frac{1}{4}$ and $z = \frac{3}{4}$ on the mirror planes in the center of Ca^{2+} triangles (in $P6_3/m$) is significantly different from that of the chloride ions which are residing between the mirror planes at $z = 0, \frac{1}{2}$ in the apatite structure, hence the observed differences in the ESR properties of the two systems are expected. It is likely that the fluorides are randomly vibrating about the mirror plane position at room temperature produc-

TABLE II. Comparison of the crystal field parameters of CrO_4^{3-} in apatite and spodiosite.

	$\lambda/\Delta E_{(xz)}$[a]	$b^2/\Delta E_{(xy)}$	λ (cm^{-1})[a]	$b^2/\Delta E_{(xy)}$	b^2
$Ca_5(PO_4)_3F$	0.0067	1.1×10^{-7}	~67	2.1×10^{-7}	...
$Ca_5(PO_4)_3Cl$[b]	0.011	2.9×10^{-7}	~110	2.6×10^{-7}	0.069[c]
$Ca_3(PO_4)_2Cl$[b]	0.0055	...	...	1.6×10^{-7}	0.0033

[a] $\Delta E_{(xz)}$ is the value of $\Delta E_{(xz)}$ obtained assuming $\Delta E_{(xz)} = \Delta E_{(yz)}$. λ is obtained by taking $\Delta E_{(xz)} = 10\,000$ cm^{-1} as indicated by optical data taken on spodiosite.[12]

[b] Results taken from Ref. 6.

[c] See Ref. 13.

ing the overall effect of the observed $P_{6_3/m}$ symmetry, however at some lower temperature the fluorines may come to an equilibrium position which is slightly off the mirror plane, resulting in a lower symmetry in fluoroapatite.

Recent low temperature x-ray diffraction studies on single crystals of $Ca_5(PO_4)_3F$ show unambiguously a hexagonal $\rightleftharpoons$ monoclinic phase transition at ~ 133 °K[15] in agreement with a previous report that such a transition occurs at about 140 °K as shown by an anomaly occurring in dielectric constant and specific heat measurements on fluoroapatite.[16,17] The x-ray data at low temperature suggests the transformation to a noncentrosymmetric $P_{2/3}$ space group which requires the phosphate tetrahedra to occupy six nonequivalent sites. The ESR results in this study indicate slight splitting of each of the three bands observed in several crystal orientation about each rotation axis [Fig. 2(a)–2(c)] such that six peaks can be accounted for: however, this effect can also be due to symmetrically related magnetically nonequivalent tetrahedra, and at present it is not possible, on the basis of ESR data, to confirm the existence of a low temperature noncentrosymmetric space group for fluoroapatite. Work is in progress to determine the structure of the monoclinic form of fluoroapatite in detail by x-ray diffraction techniques.

ACKNOWLEDGMENT

This research received support from the Biomedical Sciences Support Grant, Rutgers University, New Brunswick, N. J., and from NIDR Grant No. DE-03543 at the Polytechnic Institute of New York, Brooklyn, New York.

[4]J. C. Elliott, Nature (London) 230, 72 (1972).
[5]J. C. Elliott, P. E. Mackie, and R. A. Young, Science 180, 1055 (1973).
[6]P. E. Mackie, J. C. Elliott, and R. A. Young, Acta Crystallogr. B 28, 1840 (1972).
[7]J. S. Prener, J. Electrochem. Soc. 114, 77 (1967).
[8]H. B. Van Rees, M. Mengeot, and E. Kostiner, Mater. Res. Bull. 8, 1307 (1973).
[9]E. Banks, M. Greenblatt, and B. R. McGarvey, J. Solid State Chem. 3, 305 (1971).
[10]R. A. Young and J. C. Elliott, Arch. Oral Biol. 11, 699 (1966).
[11]S. B. Hendricks, M. E. Jefferson, and V. M. Mosely, Z. Kristallogr. 81, 352 (1932).
[12]S. Naray-Szabo, Z. Kristallogr. 75, 387 (1957).
[13]B. R. McGarvey, Inorg. Chem. 5, 476 (1966).
[14]B. R. McGarvey, *Electron Spin Resonance of Metal Complexes* (Plenum, New York, 1969).
[15]E. Banks, M. Greenblatt, and B. R. McGarvey, J. Chem. Phys. 47, 3772 (1967).
[16]The value of b^2 for chloroapatite is unreliable since the analysis assumes $\Delta E_{(xz)} = \Delta E_{(yz)}$. This is not allowable since $\Delta E_{(xz)} - \Delta E_{(yz)}$ can make a contribution to $g_x - g_y$ that is comparable to the effect of b. For example, in apatosite $g_x = g_y$ experimentally and one would then conclude $b^2 < .0008$ if one assumes $\Delta E_{(xz)} = \Delta E_{(yz)}$. But when hyperfine data are included one finds (Ref. 6) that $\Delta E_{(xz)} \neq \Delta E_{(yz)}$ and $b^2 = .0053$.
[17]E. Banks, M. Greenblatt, and S. Holt, J. Chem. Phys. 49, 1431 (1968).
[18]E. Banks (private communications).
[19]T. Arends, B. S. H. Royce, R. Smoluchowski, and D. O. Welch, "Electrical and Transport Properties of Apatites," International Symposium on Structural Properties of Hydroxyapatite and Related Compounds, 12–14 September, 1968, Princeton University, Princeton, NJ.
[20]B. S. H. Royce (private communications).

VOLUME 34, NUMBER 12 PHYSICAL REVIEW LETTERS 24 MARCH 1975

Local Character of Many-Body Effects in X-Ray Photoemission from Transition-Metal Compounds: Na_xWO_3

M. Campagna and G. K. Wertheim
Bell Laboratories, Murray Hill, New Jersey 07974

and

H. R. Shanks
Ames Laboratory—USAEC, Iowa State University, Ames, Iowa 50010

and

F. Zumsteg*
Laboratory of Atomic and Solid State Physics, Cornell University, Ithaca, New York 14850

and

E. Banks
Polytechnic Institute of New York, Brooklyn, New York 11201

(Received 27 January 1975)

X-ray photoemission spectra of W core levels in metallic sodium tungsten bronzes, Na_xWO_3, clearly show asymmetries due to many-body effects. Na and O core levels show only the expected plasmon satellite, demonstrating the importance of the local density of states in the screening of the core hole.

The importance of many-body effects in x-ray spectroscopy was pointed out in various theoretical papers a number of years ago.[1,2] Experimental evidence to support these theories has been sought in the x-ray threshold anomalies of simple metals like Li, Na, Mg, Al,[3] and the Mg_xSb_{1-x} alloys.[4] However, none of the theories seems to explain the data satisfactorily.[5] Many-body effects are also expected to be important in photoemission spectroscopy.[6] The effect of extra-atomic relaxation on binding energies[7] is, in a sense, a many-body phenomenon even though the leading term is Hartree-like. Neither this nor the well-known satellites are, however, many-body effects in the sense of Refs. 1–6. The discrepancy between the observed positive electron-spin polarization of photoelectrons from Ni and Co near threshold[8] and the prediction of negative polarization by the Stoner-Wohlfarth-Slater band theory of magnetism has been considered as among the first clear examples of the importance of these many-body interactions during the photoemission process.[9] The appearance of an asymmetry in the line shape of $3d$ and $4f$ core levels in x-ray photoemission spectroscopy (XPS) of $4d$ and $5d$ metals,[10] and similar observations in simple metals,[11,12] provide direct evidence for the fundamental role of the core-hole potential in photoemission data. The asymmetry was ascribed to the interaction of the suddenly created potential of the photohole with the conduction electrons. Apart from these first observations there is little other experimental information on the coupling between a hole state and conduction electrons in photoemission.

This Letter is a preliminary report of an XPS study of the sodium tungsten bronzes, Na_xWO_3. We show that these mixed-valence metallic oxides provide a unique opportunity for the investigation of the dependence of many-body effects on conduction-electron concentration, total density of states, local density of states at the site of a given atom in the solid, and nature of the wave functions forming the conduction band.

The cubic Na_xWO_3 are closely related to the ABO_3 ternary oxides with (distorted) perovskite structure, and have been the subject of numerous investigations.[13-15] Their electronic structure has been considered in detail from the theoretical point of view,[14] while experimental information has been derived mainly from optical studies.[15] Single-crystal specimens of Na_xWO_3 with ~16-mm^2 area were cut from larger single crystals obtained by electrolysis. Surfaces for the XPS study were prepared by cleaving as described by Wertheim *et al.*[16] Data were obtained with monochromatized Al $K\alpha$ radiation using an HP-5950A ESCA spectrometer.

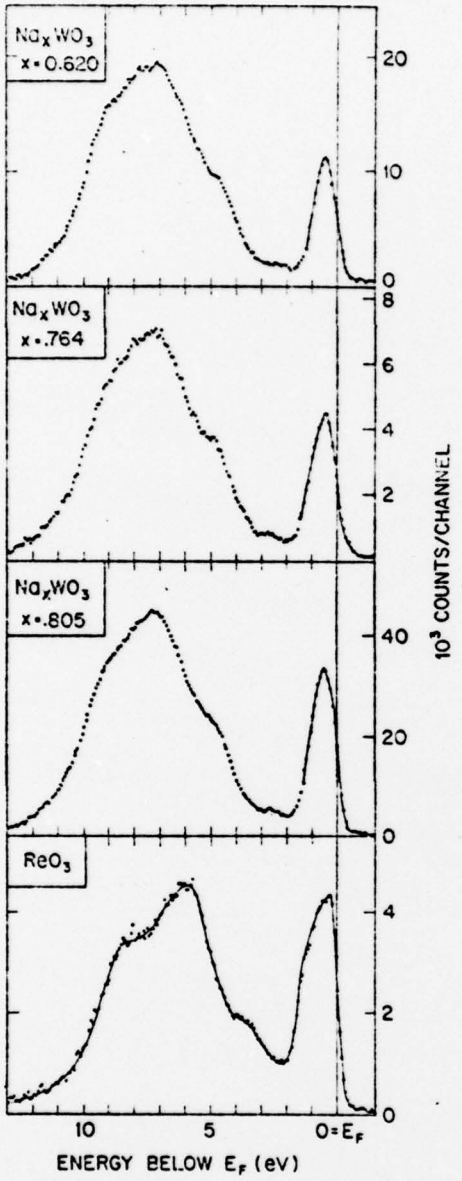


FIG. 1. Valence-band XPS spectra of vacuum-cleaved Na_xWO_3 and ReO_3.

In Fig. 1 we show the XPS valence band of Na_xWO_3 for the nominal compositions x =0.620, 0.764, and 0.805, as determined from lattice-constant measurements. For comparison we also show the valence band of ReO_3.[16] From an inspection of Fig. 1 we conclude that the electronic structure of the Na_xWO_3 is very similar to that of ReO_3, and presumably representative of the ABO_3 perovskites. Note, however, that the XPS valence-band spectrum does not reproduce the *total* density of states, but is most sensitive to the covalent admixture of higher angular momentum states into the p band.[16] The heights of the spectra of the valence bands, centered about 7 eV below E_F, have been normalized in order to show that the area of the conduction-band peak near E_F increases in proportion to the Na content. The data provide a direct visualization of the filling of a conduction band in a solid with increasing electron concentration. In fact the width of the conduction band increases slightly from an experimental full width at half-maximum of 1.00± 0.05 eV to 1.15± 0.05 eV with increasing x. This demonstrates that the conduction band, although made up of a covalent admixture of W $5d$ and O $2p$, wave functions, is filled by electrons donated by the Na, with a conduction-electron concentration equal to the sodium concentration.[13,14]

The data are in good agreement with the results of theoretical studies of the electronic structure of the perovskites,[13,14] and thus support the view that the information obtained by XPS is mostly bulk information.

The most interesting, and initially puzzling result is provided by the W $4f$ spectra, shown in Fig. 2. The $4f$ region is not a simple spin-orbit doublet of symmetrical lines with 7:5 intensity ratio as one might expect on the basis of the $4f$ spectra of W or WO_3,[17] or from simple theoretical considerations. The dominant extraneous feature is provided by the third peak at 38.5 eV, 2 eV below the $4f_{5/2}$ line. This peak is clearly broader than the other two lines suggesting that it represents a plasmon energy loss and/or other many-body satellite.[18] The former is not an unlikely interpretation in view of similar, though weaker, energy-loss features on the Na and O 1s lines and the strong 2.1-eV peak observed in the energy-loss function in Ref. 15. Either alternative implies that there must be another satellite belonging to the $4f_{7/2}$ line, lying directly beneath the $4f_{5/2}$ line. The intensity ratio of the two satellites must also be approximately in the ratio 7:5. The shape of the $4f$ core lines also requires comment. An examination of Fig. 2 shows that there is a long tail toward greater binding energy in the $4f$ spectrum. This tail, although not so pronounced, is present on each W-core-level line. It is not due to the 2-eV plasmon because a similar tail is not found in the O and Na 1s spectra, shown in Fig. 3, which do exhibit the plasmon energy loss. The Na 1s line is clearly symmetrical, even though its width greatly exceeds the natural width. According to current theoretical investigations the interaction of the

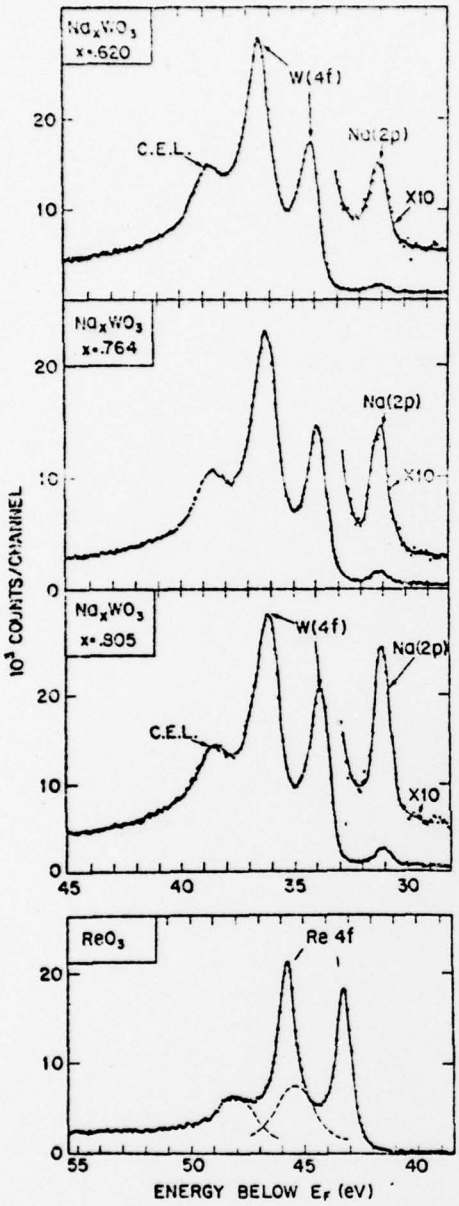


FIG. 2. XPS spectra of the $4f$ region of Na_xWO_3.

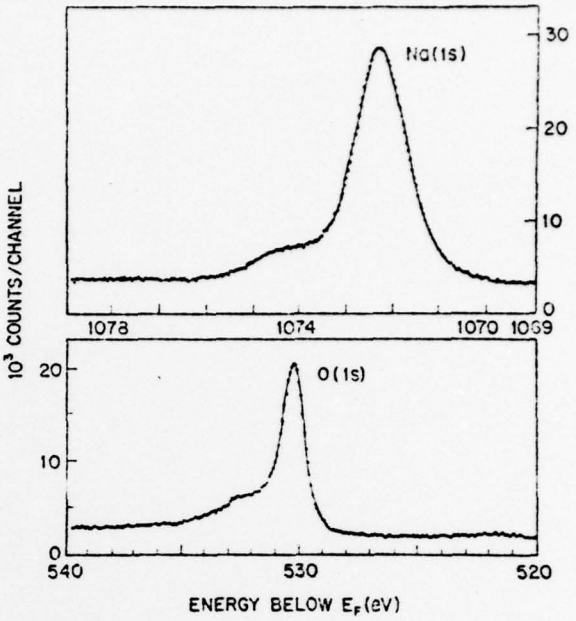


FIG. 3. XPS spectra of the Na and O 1s lines of $Na_{0.764}WO_3$.

photoelectron with other electrons during escape from the solid can be neglected (except for plasmon excitation). We therefore ascribe the long tail of the W lines to the coupling of the core hole with the Fermi sea, as suggested by Doniach and Sunjic.[6] The asymmetry parameter, α, inferred from an analysis of the spectra in Fig. 2, lies in the range ~0.15 to 0.19, with a tendency to *decrease with increasing x*. It can be understood by assuming that the f hole is effectively screened by p and d phase shifts in the $5d$ conduction band. From the absence of asymmetric broadening of the O and Na levels one concludes that the interaction of the core hole with the conduction electrons is a local effect, directly related to the nature of the wave functions forming the conduction band and not a simple "jellium" effect. The fact that the density of conduction electrons vanishes at the Na nuclei is reflected in the much weaker coupling between Na core holes and the conduction electrons. Core-level line-shape analysis therefore provides another technique for the study of covalent mixing in the conduction band.

A more precise picture of the satellites on the $4f$ lines can be obtained by subtracting the main lines under the assumption that they have the Doniach-Sunjic[6] line shape. Two broad symmetrical satellites with the proper 7:5 intensity ratio are obtained, but the strength relative to the $4f$ lines is much greater than expected on the basis of the plasmon satellites on the Na and O 1s lines. This suggests that the extra intensity is due to another mechanism, the most likely one being that proposed in a recent paper by Kotani and Toyazawa.[13] In their model photoionization of a core electron in a d-band metal may pull a normally empty d state below the Fermi energy. If that state is filled by an electron from the conduction band the asymmetrical main line is obtained; if it remains empty a lifetime-broadened satellite appears at greater binding energy. This

corresponds very closely to what is found in Na_xWO_3; even the 2-eV separation corresponds well to the shift expected for removal of one electron.

A detailed discussion of (1) the relationship between the electronic structure of the bronzes and XPS valence-band data, (2) the connection between XPS binding energies of W and Na core levels and spin-relaxation[20] and Knight-shift[21] experiments, and (3) the implications of the detection of a unique W 4*f* doublet on conduction-electron delocalization will be published elsewhere. A more extensive investigation of the dependence of α on x and on the local environment is in progress.

---

*Present address: Central Research Department, Dupont Chemicals, Wilmington, Del. 19898.

[1]G. D. Mahan, Phys. Rev. 163, 612 (1967).

[2]P. Nozières and C. T. deDominicis, Phys. Rev. 178, 1097 (1969).

[3]J. D. Dow and B. F. Sonntag, Phys. Rev. Lett. 31, 1461 (1973).

[4]J. D. Dow, J. E. Robinson, J. H. Slowik, and B. F. Sonntag, Phys. Rev. B 10, 432 (1974).

[5]J. D. Dow, in Proceedings of the Fourth International Conference on Vacuum Ultraviolet Radiation Physics, Hamburg, West Germany, 22–26 July 1974 (unpublished).

[6]S. Doniach and M. Sunjic, J. Phys. C: Proc. Phys. Soc., London 3, 285 (1970).

[7]L. Ley *et al.*, Phys. Rev. B 8, 2392 (1973).

[8]G. Busch, M. Campagna, and H. C. Siegmann, Phys. Rev. B 4, 747 (1971).

[9]P. W. Anderson, Phil. Mag. 24, 203 (1971); S. Doniach, in *Magnetism and Magnetic Materials—1971*, edited by C. D. Graham, Jr., and J. J. Rhyne, AIP Conference Proceedings No. 5 (American Institute of Physics, New York, 1972), p. 549.

[10]S. Hüfner, G. K. Wertheim, D. N. E. Buchanan, and K. W. West, Phys. Lett. 42A, 420 (1974); S. Hüfner and G. K. Wertheim, Phys. Rev. B 11, 678 (1975).

[11]P. H. Citrin, Phys. Rev. B 8, 5545 (1973).

[12]L. Ley, F. R. McFeely, S. P. Kowalczyk, J. G. Jenkin, and D. A. Shirley, to be published.

[13]See P. Hagenmuller, in *Progress in Solid State Chemistry*, edited by H. Reiss (Pergamon, Oxford, England, 1971), Vol. 5, p. 71, and references cited therein.

[14]J. B. Goodenough, Bull. Soc. Chim. Fr. [illegible] 1200, and Progr. Solid State Chem. 5, 145 (1971); L. F. Matheiss, Phys. Rev. B 6, 4718 (19[illegible].

[15]D. W. Lynch, R. Rosei, J. H. Weave[illegible] and C. G. Olson, J. Solid State Chem. 8, 242 (1973), and references cited therein.

[16]G. K. Wertheim, L. F. Matheiss, M. Campagna, and T. P. Pearsall, Phys. Rev. Lett. 32, 997 (1974).

[17]T. A. Carlson and G. E. McGuire, J. Electron Spectrosc. Relat. Phenomena 1, 161 (1972/1973).

[18]The alternate interpretation of the W 4*f* spectrum in terms of separate contributions from W^{6+} and W^{5+} is not tenable for various reasons. The intensity ratios $[W^{5+}]/[W^{6+}]=x/(1-x)$ for the three samples range from 4.1 for $x=0.805$ to 1.63 for $x=0.620$. This is contrary to the data. Neither the x-dependent shift of the narrower line at smaller binding energy, nor the x-dependent change in the separation between the two sets of lines fits into this picture.

[19]A. Kotani and Y. Toyazawa, J. Phys. Soc. Jpn. 37, 912 (1974).

[20]W. H. Jones, Jr., E. A. Garbaty, and R. G. Barnes, J. Chem. Phys. 36, 494 (1962).

[21]A. T. Fromhold, Jr., and A. Narath, Phys. Rev. 136, A487 (1964).

Reprinted from JOURNAL OF THE ELECTROCHEMICAL SOCIETY
Vol. 125, No. 10, October 1978
Printed in U.S.A.
Copyright 1978

75-Year Review Series—Luminescence—The Past 25 Years

Ephraim Banks*

Department of Chemistry, Polytechnic Institute of New York, Brooklyn, New York 11201

In an article (1) entitled, "The Growth of the Luminescence Section" Rudolph Nagy summarized the major developments in lighting and phosphors for the previous fifty years, citing 50 selected papers from *This Journal* or presented at Society meetings through 1951. Although he disclaimed complete coverage, the major trends were well represented by those papers. The luminescence symposia which featured the spring meetings had begun in 1945 and of the 50 references cited by Nagy, just 25 dealt with phosphors or their behavior in lamps and other devices, including two reviews (2) by Fonda of annual progress. These became biennial, the last appearing in 1957 (3). Four references were on semiconductors, which have blossomed into the dominant subdivision of the Electronics Division. A number of references to gas discharge studies were also included.

A search through the index of *This Journal* for the period 1952-1976 revealed that almost 500 papers on luminescence were published during this period in *This Journal* alone. Much of this research was directed to meeting the needs stated in Nagy's survey: "There is a great deal to be learned regarding the mechanisms of luminescence. We are in need of better phosphors for fluorescent lamps and television tubes, and of more efficient high temperature and ultraviolet emitting phosphors." The Electronics Division has indeed played a major role.

Luminescence research has come a long way in the last quarter-century, from an empirical art to a field in which considerable physical and chemical understanding has developed. Modern phosphor laboratories use a variety of sophisticated techniques in attempts to understand the processes of luminescence. These have ranged from low temperature, high resolution spectroscopy to electron spin resonance, NMR, etc. In Nagy's review, the first use of powder x-ray diffraction in phosphor chemistry was cited—today it is a routine procedure.

Since the publication of Pringsheim's monograph (4) in 1949, there have been no such books published. The field has grown too large, and the only book which has attempted to cover the entire field, edited by Goldberg (5), is a symposium with several contributing authors. Other books and chapters include Curie (6), Klick and Schulman (7), Garlick (8), Riehl (9), Henisch (10), Ivey (11), Nassau (12), and Day (13, 14). Some of these are brief reviews or introductions to the field, while others select a single topic for discussion.

During these years there have been frequent international conferences and symposia on luminescence. These were held at New York University in 1961 (15), Balatonvilagos, Hungary in 1961 (16), Torun, Poland in 1963 (17), Munich, Germany in 1965 (18), Budapest, Hungary in 1966 (19), the University of Delaware in 1969 (20), Leningrad, U.S.S.R. in 1972 (21), Tokyo, Japan in 1975 (22), and this year, the conference was held in Paris, France. A new journal, the "Journal of Luminescence," began publication in 1970, and has been the medium of publication for many of these symposia, as well as research papers and review articles on many topics in luminescence.

The fields of research covered in these years include fluorescent lamp phosphors, high temperature phosphors for color correction in HPMV[1] lamps, cathode ray phosphors for color and monochrome television, electroluminescent materials and phosphors for x-ray intensification, to classify the phosphors by their technical application. Little attention has been given in the Luminescence Division of the ECS to organic luminescence, whose major applications are in such devices as liquid scintillation counters.

Electroluminescence has been the subject of much research as it moved from an effect whose existence was disputed by many after it was first reported by Destriau (23) through a stage of intense development as a possible area light source to the development of light-emitting diodes and semiconductor lasers. This progression was reviewed by Ivey (24), who had presented a similar review of cathodoluminescence and electroluminescence in 1957 (25). Ivey has also compiled a continuing bibliography on electroluminescence and related topics through 1967 (26), with 3700 references to papers and patents worldwide. It is somewhat ironic that the present applications of electroluminescence are based not on the Destriau effect, but on the type of electroluminescence observed in SiC crystals by Lossev (27) in 1924, namely p-n junction injection EL. Modern devices are fabricated from single crystal material, chiefly GaAs and GaAs-GaP alloys, with grown junctions prepared by counterdoping melts during growth, and more recently, by epitaxial vapor growth on prepared single crystal substrates. Semiconductor diodes have been constructed to show laser action by confining the p-n junction in a feedback cavity made of polished surfaces normal to the junction plane, and a substantial technology has been developed (24).

The development of light-emitting diodes and semiconductor lasers has reached the point where, at least for LED's, they have reached into the consumer market. In conjunction with silicon-integrated circuits, LED display devices are now found in wristwatches and the ubiquitous pocket calculators to be found in the pocket of every college freshman. All these devices are based on the generation of recombination luminescence at p-n junctions in alloys of GaAs-GaP. Because GaP has an indirect bandgap, while GaAs has a direct bandgap, the efficiency of light generation is high for compositions near GaAs and falls off rapidly when the band structure of the alloy becomes GaP-like, i.e., having an indirect bandgap. This has limited

* Electrochemical Society Active Member.

[1] High pressure, mercury vapor.

the emission color of the devices now on the market to the red region of the spectrum, and incidentally stimulated considerable effort in the development of infrared-visible upconversion phosphors. The limitation has been partly overcome by the discovery of the effect of the isoelectronic trap, nitrogen, in GaP. The nitrogen center introduces a short-range, noncoulombic attractive potential with a binding energy of about 8 meV. The negative (N^-) site now may capture a hole, forming a trapped exciton which may be destroyed by radiative recombination, emitting green light. Although the efficiency of this process is low (about 1%), the superior eye response in the green region of the spectrum makes such devices promising for future display devices. Experimental diodes are now available. Several reviews have been published on the development of light-emitting diodes and diode lasers subsequent to Ref. (24), including the reviews by Lorenz (28), Casey and Trumbore (29), Nuese *et al.* (30), Dean (31), and a very personal review by Loebner (32).

At the time of Nagy's article, the process of replacing phosphor blends in standard fluorescent lamps by a single phase material was underway, stimulated by the tragic problem of toxicity of zinc beryllium silicates and the ease of fabrication when a white appearance could be obtained by varying the concentration of Sb and Mn in a single-phase material (33), blending being required only for extending the spectral range in deluxe lamps. *This Journal* published only 23 papers on halophosphate phosphors in the next 25 years—a surprisingly small number. Of course, there have been many papers published elsewhere and much of the development work appears only in the patent literature. In the lamp phosphor field, blends appear to be making a comeback, with the report of new efficient narrow-band blue phosphors based on Eu^{2+} in apatite (34), and the development of the three narrow-band lamps by Verstegen (35) and by Thornton (36). A very recent development involving the reintroduction of blends is the blending of a phosphor with a narrow blue band, such as Sr chlorapatite:Eu^{2+}, with a "yellow" broad-band phosphor, for example, a fluorapatite activated with Sb^{3+} and Mn^{2+} to favor the Mn band. This combination was blended in a lamp having total output efficiencies up to about 85 lpw in a blend containing about 6% of the Eu^{2+}-activated phosphor (37, 38).

There has been considerable discussion of sensitized luminescence, whose importance in phosphors for 254 nm excitation is well known. This topic is discussed by Ivey in a review (39), and in several papers in *This Journal* (40-42). Much discussion of the theory of resonance transfer in doubly activated phosphors has appeared in other journals, and many references can be found in Ivey's review.

Over one hundred papers on zinc sulfide phosphors and related II-VI compounds appeared in *This Journal*, on topics including the identification of trapping levels with coactivators (43, 44) the study of polarized luminescence of single crystals (45, 46), the properties of phosphors with new impurities, and electroluminescent and cathodoluminescent behavior.

The major breakthrough in cathodoluminescent materials was the development of efficient red phosphors with suitable decay characteristics, beginning with YVO_4:Eu (47) and including oxysulfides and the currently used Y_2O_3 (48). These phosphors have been the most important technical step, making possible today's mass market for color television (together with solid-state electronic devices) because a suitable red phosphor had been a perennial bottleneck. Wickersheim (49) has presented a personal history of the development of the red Y_2O_3:Eu phosphor (50, 51) and some of the background of the development of rare earth activated phosphors for x-ray intensifying screens. Wickersheim's account suggests that sometimes invention may be the mother of necessity, as the first new successful x-ray phosphor, Gd_2O_2S:Tb, was based on research supported by the U.S. Atomic Energy Commission on the basis of its potential as a scintillation counter. The greater x-ray stopping power of phosphors based on rare earths suggested their advantage over conventional $CaWO_4$-intensifying screens for improved resolution in medical radiography or for reduced dosage to patients and operators at equivalent resolution (52). The disadvantage that the green-emitting Tb^{3+} requires green-sensitive film for optimum results has led to an intensified search for new x-ray phosphors with high x-ray absorption and efficient blue emission (53). Recent candidates are largely based on the blue emission of Eu^{2+} in hosts containing heavy elements such as barium and bismuth.

Another area in which rare earth activators play a significant role is the infrared-visible upconversion phosphor (54-57), in which two quanta of near infrared are absorbed by the phosphor, and a visible light quantum is emitted. Resonant energy transfer, usually from Yb^{3+} to Er^{3+}, is the dominant mechanism. These phosphors are useful in converting the infrared emission of GaAs LED's to visible light for displays, etc. Their applicability seems to have been superseded by the appearance of green-emitting LED's based on GaP (58), but there may continue to be applications where high power densities are required, such as in fiber optics communications.

Rare earth activators play a prominent role in solid-state lasers. Although the first optically pumped laser was based on Al_2O_3:Cr^{2+} (ruby) (59), the next to be reported was based upon bivalent samarium in fluorite crystals (60, 61). Rare earth ions have been especially significant in solid lasers because they can operate in a four-level mode, i.e., the terminal state of the stimulated transition is a normally empty state above the ground electronic state. This permits laser action to start at modest levels of excitation, rather than requiring the excitation of more than half the activator atoms to achieve population inversion. These were followed by a veritable explosion of papers describing the physical characteristics and new materials showing laser action. The most important solid-state lasers today use trivalent neodymium as the activator in a variety of hosts including yttrium aluminum garnet, $Y_3Al_5O_{12}$ (62), glasses (63), apatites (64, 65), and other compounds (66, 67). Currently, neodymium glass lasers are being assembled for experiments with laser fusion, in which several intense laser beams are focused on a tiny volume into which small pellets of deuterium-tritium mixtures are dropped. The intense concentration of energy in the laser beams causes rapid ablation of the outer pellet material, creating a recoil shock wave which implodes the remainder of the pellet and raises its temperature and density to very high levels, where it is hoped that nuclear fusion will occur, generating more energy than was required to initiate thermonuclear processes.

Fluorescence in liquids has received rather little attention in the field of inorganic luminescence, although there has been intensive activity in the field of organic fluorescence in solution, including many biochemical applications. Interest in liquid lasers was stimulated by certain obvious advantages for optically pumped lasers, notably the elimination of the need for solid rods of high perfection, (either single crystals or glasses) liquids simply requiring appropriate expansion volumes to accommodate temperature changes. Another advantage is that liquids may be circulated for cooling purposes. The liquid lasers which have been most successful have been those based on europium III chelates such as the tris-dibenzoylmethide europium molecule in solution in alcohol, acetonitrile, or other solvents (68), solutions of rare earth oxides in $SeOCl_2$ and similar solvents (69, 70), and organic dye lasers (71, 72) in which a laser may be tuned over the broad fluorescence emission band of an organic dye in solution by methods such as varying the setting of a grating used as one reflector in the optical cavity, etc. Such

tunable lasers have been actively taken up in scientific instrumentation, as they provide an intense coherent light source of variable frequency.

The previous paragraphs were organized in terms of the areas of application of phosphors. Included in the work were a number of theoretical and fundamental experimental studies published in *This Journal* and elsewhere. Several such fundamental issues occupied considerable time at the annual meetings of the Luminescence Division and, in my opinion, have contributed much to the understanding of phosphors and led to new materials for practical application. The work of Wickersheim and co-workers, mentioned above (49, 50), is a case in point. Another example is the work of Blasse (73, 74) and co-workers at Philips Laboratories and later in a university setting on the fluorescence of rare earth ions in a variety of crystalline environments, resulting in correlations of theory and experimental behavior of rare earths in a variety of oxide hosts. Struck and Fonger (75) have presented a quantitative theoretical discussion of the interaction between charge-transfer states and localized 4f states based on a configuration coordinate model. This model had been elaborated by Williams (76) in his program to calculate the luminescence properties of YOCl:Pr from first principles, and was the subject of considerable theoretical and experimental study by Klick, Schulman, and their co-workers (7).

Other fundamental studies on ZnS-type phosphors led to the appreciation of the role of coactivators, already prefigured at the time of Nagy's review in the paper by Kröger and Hellingman (77) on the role of chlorine in self-activated ZnS. At the time, there was much doubt about the facts, but over the years, the role of halogens and trivalent ions was firmly established (43, 44). The necessity for the coactivator led Prener, Apple, and Williams (78, 79) to formulate a donor-acceptor pair model for luminescence in these phosphors. These concepts have also contributed to developments in semiconductor lasers and light-emitting diodes.

This review has skimmed very lightly over some of the highlights in the field of luminescence in the past quarter-century. Some important topics have been omitted. In 1952, it was possible for a review to cover developments of the previous 50 years from the early discoveries of the basic devices (fluorescent lamps and cathode-ray tubes) to the most recent developments, with coverage of recent studies in luminescent material drawn from *This Journal* alone and personal attendance at the Electrochemical Society meetings where the papers were presented. This has not been possible for this author. The field has progressed to the point where it cannot readily be reviewed in a short article. Papers on luminescence are appearing in many journals. The solid-state optically pumped laser, an outgrowth of luminescence research, is the subject of numerous studies, and the semiconductor laser, based on electroluminescence research, has also been intensively studied, as mentioned above. Most of the needs cited in Nagy's article have been met, and developments which could not have been foreseen in 1952 are now commonplace in our technology. Although discussion and publication are now much more widely spread than at that time, the Luminescence Division of The Electrochemical Society has continued to be a significant forum for the presentation of the results in this field. Research in luminescence and luminescent devices has matured, and it would be presumptuous to predict new devices, such as the flat solid-state television tube (which has already been predicted). However, we have seen many surprises in the last 25 years, and it would be very surprising if there were no new ones to review on the occasion of the Society's centenary.

Acknowledgments

I wish to thank all the people who helped assemble the material for this review, especially Dr. Henry Ivey, Dr. Jerry Prener, Dr. George Blasse, and Dr. Kenneth Wickersheim.

116.

REFERENCES

1. R. Nagy, *This Journal*, 99, 81C (1952).
2. G. R. Fonda, *ibid.*, 97, 8C (1950); *ibid.*, 98, 35C (1951).
3. G. R. Fonda, *ibid.*, 104, 524 (1957).
4. P. Pringsheim, "Fluorescence and Phosphorescence," Interscience, New York (1949).
5. P. Goldberg, "Luminescence of Inorganic Solids," Academic Press, New York (1966).
6. D. Curie, "Luminescence in Crystals," John Wiley & Sons, New York (1959).
7. C. D. Klick and J. Schulman, in "Solid State Physics," Vol. 5, F. Seitz and D. Turnbull, Editors, p. 27, Academic Press, New York (1957).
8. G. F. J. Garlick, "Luminescent Materials," Oxford, London (1949).
9. N. Riehl, "Einführung in Die Lumineszenz," Karl Thiemig, München (1971).
10. H. K. Henisch, "Electroluminescence," Macmillan, New York (1962).
11. H. F. Ivey, "Electroluminescence and Related Effects," Academic Press, New York (1963).
12. K. Nassau, *Appl. Solid State Sci.*, 2, 173 (1971).
13. P. Day, Chemical Society, Specialist Reports, Chemical Society, London (1970).
14. P. Day, *ibid.* (1977).
15. "Luminescence of Organic and Inorganic Materials," H. Kallmann and G. M. Spruch, Editors, John Wiley & Sons, New York (1962).
16. *Acta Phys. Acad. Sci. Hung.*, 14, No. 2, 3 (1962).
17. *Acta Phys. Pol.*, 26, (1964).
18. International Symposium on Luminescence: Physics and Chemistry of Scintillators, N. Riehl and H. Kallmann, Editors, Karl Thiemig, Munich (1966).
19. Proceedings of the International Conference on Luminescence, 1966, Publishing House of the Hungarian Academy of Sciences, Budapest (1967).
20. Proceedings of the International Conference on Luminescence 1969, F. E. Williams, Editor, *J. Lumin.*, 1, 2 (1970).
21. "Luminescence of Crystals, Molecules and Solutions," F. E. Williams, Editor, Plenum Press, New York (1973).
22. *J. Lumin.*, 12, 13 (1976).
23. G. Destriau, *J. Chim. Phys.*, 34, 117 (1937).
24. H. F. Ivey, *IEEE J. Quant. Electronics*, qe-2, 711 (1966).
25. H. F. Ivey, *IRE Trans.*, CP-4, 114 (1957).
26. H. F. Ivey, "Bibliography on Electroluminescence and Related Topics," I. *IRE Trans. Electron Devices*, ed-6, 203 (1959); II. *This Journal*, 108, 590 (1961); III. *Electrochem. Technol.*, 1, 42 (1963); IV. *ibid.*, 3, 137 (1965); V. *ibid.*, 5, 451 (1967).
27. O. W. Lossev, *Phil. Mag.*, 6, 1024 (1928).
28. M. Lorenz, *Science*, 159, 1410 (1968).
29. H. J. Casey and F. A. Trumbore, *Mater. Sci. Eng.*, 6, 69 (1970).
30. C. J. Nuese, H. Kressel, and I. Ladany, *J. Vac. Sci. Technol.*, 10, 772 (1973).
31. P. J. Dean, *J. Lumin.*, 12/13, 83 (1976).
32. E. E. Loebner, "Subhistories of the Light-Emitting Diode," *IEEE Trans. Electron Devices*, ed-23, 675 (1976).
33. H. G. Jenkins, A. H. McKeag, and P. W. Ranby, *This Journal*, 96, 1 (1949).
34. F. C. Palilla, and B. E. O'Reilly, *ibid.*, 115, 1076 (1963).
35. J. M. P. J. Verstegen, D. Radislovic, and L. E. Vrenken, *ibid.*, 121, 1627 (1974).
36. H. H. Haft and W. A. Thornton, *J. Illum. Eng. Soc.*, 2, 29 (1972).
37. W. W. Piper, J. S. Prener, and G. R. Gilooly, U.S. Pat. 4,075,532, Feb. 21, 1978.
38. W. W. Piper, Abstract 338A, p. 842, The Electrochemical Society Extended Abstracts, Spring Meeting, Seattle, Washington, May 21-26, 1978.
39. H. F. Ivey, in Laser Materials, "Proceedings of the International Conference on Luminescence," p. 128, Publishing House of the Hungarian Academy of Science, Budapest, (1966).
40. E. W. Clarly and C. C. Klick, *This Journal*, 104, 445 (1957).

41. R. J. Ginther, *ibid.*, 101, 248 (1954).
42. R. L. Amster, *ibid.*, 117, 791 (1970).
43. H. A. Klasens, *ibid.*, 100, 72 (1953).
44. W. Hoogenstraaten, *ibid.*, 105, 365 (1958).
45. A. Lempicki, *ibid.*, 107, 404 (1960).
46. J. L. Birman, *ibid.*, 107, 409 (1960).
47. F. C. Palilla, A. K. Levine, and M. Rinkevic, *ibid.*, 112, 776 (1965).
48. S. S. Trond, J. S. Martin, and A. L. Smith, *ibid.*, 116, 1047 (1969).
49. K. A. Wickersheim, Abstract 126, p. 337, The Electrochemical Society Extended Abstracts, Spring Meeting, Philadelphia, Pennsylvania, May 8-12, 1977.
50. K. A. Wickersheim, and R. A. Lefever, *This Journal*, 111, 47 (1964).
51. R. A. Buchanan, K. A. Wickersheim, J. L. Weaver, and E. E. Anderson, *J. Appl. Phys.*, 39, 4212 (1968).
52. R. A. Buchanan, S. I. Finkelstein, and K. A. Wickersheim, *Radiology*, 105, 105 (1972).
53. A. H. Waller, Abstract 147, p. 368, The Electrochemical Society Extended Abstracts, Spring Meeting, Washington, D.C., May 2-7, 1976.
54. F. Auzel, *Compt. Rend.*, 262B, 1016 (1966).
55. F. W. Ostermayer, Jr., *Metall. Trans.*, 2, 747 (1971).
56. L. Ozanne, *Philosophical Mag.*, 26, 1783 (1972).
57. F. Auzel, D. Pecile, and D. Morin, *ibid.*, 128, 181 (1973).
58. T. L. [illegible], R. T. [illegible], and E. H. [illegible], U.S. Pat 3,308,310, Aug. 20, 1963.
59. T. H. Maiman, *Nature (London)*, 187, 493 (1960).
60. W. Kaiser, C. G. B. Garrett, and D. L. Wood, *Phys. Rev.*, 123, 766 (1961).
61. P. P. Sorokin, M. J. Stevenson, J. R. Lankard, and G. D. Pettit, *ibid.*, 127, 503 (1962).
62. G. E. Geusic, H. M. Marcos, and L. G. Van Uitert, *Appl. Phys. Lett.*, 4, 182 (1964).
63. E. Snitzer, *Phys. Rev. Lett.*, 7, 444 (1961).
64. R. Mazelsky, R. C. Ohlmann, and K. B. Steinbrugge, *This Journal*, 115, 68 (1968).
65. R. H. Hopkins, G. W. Roland, K. B. Steinbrugge, and W. D. Partlow, *ibid.*, 118, 627 (1971).
66. L. H. Brixner, and P. A. Flournoy, *ibid.*, 112, 303 (1965).
67. P. A. Flournoy and L. H. Brixner, *ibid.*, 112, 779 (1965).
68. A. Lempicki and H. Samelson, "Organic Laser Systems," in "Lasers," A. K. Levine, Editor, Marcel Dekker, New York (1966).
69. A. Heller, *Appl. Phys. Lett.*, 9, 106 (1966).
70. A. Lempicki and A. Heller, *ibid.*, 9, 108 (1966).
71. P. P. Sorokin, J. R. Lankard, E. C. Hammond, and V. L. Moruzzi, *IBM J. Res. Dev.*, 11, 130 (1967).
72. B. B. Snavely, *Proc. IEEE*, 57, 1374 (1969).
73. G. Blasse and A. Bril, *This Journal*, 114, 250 (1967).
74. G. Blasse and A. Bril, *Philips Tech. Rev.*, 31, 304 (1970).
75. C. W. Struck and W. H. Fonger, *J. Chem. Phys.*, 64, 1784 (1976).
76. F. E. Williams, *J. Phys. Chem.*, 57, 780 (1953).
77. F. A. Kröger and J. R. Hellingman, *This Journal*, 89, 39 (1946).
78. J. S. Prener and F. E. Williams, *ibid.*, 103, 342 (1956).
79. F. E. Williams and E. F. Apple, *ibid.*, 106, 224 (1959).

117.

Unclassified

SECURITY CLASSIFICATION OF THIS PAGE (When Data Entered)

REPORT DOCUMENTATION PAGE

READ INSTRUCTIONS BEFORE COMPLETING FORM

1. REPORT NUMBER: 12613.1-C and 15558.1-C
2. GOVT ACCESSION NO.
3. RECIPIENT'S CATALOG NUMBER

4. TITLE (and Subtitle): Compounds with Defect Lattice Structures
5. TYPE OF REPORT & PERIOD COVERED: Final Report: 1 Mar 75 - 31 Dec 78
6. PERFORMING ORG. REPORT NUMBER

7. AUTHOR(s): E. Banks
8. CONTRACT OR GRANT NUMBER(s): DAAG29-75-G-0096; DAAG29-78-G-0105

9. PERFORMING ORGANIZATION NAME AND ADDRESS: Polytechnic Institute of New York, Brooklyn, New York 11201
10. PROGRAM ELEMENT, PROJECT, TASK AREA & WORK UNIT NUMBERS

11. CONTROLLING OFFICE NAME AND ADDRESS: U. S. Army Research Office, P. O. Box 12211, Research Triangle Park, NC 27709
12. REPORT DATE: Nov 78
13. NUMBER OF PAGES: 117 (124 p.)

14. MONITORING AGENCY NAME & ADDRESS (if different from Controlling Office)
15. SECURITY CLASS. (of this report): Unclassified
15a. DECLASSIFICATION/DOWNGRADING SCHEDULE

16. DISTRIBUTION STATEMENT (of this Report)

Approved for public release; distribution unlimited.

18 ARO, ARO

17. DISTRIBUTION STATEMENT (of the abstract entered in Block 20, if different from Report)

19 12613.1-C, 15558.1-C

18. SUPPLEMENTARY NOTES

The view, opinions, and/or findings contained in this report are those of the author(s) and should not be construed as an official Department of the Army position, policy, or decision, unless so designated by other documentation.

19. KEY WORDS (Continue on reverse side if necessary and identify by block number)

Defect Lattice Structures	Fluorides	Phthalocyanine
Point Imperfections	Luminescent Fluorides	Fluorapatite
Solid Electrolytes	Rare Earths	Cadmium Fluoride
Electrolytes	Divalent Rare Earths	

20. ABSTRACT (Continue on reverse side if necessary and identify by block number)

This report contains results of studies of (1) new bivatent rare-earth magnesium fluorides, (2) complex transition metal fluorides (3) upconversion and NMR studies of CdF_2: rare earth, (4) synthesis of potential solid electrolytes, (5) Eu Mossbauer study of EU_xMoO_4, (6) phase transition and ESR of Cr(V) in fluorapatite, and (7) possible linear conductors based on (VO) phthalocyanine.

408 704

DD FORM 1 JAN 73 1473 EDITION OF 1 NOV 65 IS OBSOLETE

Unclassified

SECURITY CLASSIFICATION OF THIS PAGE (When Data Entered)